UNIVERSITY OF CALIFORNIA
SANTA CRUZ

THE SPEED OF SIGHT: HOW CHARACTERISTICS OF ALPHA OSCILLATIONS RELATE TO RHYTHMIC SAMPLING AND TIME PERCEPTION

A dissertation submitted in partial satisfaction
of the requirements for the degree of

DOCTOR OF PHILOSOPHY
in
PSYCHOLOGY

by

Audrey Morrow

September 2024

The Dissertation of Audrey Morrow is approved:

_____
Professor Jason Samaha, Chair

_____
Professor Nicolas Davidenko

_____
Professor Megan Boudewyn

_____
Peter Biehl
Vice Provost and Dean of Graduate Studies

Table of Contents

List of Figures

List of Tables

Abstract

The Speed of Sight: How Characteristics of Alpha Oscillations Relate to Rhythmic Sampling and Time Perception

Audrey Morrow

Despite a large body of research indicating that alpha oscillations are involved in visual processing, and particularly that alpha frequency relates to temporal resolution and discriminability of stimuli, the mechanisms underlying exactly how alpha shapes our conscious perception are still unclear. According to one account, perception could be discretely windowed by each alpha cycle into a series of "snapshots" (discrete sampling theory), while another account posits that just the strength of perception continuously waxes and wanes across each alpha cycle (rhythmic sampling theory). This dissertation examines features of alpha oscillations in the context of these theories of perceptual sampling. We demonstrate that perception is unlikely to occur in discrete snapshots, given that an individual's alpha frequency (IAF) does not relate to the magnitude of their percepts across similar visual illusions that are thought to depend on discrete sampling, nor does it relate to the timing of sensory responses associated with visual percepts. Finally, we find that alpha does not relate to a bias in duration estimation, which should occur if individuals accumulate varying amounts of visual information via discrete perceptual snapshots due to their varying IAFs. However, we found support for the role of alpha oscillations in modulating the strength of our sensory percepts by demonstrating that alpha phase – and its interaction with alpha power – relates to the strength of sensory responses associated with visual perception, and that IAF relates to individual differences in sensitivity when estimating and discriminating

the durations of visual events. These studies provide novel insights into how alpha oscillations play a role in visual processing, not just around the timing of a single alpha cycle, but also at longer durations of stimulus processing in a way that facilitates our perception of time.

Acknowledgements

As the King in Alice in Wonderland instructed, “begin at the beginning… and go on till you come to the end: then stop.” In terms of my scholastic journey, I’ve finally done this, and I might as well do it for my acknowledgements too. So, to “begin at the beginning,” I must acknowledge my parents, Rick and Denise. I wouldn’t be here without you. Thank you for always pushing me to learn and try new things, to reach for bigger goals, and to attend every possible graduation. And I wouldn’t be the person I am today without my brother, Alex, who taught me to sing and dance and not take life too seriously (except when it came to getting the better report card, which I took very seriously, and which clearly got me hooked on academic success. So, thanks for that…). I could go on and on before the end – it was a long journey, and I have many friends to acknowledge along the way. But I think you know who you are, I just hope you also know how much I appreciate you being my hype team. Many thanks, of course, to my committee for the brilliant ideas you shared with me – particularly my advisor, Jason, who reviewed countless versions of every project, analysis, figure, talk, poster, and manuscript I ever made (and let me go to a castle in Germany to learn even more about beer – I mean, friendship – I mean, visual neuroscience); I truly couldn’t have asked for a better mentor. At the end, though, I have to thank my partner, Nathan. You were my boots-on-the-ground support system, giving me the love and dinners, rides and listening ear, cozy nights and stimulating discussions, that carried me through my final milestones. Thank you.

CHAPTER 1: Introduction to Alpha Oscillations and Theories of Perception

Our conscious perceptual experience does not always match the physical sensory stimuli which evoke that experience, as has been demonstrated by various visual and multisensory illusions. Theories of visual perception often try to explain the discrepancies between what is real and what is perceived by examining the neural dynamics associated with changes in perception, illusory or otherwise. Experimentally testing the predictions of theories of perception can help bolster our understanding of how neural dynamics shape our perceptual experience.

Measuring Neural Activity

To study temporal aspects of visual perception it is critical to understand how the neural activity underlying perceptual processes can be measured. Perception typically occurs in response to a stimulus, but perception can also occur in the absence of a stimulus, and ongoing neural activity can modulate these perceptual experiences. Two fundamental aspects of neural dynamics that underlie perceptual processing are neural oscillations and stimulus-evoked responses. Neural oscillations are rhythmic patterns of electrical activity produced by local populations of neurons referred to as neural generators. The firing of a neuron is an electrochemical process in which charged chemicals initiate an action potential by moving into the cell body of the neuron; this creates a change in the electrical charge surrounding the neuron and also promotes the release of additional chemicals that signal for neighboring neurons to fire (Barnett & Larkman, 2007). When this process affects a population of neurons in the cortex, the electrical charge is often strong enough to travel through the skull and be measured with electrodes on the scalp via electroencephalography (EEG; Buzsáki et al., 2012; Cohen, 2017; Jackson & Bolger, 2014). Importantly, this process is ongoing and often has characteristic temporal regularities, both locally and across brain layers and regions, that

are referred to as neural oscillations.

Neural oscillations have several characteristics that can play different roles in cognitive and perceptual processing: frequency, amplitude, and phase. Oscillations are defined by their frequency-band range, as measured in Hertz (Hz) or cycles per second, and the brain region(s) or process they are associated with. Alpha oscillations, for example, which range from 7-14Hz, were discovered over posterior electrode locations, and subsequent research has shown activity in this frequency range (and cortical region) to be strongly associated with sensory perception (Hindriks et al., 2014; Hindriks & van Putten, 2013). Amplitude refers to the height of the wave, or the distance from the peak or trough to the mean position of the wave, and it relates to the amount or synchrony of neural activity at a given frequency, typically measured in microvolts (μV). Amplitude can be squared to give a measure of power (μV^2) which represents the amount of energy of an ongoing signal at a particular frequency. Finally, phase captures the specific phase angle of an oscillation relative to a specific starting point, measured in degrees or radians. In other words, phase describes the shift in the wave relative to a reference angle of 0°. While intrinsically related, each of these attributes of neural oscillations can be extracted separately and can be studied alone or in combination with other oscillatory attributes, stimulus-evoked responses, and behavioral measures, to better understand their functional significance.

Stimulus-evoked response refers to the simultaneous firing of action potentials in neurons that are specialized to process a given stimulus. Responses are driven by particular sensory properties of the stimulus such as color or spatial location as well as the cognitive mechanisms underlying processing that stimulus, such as surprise or decision-making (Luck, 2005; Sur & Sinha, 2009). These responses do not occur in isolation in the brain (they tend to be understood as adding to the ongoing or background oscillatory activity), making them

difficult to detect in a single instance due to ongoing neural activity that is not associated with stimulus processing. Thus, in order to measure stimulus-evoked activity in humans using non-invasive methods, neural activity is typically averaged across a large number of trials causing the random activity to cancel out and the stimulus-evoked activity, which always occurs at a similar timepoint relative to the stimulus presentation, to emerge (Luck, 2005; Sur & Sinha, 2009). These stimulus-evoked responses may be referred to as event-related potentials (ERPs), referring to the electrical potential or voltage that changes in the population of neurons processing that stimulus "event". It is important to study both ERPs and neural oscillations, and the interactions between these types of activity, to fully understand how perception varies from moment-to-moment within an individual, and how perception may be different across different individuals.

Alpha Oscillations in Visual Perception

Alpha oscillations are involved in many cognitive processes, from bottom-up sensory processing in sensory areas, to top-down, long-range communication between sensory and frontal areas (Clayton et al., 2018) and frequency, as well as amplitude and phase, are known to be involved in different aspects of perception. Alpha oscillations are typically around 10Hz in adults, but every individual has a specific peak frequency within the alpha-band range with the highest amount of power, referred to as the peak individual alpha frequency (IAF). IAF varies across individuals yet is relatively stable within an individual throughout adulthood (Grandy et al., 2013; Knyazeva et al., 2018). Alpha frequency is related to the temporal resolution of visual perception and the integration of multisensory information. Specifically, faster IAF is predictive of better discrimination between successive flashes of light and is associated with shorter binding windows within which a number of multisensory illusions occur (Cecere et al., 2015; Cooke et al., 2019; Migliorati et al., 2020; Noguchi, 2022; Samaha

& Postle, 2015; Venskus et al., 2021). These findings have been supported by research modulating IAF using rhythmic-transcranial magnetic stimulation (rTMS), highlighting a causal relationship between alpha frequency and improved sensitivity in visual detection (Di Gregorio et al., 2022). This wealth of research examining the role of IAF in visual perception suggests that alpha frequency is correlated with perceptual sensitivity, particularly around temporal aspects of perception.

Alpha power has long been thought to be linked to cortical excitability in an inhibitory manner (Coffin & Ganz, 1977; Kelly et al., 2009; Melcón et al., 2023; Thut et al., 2006). Reductions in alpha power are observed during states of spatial attention (Dockree et al., 2007; Gould et al., 2011; Thut et al., 2006), and increases in alpha power occur when participants close their eyes (Goldman et al., 2002). These changes in alpha power also relate to visual perception, such that participants are more likely to report seeing a near-threshold stimulus on trials when alpha power is low compared to trials when alpha power is high (Ergenoglu et al., 2004; Lange et al., 2013; van Dijk et al., 2008). It is also thought that prestimulus alpha power can drive sensory representations by modulating the strength of early sensory ERPs (Jensen & Mazaheri, 2010; Klimesch, 2011; Samaha et al., 2018). For example, Iemi and colleagues (2019) showed that stronger prestimulus alpha power in a passive viewing paradigm led to a reduced (inhibited) C1 response – the earliest ERP component, thought to reflect afferent activation of the primary visual cortex (V1). These findings highlight the role of alpha power in bottom-up sensory processing, but a large body of research has also focused on the top-down modulations of alpha-band activity. The literature has primarily focused on how alpha power changes in an inhibitory manner during preparatory visual attention (Foxe & Snyder, 2011), and an early macaque study demonstrated that attention can modulate alpha power even at the layer-specific level of

visual cortex (Bollimunta et al., 2011). In conditions with visual stimulation, the local field power (LFP) measure of alpha power decreased significantly in certain layers of visual cortex. This result indicates how top-down mechanisms such as attention can alpha modulate alpha power and support models of alpha oscillations as an inhibitory gating mechanism (Jensen & Mazaheri, 2010; Klimesch et al., 2007). Similar findings have been demonstrated in human studies and suggest that attention can affect the distribution of alpha power across cortical locations (not just layers) when attending to different spatial locations or features (Dockree et al., 2007; Gould et al., 2011; Thut et al., 2006). Additionally, these changes in alpha power are associated with improvements in task performance, and changes in the strength of ERPs (Foxe & Snyder, 2011; Fu et al., 2005; Kelly et al., 2008; Kelly & O'Connell, 2013; Sauseng et al., 2005; Slagter et al., 2016). Overall, alpha power seems to be related to both spontaneous cortical excitability and endogenous changes in excitability via attention.

Several studies have also shown that the phase angle of prestimulus alpha is related to the perceptual detection and the strength of sensory responses. Specifically, research has demonstrated a relationship between prestimulus alpha phase and detection in tasks that use near-threshold stimuli, such that participants are more likely to detect or correctly discriminate stimuli at some phase angles compared to others (Busch et al., 2009; Busch & VanRullen, 2010; Mathewson et al., 2009; Ronconi et al., 2017; Samaha et al., 2015, 2017; Sherman et al., 2016), but see (Benwell et al., 2017; Ruzzoli et al., 2019). This variation in perceptual performance may be due to a phasic modulation of sensory responses. When examining the global field power associated with the time window of C1 (the earliest visual-evoked response), Dou et al. (2022) found that GFP varied based on the alpha-band phase angle just before stimulus presentation. This finding suggests that alpha phase may be

modulating the strength of the sensory percept via the strength of early sensory activity. Interestingly, phase angle was found to interact with alpha power, such that phase angle modulated GFP response to a greater extent on trials with higher alpha power compared to trials with low alpha power (Dou et al., 2022). In other words, while phase, amplitude, and frequency likely each play specific roles in perceptual processing, these oscillatory features also interact in nuanced ways to shape our perceptual experience and are worth examining in a variety of contexts.

Theories of Visual Perception

To better understand how alpha oscillations relate not just to the sensitivity of perceiving an event, but the sensitivity of discriminating events in time, and the way we perceive time more broadly, it is important to understand temporal theories of visual perception. Driven by research highlighting the role of IAF in sensitivity of visual illusions (Chota & VanRullen, 2019), VanRullen (2016) proposed two possible theories of how alpha frequency might explain these different perceptual outcomes: the discrete sampling theory and the rhythmic sampling theory.

The discrete sampling theory suggests that our perceptual experience is modulated by alpha cycles in a way that mimics the frame rate of a film (VanRullen, 2016). Each alpha cycle is thought to capture a "snapshot" of the visual environment that is taken at, for example, each peak of the wave. These snapshots then get stitched together to form our conscious visual perception, losing information that occurred between snapshots. If each alpha cycle provides an updated visual percept, IAF should relate to how quickly or slowly an individual updates their conscious perception. Thus, this theory has implications for temporal aspects of visual perception, such as the perception of certain visual illusions, and, perhaps, the perception of the timing or the durations of visual events. Individual differences in the

perception of illusions and durations should relate to IAF and IAF in general should relate to the timing of sensory responses that index the conscious perceptual experience. If the discrete sampling theory is an accurate description of the role of alpha in visual perception, we would expect that visual illusions that rely on motion stimuli are not actually processed as continuous motion but rather perceived as snapshots which are updated in our conscious perception to be moving. For example, in the flash-lag illusion, a stationary flash and a moving object that appear in the same location appear to be displaced such that the moving object is perceived to have appeared farther along in its trajectory. The magnitude of the illusion, or in the flash-lag example the amount of displacement of the moving object, should be greater for individuals with slower IAF and who update their percept less frequently and thus update the movement of the object later than individuals with faster IAF. This question is explored in depth in Chapter 2, by comparing the magnitude of two visual motion illusions and a control task. The discrete sampling theory could also relate to how an individual perceives time or, more specifically, durations of visual events. If each alpha cycle represents a snapshot of the visual environment, then individuals with faster IAF should take more snapshots may have a bias towards over-estimating durations. A study by Mioni et al. (2020) found a similar effect: when stimulating alpha frequency to be above or below IAF, participants tended to over- or under-estimate durations. However, given the stability of IAF across adulthood, it is possible that an individual learns to calibrate their time judgments and would show no bias at their own non-manipulated IAF relative to an individual with faster or slower IAF. In addition to variations in temporal perception, IAF should map on to other neural mechanisms, such as the timing of sensory ERPs. If the alpha cycle is actually modulating the timing of our visual percepts, so should it modulate the timing of stimulus processing; individuals with faster IAF who are updating their perceptual snapshots of visual

stimuli more often should also have faster (or earlier) sensory-evoked responses. In other words, the latencies of sensory ERPs should be related to the speed of IAF, a hypothesis that is evaluated in Chapter 3. Despite some evidence linking IAF to the magnitude of illusory percepts (Chota & VanRullen, 2019; Händel & Jensen, 2014), there is little evidence linking the magnitude of individual differences across different but related illusions, nor is there evidence that IAF is related to the timing of early sensory responses. Thus, to understand whether discrete sampling indeed plays a role in how we form our visual percepts, the timing of illusory percepts and the timing of sensory responses should be further evaluated in the context of IAF.

The rhythmic sampling theory, on the other hand, suggests that our perceptual experience is modulated by alpha cycles in a way that mimics the brightening and dimming of a lightbulb (VanRullen, 2016). According to this account, the conscious representation of our visual environment is proposed to, for example, become stronger with each peak of the wave and weaker with each trough of the wave. Rather than updating the entire percept with each cycle, this theory proposes that our visual perception is continuous and instead, the strength or sensitivity of our perception changes throughout the alpha cycle. If our perception functions like the rhythmic sampling theory suggests, it would mean that individuals with faster IAF have more frequent fluctuations in the strength of their sensory representations than individuals with slower IAF. Thus, even though high (fast) IAF would theoretically lead to the experience of more weak representations in a second, it would also lead to the experience of more strong representations in that timeframe, which are critical for making perceptual judgements. In addition, IAF should relate to other underlying mechanisms of perceptual sensitivity, such as the strength of early sensory ERPs which have been thought to map on to the strength and saliency of the perceptual representation (Luck et al., 1990; Salti

et al., 2012; Woodman, 2010). Whether the prestimulus phase of IAF is linked to the magnitude of sensory responses is explored in Chapter 4. We would also expect behavioral differences according to the rhythmic sampling account, such that IAF should be related to sensitivity of perceiving ongoing or very brief visual stimuli given that the conscious visual percept is continuously representing actual physical stimuli. It has been demonstrated by some studies that participants with faster IAF are more sensitive at perceiving brief events (Chaumon & Busch, 2014; Tarasi & Romei, 2023; Zhou et al., 2021), but few studies have been done to explore whether participants with faster IAF are better at discriminating durations of visual stimuli. One study has explored the role of phase in duration perception, suggesting it relates to sensitivity in discriminating durations (Milton & Pleydell-Pearce, 2016), but while phase is intrinsically related to alpha frequency, the relationship between IAF and duration perception sensitivity is not well understood. In Chapter 5, we evaluate the role of IAF in duration perception, with the hypothesis that the rhythmic sampling account would explain differences in task sensitivity, while the discrete sampling account would explain differences in bias in the task. This chapter is critical to understanding how these theories of visual perception play a role in more long-term perception. By evaluating the discrete and rhythmic sampling theory in the context of illusory perception, duration perception, and stimulus processing, we can establish support for which perceptual mechanism is underlying our visual processing. Overall, the studies outlined in the subsequent chapters help to expand on what we know of the role of alpha oscillations in sensory processing and shed new light on the role of alpha oscillations in the intriguing but understudied topic of time perception.

CHAPTER 2: No Evidence for a Single Oscillator Underlying Discrete Visual Percepts

Published in the European Journal of Neuroscience as Morrow and Samaha (2022)

Whether conscious visual perception unfolds continuously or as a series of discrete updates remains a topic of much debate (Anliker, 1963; Doerig et al., 2019; Fekete et al., 2018; Harter, 1967; Herzog et al., 2020; James, 1980; Kristofferson, 1967a; Valera et al., 1981; VanRullen, 2016; VanRullen & Koch, 2003; C. T. White, 1963; P. A. White, 2018). Vision appears continuous to introspection, yet a number of perceptual phenomena are difficult to reconcile with a continuously updating perceptual process (Herzog et al., 2020; Sokoliuk & VanRullen, 2019). The flash-lag effect and the Fröhlich effect are two such examples. In the flash-lag illusion, a brief stationary stimulus (the 'flash') is misperceived as lagging behind a moving stimulus when the two stimuli are, in fact, spatially aligned (Metzger, 1932; Murakami, 2001; Nijhawan, 1994). The Fröhlich illusion refers to the observation that the onset of a moving stimulus is often mislocalized as being further along the trajectory of motion than it really is (Fröhlich, 1923; Kerzel, 2010). Many variants of discrete sampling models have been proposed to account for each effect separately (for reviews, see: Herzog et al., 2020; VanRullen, 2016; P. A. White, 2018), but recently Schneider (2018) proposed a unifying account of both the flash-lag and Fröhlich illusions based on discrete sampling.

In the model, a repeating process of sampling followed by reconstruction occurs, with the sampling process lasting for a specified duration (a 'perceptual moment'). At the end of the perceptual moment, stimuli are registered in their last-known positions and this estimate forms the basis of the conscious reconstruction of events. Because moving stimuli will be in a different position at the end of the moment than a stationary stimulus, this leads to the kind of discrepancy observed between the flash and motion stimulus (flash-lag) or

between the onset of the motion and the position the stimulus is in when conscious perception was updated (Fröhlich). Thus, the duration of an individual's perceptual moment is the sole parameter in the model and half of this quantity corresponds to the average flash-lag and Fröhlich magnitude. This single-parameter model (Schneider, 2018) provided good fits to a large flash-lag dataset from Murakami (2001).

At the neural level, oscillations in brain activity have long been speculated to be involved in discrete perceptual sampling. For instance, within- and between-subject variation in alpha-band frequency (7-14 Hz) is predictive of temporal properties of visual (Baumgarten et al., 2018; Coffin, 1977; Coffin & Ganz, 1977; Gray & Emmanouil, 2020; Gulbinaite et al., 2017; Kristofferson, 1967b; Minami & Amano, 2017; Ro, 2019; Samaha & Postle, 2015; Shen et al., 2019) and cross-modal perception (Cecere et al., 2015; Cooke et al., 2019; Keil & Senkowski, 2018), with higher-frequency oscillations being associated with finer-grained temporal resolution. Moreover, the phase of ongoing alpha activity predicts perception of near-threshold visual stimuli (Alexander et al., 2020; Busch et al., 2009; Dugué et al., 2011; Mathewson et al., 2009; Samaha et al., 2015, 2017; Sherman et al., 2016). Indeed, it has been shown that trial-to-trial variability in the magnitude of the flash-lag effect is predictable by the phase of ~7 Hz oscillations prior to flash onset (Chakravarthi & VanRullen, 2012), consistent with the model proposed by Schneider (2018). And a recent experiment presented a luminance-modulating annulus at 10 Hz surrounding a flash-lag display and found that the flash-lag magnitude was correlated with the phase of the luminance modulation, suggesting that entraining brain activity at an alpha frequency causes changes in flash-lag perception at that frequency (Chota & VanRullen, 2019). Thus, discrete sampling at alpha frequencies has been advanced as a possible explanation for the flash-lag effect (Chakravarthi & VanRullen, 2012; Chota & VanRullen, 2019; Sokoliuk & VanRullen, 2019) and the Fröhlich effect has

been argued to follow from the same underlying mechanism as the flash-lag effect (Eagleman & Sejnowski, 2007).

Importantly, variations in the flash-lag and Fröhlich effects, if driven by discrete sampling at alpha frequencies, should be seen across participants given that significant differences in peak IAF have been reliably observed (Grandy et al., 2013; Haegens et al., 2014). Peak alpha frequency has been described as a trait variable due to evidence linking it to genetic factors (Bodenmann et al., 2009). Additionally, an average standard deviation of 1Hz has been reported for IAF in age-matched participants, suggesting substantive variation across individuals (Klimesch, 1997). For these reasons, we expect that IAF will vary within a random sample, even without having recorded EEG data.

The goal of this study was to test the proposition that, if the flash-lag and Fröhlich effects are driven by discrete sampling at the alpha frequency, then the magnitude of the illusion should be correlated across individuals. That is, given the relative stability of an individual's alpha frequency (Grandy et al., 2013; Haegens et al., 2014), an individual with a large flash-lag magnitude (putatively caused by a lower alpha frequency and thus less frequent updating) should also have a large Fröhlich effect. Alternatively, no correlation between illusion strengths could indicate either that the Fröhlich and flash-lag do not reflect the same discrete sampling mechanism, or that they do reflect discrete sampling but at different frequencies that are not meaningfully related to one another across individuals. This latter notion is supported by a general lack of convergence in the literature on a single time scale of the 'perceptual moment' across tasks and stimuli, and a lack of a single oscillation frequency being related to temporal perception (Herzog et al., 2020; Ronconi et al., 2017; VanRullen, 2016). Thus, a correlation between illusion magnitudes would provide a compelling (albeit not sufficient) pre-condition for the theory that alpha sampling underlies

both illusions. There is also a more general question of whether the flash-lag and Fröhlich effects are based on the same mechanism (whatever that may be), which remains controversial (Kreegipuu & Allik, 2003; Krekelberg & Lappe, 2001; Whitney & Cavanagh, 2000) but which can be informed by an individual differences approach.

We quantified the magnitude of the flash-lag and Fröhlich illusion psychophysically by determining the spatial offset required between a motion stimulus and a stationary reference stimulus to make the two stimuli appear spatially aligned (i.e., the point of subjective equality; PSE). Robust flash-lag and Fröhlich illusions were present in our displays and despite the two displays being highly similar, we observed no correlation between individual differences in the illusion magnitudes. A Bayesian analysis provided moderate support for the null hypothesis of no correlation. It is possible that our stimulus parameters were ill-suited to detect a true relationship, or that a true relationship exists between each illusion and IAF, but the two illusions do not correlate with each other. However, follow-up research performed a robust examination of eight different motion position illusions across 104 participants and found no significant relationship between the flash-lag and Fröhlich illusions (Cottier et al., 2023). Furthermore, Cottier et al. (2023) performed an exploratory factor analysis on clusters of illusions that did show significant correlations with one or more other illusions and found that each cluster was likely explained by a different factor or mechanism. Thus, we conclude that the lack of a relationship between the flash-lag and Fröhlich effects is because 1) these two illusions are supported by different mechanisms, perhaps based on sampling rates determined by different oscillatory frequencies in the brain or 2) distinct mechanisms not based on discrete sampling underlie each illusion.

Method

Participants

Twenty-four participants (15 female, 8 male, 1 prefer not to say; age range: 18-29)

were recruited from the University of California Santa Cruz's (UCSC) online psychology research pool. The experiment was approved by the UCSC Institutional Review Board. All participants had normal or corrected-to-normal vision and provided written consent to participate. One participant's data was excluded for indicating, during debriefing, that they did not understand the instructions. As a result, their data did not follow a typical psychometric curve.

A post hoc power analysis (G*power 3.1; Faul et al., 2007) indicated that 23 participants achieved 80% power to detect a one-tailed correlation of magnitude 0.5 (alpha level = 0.05). Given that the theory we are testing proposes that both illusions are based on the same mechanisms of alpha-band sampling, this would predict a strong correlation between the two illusion magnitudes. Our group has published similarly sized samples when investigating individual differences in theoretically-large associations (Samaha & Postle, 2015, 2017). However, we sought to quantify more precisely the degree of evidence in favor of the null hypothesis provided by our results by using Bayesian analyses (described later).

Design

The experiment took place in a dimly lit room with participants positioned in a headrest to maintain a distance of 74cm from the computer monitor. Stimuli were generated using Psychtoolbox-3 (Kleiner, 2007) running in the MATLAB environment (version 9.8) under the Ubuntu (version 18.04) operating system. Stimuli were presented on a middle-gray background of 50cd/m^2 luminance on a gamma-corrected VIEWPixx EEG monitor (1920 x 1200 pixels, 120 Hz refresh rate). A central fixation, consisting of a gray crosshair superimposed over a black circle 0.4° of visual angle, was present on the screen throughout each task.

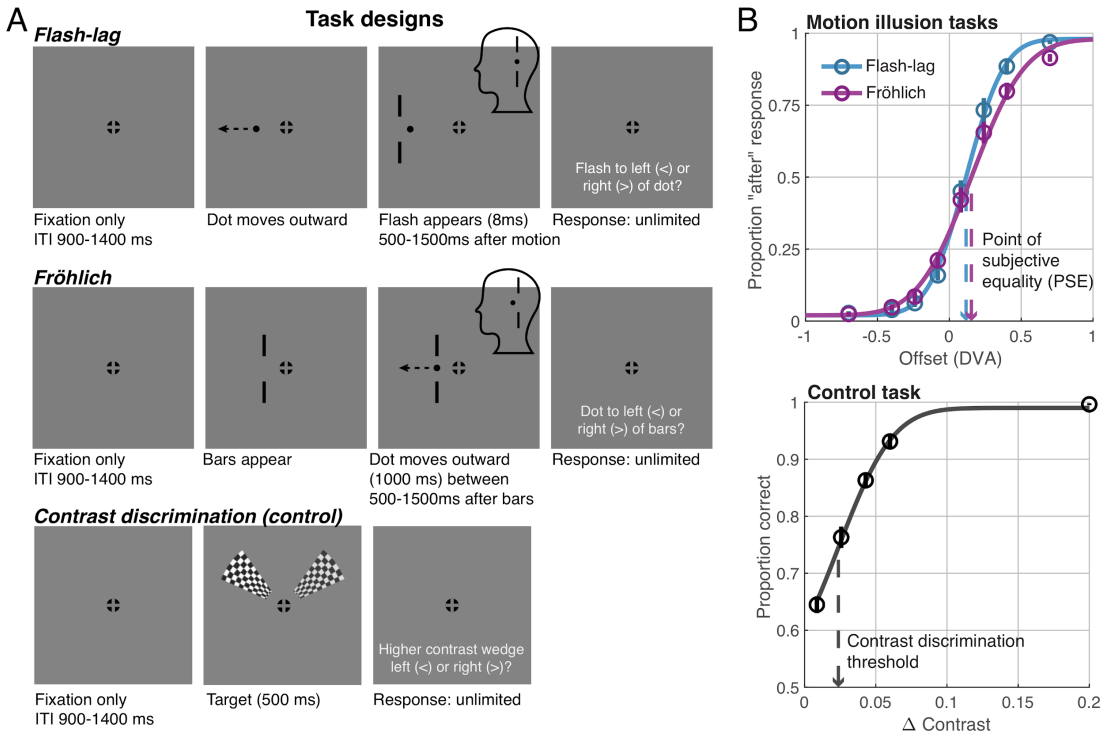

Figure 1: Diagrams for the flash-lag, Fröhlich, and control tasks, and group-level psychometric functions.

A) From top-to-bottom, example trials of the flash-lag, Fröhlich, and control tasks are shown. For the two illusion tasks (flash-lag and Fröhlich), participants judged the location of the vertical bars relative to the moving dot. All that differed between tasks was whether the moving dot appeared before the vertical bars (flash-lag condition) or after (Fröhlich) and whether the bars were presented briefly (8ms; flash-lag) or remained on screen throughout the trial (Fröhlich). In the example flash-lag trial, a positive offset is shown which refers to the fact that the vertical bars flashed further away from fixation than the moving dot. The cartoon head insert represents the perceived illusion and was not part of the display participants saw. In the flash-lag effect, the flashed bars appear to lag behind the motion stimulus which, for a positive offset, would manifest as the bars appearing to be aligned with the dot. In the example Fröhlich trial, the offset equals zero, but the initial position of the dot is perceived as advanced along the trajectory of motion. In the contrast discrimination (control) task, two wedges were shown simultaneously, one with higher contrast (the left wedge in this example) and participants judged the location with highest contrast. The white text shown in these schematics was not present on the actual displays. B) Group-level behavior (circles) and psychometric function fits (lines) for the two illusion tasks (top) and control task (bottom). In both the flash-lag and Fröhlich data, the PSE is reliably non-zero, indicating that a positive offset between the dot and bars are required for participants to perceive the two stimuli as being aligned. Contrast discrimination thresholds provided control data in that they were hypothesized to be independent of the illusion PSEs. Error bars represent ±1 SEM across subjects and sometimes too small to be clearly visible.

Flash-Lag Illusion

A 0.3° black dot moved horizontally outwards from the center in either the left or right hemifield (randomly determined on each trial with equal probability). The dot trajectory started at 2° from central fixation and moved horizontally away from fixation for 2000ms at a speed of 6° per second. At a randomly selected interval between 500-1500ms during the dot's trajectory, a set of vertical black bars (the "flash") flashed above and below the dot for 8ms. The two bars were 0.13° W x 0.83° H with a distance of 0.83° between them. The flash appeared at one of 8 offsets (randomly selected with equal probability on each trial) from the set [-0.70°, -0.40°, -0.24°, -0.08°, +0.08°, +0.24°, +0.40° +0.70°] relative to the location of the moving dot, which translates to between 4.3° to 11.7° away from central fixation. This variation in offset caused the flash to appear "ahead of" or "behind" the dot to varying extents (Figure 1).

Fröhlich Illusion.

This task used the same parameters as the flash-lag for the moving dot and the set of bars except that the bars appeared first (either to the left or right if fixation, randomly determined), and remained on screen for 2000ms. The dot then appeared midway into the 2000ms (between 500-1500ms) and immediately began moving (Figure 1). The bars were placed using the same set of possible offsets between the onset of the dot trajectory ([-0.70°, -0.40°, -0.24°, -0.08°, +0.08°, +0.24°, +0.40° +0.70°], randomly selected on each trial), which translates to between 5° to 11° from fixation. Similar to the flash-lag illusion, this offset caused the dot to appear "ahead of" or "behind" the set of bars to varying degrees.

Contrast Discrimination (Control) Task.

In addition to the two illusion tasks, we included a third control task that was

intended to measure perceptual processes (here, contrast discrimination) different from those underlying the flash-lag and Fröhlich illusions. The control task was adapted using stimuli from (Iemi et al., 2019) and presented two checkerboard wedges to the left and right of fixation (Figure 1). The wedges corresponded to segments of an annular checkerboard with a spatial frequency of 5 cycles per degree. The two wedges appeared for 500ms in either the upper or lower hemifield with the inner edge of the wedges 3° from central fixation and the outer edge 10° away. The right wedge was designated a 'standard' and was held constant at 0.8 contrast (i.e., 80% Michelson contrast) and the left wedge varied randomly across the following 10 levels [0.60, 0.740, 0.757, 0.774, 0.791, 0.808, 0.825, 0.842, 0.860, 1.0]. This task was a control in the sense that the specificity of any correlation observed between the flash-lag and Fröhlich illusions could be tested by comparing this effect to the correlation obtained between the illusion PSEs and contrast discrimination thresholds (which, we hypothesized, would be uncorrelated).

Procedure

Participants were instructed on each task before engaging in practice blocks of 20 trials. Researchers monitored the practice blocks to ensure participants understood the task instructions and reviewed the response curves after each block. Additional practice blocks were conducted as necessary. The order of the three tasks was counterbalanced across participants. For all tasks, the intertrial interval varied randomly between 900ms and 1400ms and response duration was unlimited so that participants would focus on accuracy over speed of response. Participants were instructed to maintain fixation on the central crosshair throughout the whole trial and not to track the moving object.

Participants completed 312 trials, split across three blocks, of each illusion task. Participants were instructed to respond using the "<" and ">" keys to indicate whether the

new object appeared to the left or right of the original object, respectively. In other words, participants responded to whether the flash appeared to the left or right of the moving dot in the flash-lag illusion or to whether the moving dot first appeared to the left or right of the stationary bars in the Fröhlich illusion.

Participants completed 300 trials of the control task, split into three blocks. In this task, participants engaged in contrast discrimination between the two checkerboard wedges. The participants responded with the same "<" and ">" keys to indicate whether the left or right wedge, respectively, had a greater level of contrast.

Data Analysis

Psychometric Functions

Responses were mirrored to remove relative location information (i.e., responses were re-coded to reflect "before" or "after" responses rather than "left" or "right" responses, the meaning of which was dependent on the hemifield of presentation). When analyzing data from the contrast discrimination task, the contrast of the variable-contrast wedge was expressed in units of absolute difference from the standard contrast wedge (i.e., Δ contrasts = [0.008, 0.025, 0.042, 0.060, 0.2]) and accuracy (proportion correct) was computed for each Δ contrast level.

A cumulative normal function was fit to each subject and task using maximum-likelihood estimation as implemented in the Palamedes toolbox (version 1.9.1; Prins & Kingdom, 2018). For the flash-lag and Fröhlich task, the PSE and slope were free parameters whereas the lower and upper asymptotes of the curve were fixed at 0.02 and 0.98, respectively, to allow for lapses (Prins, 2012). For the contrast discrimination data, the threshold and slope were free parameters, and the guess rate was fixed at 0.5 and lapse rate at 0.02. The across-subject correlation between psychometric parameters in each task was then

computed using a Spearman correlation (rho), to mitigate the influence of any potential outliers.

Data from the right and left visual hemifield of each illusion task were initially analyzed separately to check for an effect of the visual field location on the correlations between illusion response curves. We fit the response curves for right and left hemifield trials for the flash-lag and Frohlich illusions separately in order to compare PSEs from the right and left visual field. The flash-lag illusion did not produce significantly different PSEs at right and left visual fields ($t(22) = -0.67$, $p = 0.51$), while the Fröhlich illusion did produce significantly different PSEs at right and left visual fields ($t(22) = 2.68$, $p = 0.01$) such that trials in the right visual field produce a larger Fröhlich effect. To ensure this significant difference in PSEs across hemifield was not masking potential correlation between illusion magnitudes, we performed a Spearman correlation of the flash-lag and Fröhlich PSEs for each visual field. Neither right nor left visual field trials show a significant correlation between illusion PSEs (right: $r(22) = -0.29$, $p = 0.19$; left: $r(22) = 0.07$, $p = 0.75$). Thus, we collapsed all trials for further analyses.

Bayes Factor Analysis

To interpret the weight of evidence our data provide for and against the null hypothesis of no correlation, we computed Bayes factors (BF). Here, BF reflects the ratio of likelihoods (L) of the data under the alternative hypothesis (the theory; H1) to that of the null hypothesis (H0); that is $BF_{1,0} = L_{H1}/L_{H0}$. Thus, a BF increasing from 1 indicates more evidence for H1, whereas a BF approaching zero indicates increasing evidence for H0. Meaningful interpretation of a BF requires specifying an appropriate H1, which amounts to specifying a theoretically-plausible distribution of effects according to a theory (Dienes, 2014; Rouder et al., 2016). We specified two models of H1, corresponding respectively to weak and strong

versions of the theory that alpha-based sampling underlies both illusions.

The first model instantiates the relatively minimal assumption that the theory just predicts a positive correlation (rho) between the flash-lag and Fröhlich effect. This was specified in the MATLAB implementation of the BF calculator by Zoltan Dienes (http://www.lifesci.sussex.ac.uk/home/Zoltan_Dienes/inference/Bayes.htm) as a uniform distribution spanning 0 (lower bound of rho) to 0.9 (upper bound of rho; values greater than 0.9 were considered unrealistic). (Note that values were Fisher's z-transformed prior to input into the calculator.) This expresses the view that the theory predicts some positive relationship that is equally likely to be of small, medium, or large effect size. We refer to this as $BF_{U(0, 0.9),0}$. The actual mean and spread of the observed effect ("sample mean" and "sample SE" in the calculator) were taken as the Fisher's z-transform of the actual rho value computed between the illusions with SE = 1/sqrt(df - 1).

The second BF represents H1 in a more theoretically-motivated way using the ratio-of-scales heuristic from Dienes (2019). This approach rests on the logic that, if the two illusions are caused by the same underlying mechanism, and because both are measured in the same units (PSE in degrees of visual angle, or DVA), a strong version of the theory predicts that they should be identical. That is, the slope (β) of a line fit to the Fröhlich by flash-lag PSEs (e.g., Figure 3A) should equal 1. This predicted effect size for H1 was specified in the Dienes code as a half-normal distribution (to reflect the directional nature of the hypothesis) with a mean of zero and an SD of $\beta/2 = 0.5$. Since the prediction that $\beta = 1$ is a maximum effect that assumes no error, the specification of a half normal with a mean of zero is a conservative estimate of the H1 mean since it predicts that smaller effects are more likely. Dividing the predicted value by 2 to achieve an SD of 0.5 is a further conservative correction that halves the predicted effect, as recommended in the literature (Dienes, 2014,

2019). We refer to the BF according to this model of H1 as $BF_{HN(0,\ 0.5),0}$. The observed β and SE from the data were estimated as the slope and standard error of an ordinary least-squares regression predicting the flash-lag PSE from the Fröhlich PSE and were input into the BF calculator.

Results

We quantified the magnitude of the flash-lag and the Fröhlich illusion within the same individuals to assess their correlation. The data were well-described by a psychometric function (R^2 across all subjects in both tasks: mean = 0.98, range = [0.92, 0.99]; see Figures 1 and 2). As a first step, we tested whether illusory percepts consistent with the flash-lag and the Fröhlich effects were observed in our displays. Because each illusion was quantified as the PSE whereby the offset between the dot and bar stimuli would be judged as either "before" or "after" 50% of the time, a PSE of zero DVA would correspond to veridical perception, or a 0ms difference between dot and bar stimuli. Consistent with illusory percepts, however, the mean (±SEM) PSE in the flash-lag task was 0.12 (±0.02) DVA or 20 (±3.33) ms (given a dot speed of 6 degrees per second), which was significantly different from zero, as assessed with a repeated-measures t-test ($t(22) = 5.74$, $p < 0.0001$). The mean Fröhlich PSE was 0.15 (±0.03) DVA or 25 (±5) ms, which also differed from zero ($t(22) = 5.43$, $p < 0.0001$). A positive PSE indicates, in the flash-lag case, that the bars needed to be flashed further from fixation than the moving dot by 20ms (0.12 DVA) in order to be perceived as aligned with the dot (i.e., to offset the illusory lag of the flash). In the Fröhlich task, the bars needed to be 25ms (0.15 DVA) further from fixation than the onset of motion in order for the motion onset to be perceived as aligned with the bars (consistent with a misperception of the motion stimulus as being advanced along the motion trajectory). Under comparable conditions to those used here, similar magnitude illusions have been reported for

both the flash-lag and Fröhlich effect (Eagleman & Sejnowski, 2007). Additionally, Kanai et al. (2004) found flash-lag effects in the range of 20-60ms, with the flash-lag magnitude increasing with increasing eccentricity of the moving stimulus, decreasing eccentricity of the flashing stimulus, and increasing distance between the stimuli, among other factors. Contrast thresholds from the control task were Δ0.024 (±0.002), indicating that observers could discriminate, on average, a contrast difference between wedges of 2.4% with 75% accuracy.

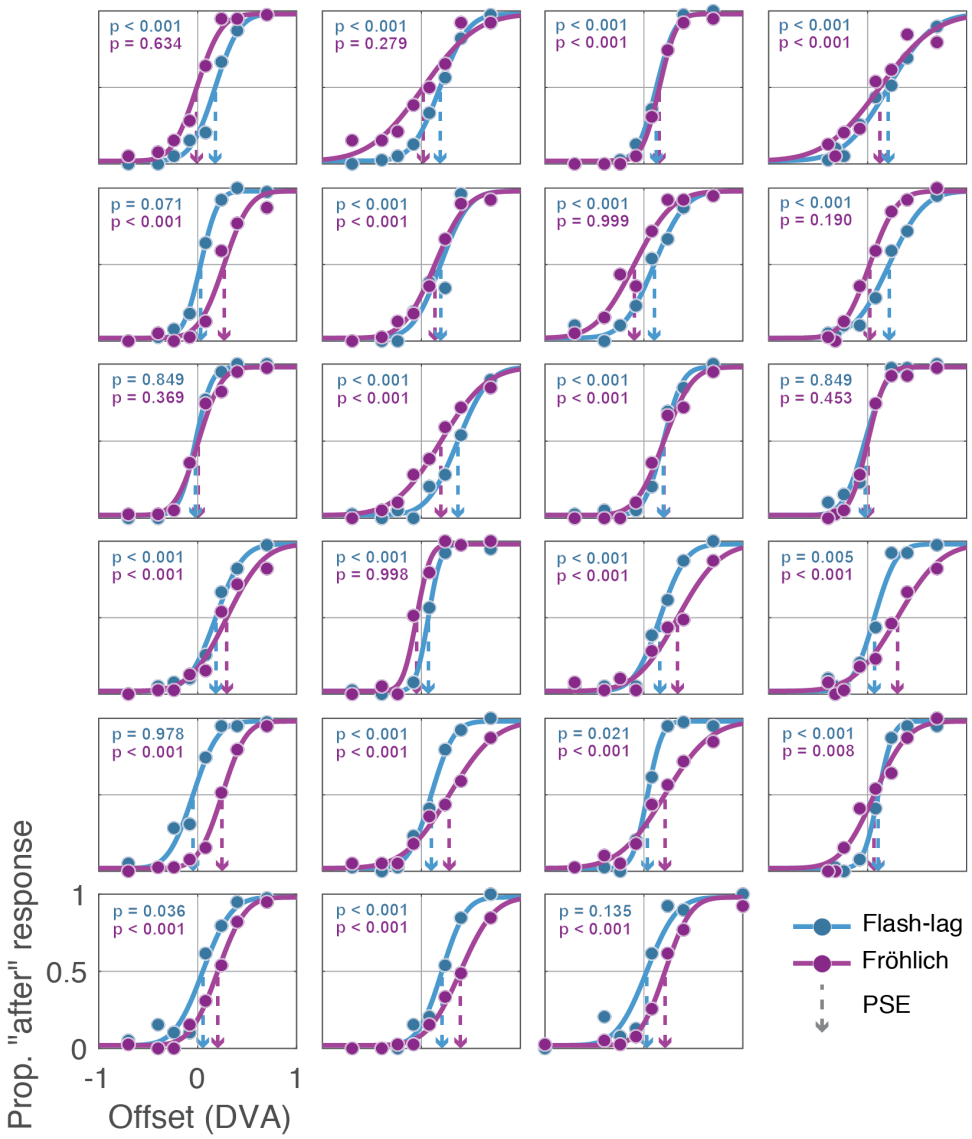

Figure 2: Subject data and psychometric function fits for the flash-lag and Fröhlich illusion tasks.

Individual subject data, shown in circles, and psychometric function fit lines for the two illusion tasks. Dashed lines denote the PSE for each subject. P-values inset in each panel show the result of a one-tailed bootstrap analysis determining if a positive PSE was present for each subject (i.e., if the illusion magnitude was significant).

We also checked whether participants showed significant illusory percepts at the single subject level using a bootstrap method. A bootstrap analysis was performed on each participant's data where the total number of trials were randomly selected, with replacement, from each participant's trials. This means a trial could have been left out or included multiple times in any given bootstrap sample. The bootstrap sampling procedure was performed 5,000 times to create a distribution of PSEs for each participant from their own data. Using these distributions, we calculated the proportion of bootstraps that had PSEs below zero, which would indicate the lack of an illusory percept. This was done to generate a p-value (one-tailed) for each participant for each illusion (Figure 2). A total of five and seven participants, for the flash-lag and Fröhlich illusions, respectively, did not have a significant illusory effect. These participants were not removed from the analysis, however, since all but two participants had a significant illusion effect in at least one of the illusions, and we are interested in the relationship (or lack thereof) between illusion PSEs in each subject.

We next directly compared the magnitudes of the two illusions as well as the split-half reliability of the PSE found for each illusion. The two illusions were of a comparable magnitude as they did not significantly differ from one another when assessed with a paired-samples t-test ($t(22) = 1.05$, $p=0.304$). To ensure reliability of our PSE measurement (an important prerequisite for detecting a correlation across subjects), we performed a split-half reliability analysis by fitting psychometric functions to all odd or even trials from each illusion and computing the Spearman-Brown split-half reliability to quantify the proportion of variance explained in PSE by random variation (Eisinga et al., 2013; Salkind, 2006). A repeated-measures t-test showed that the PSEs derived from each half of the data were not

significantly different for either illusion task (Flash-lag: $t(22) = 1.26$, $p = 0.22$; Fröhlich: $t(22) = -1.31$, $p = 0.20$) and a Spearman correlation showed the PSEs from each half of the data were strongly correlated for both illusions (Flash-lag: $r(22) = 0.82$, $p < 0.001$; Fröhlich: $r(22) = 0.91$, $p < 0.001$). Finally, both tasks show high reliability according to the Spearman-Brown split-half reliability score, for which the flash-lag PSE was 0.915 and the Fröhlich PSE was 0.967. This indicates that only about 8.5% and 3.2% of the variance in our quantification of the flash-lag and Fröhlich illusion PSEs, respectively, is due to random variation.

Regarding our main hypothesis, we next asked whether the magnitude of an individual's flash-lag illusion (flash-lag PSE), was predictive of the magnitude of their Fröhlich illusion (Fröhlich PSE). A relationship between the flash-lag illusion PSEs and the Fröhlich illusion PSEs would be expected if the two illusions result from each individual's unique underlying oscillatory sampling frequency. However, the across-task correlation in PSEs was virtually zero ($rho(22) = -0.001$, $p = 0.97$, 95% bootstrap CI = [-0.41, 0.39], indicating no evidence for a relationship between these illusions (Figure 3A). To appreciate the uncertainty associated with each correlation value, we conducted a bootstrap analysis that randomly sampled with replacement 23 PSEs from the pool of all participant data, meaning that the same participant may be represented multiple times in a sample. This was done 50,000 times to generate a distribution of samples. For each bootstrap sample, we correlated PSEs across tasks in order to also generate a distribution of correlations (Figure 3, right column), representing the uncertainty associated with the correlation between tasks. As evident from the bootstrap distributions presented in Figure 3A, the true correlation could plausibly span a wide range between ±0.4, though the mean of this bootstrap distribution is virtually zero (-0.006).

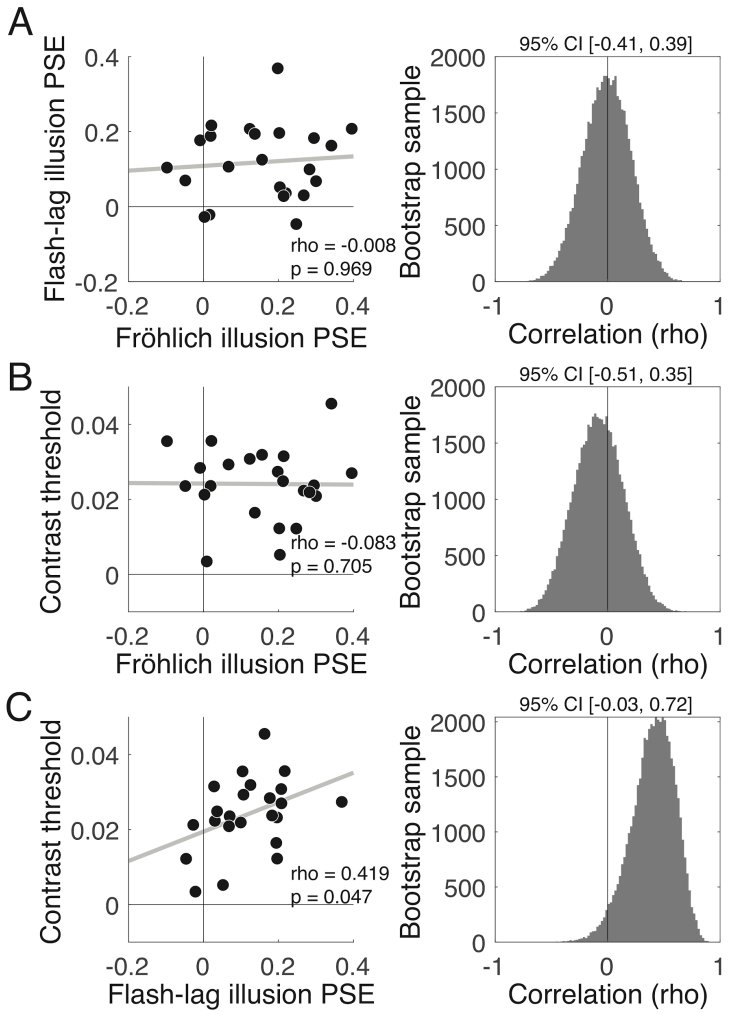

Figure 3: Across task correlations between psychometric thresholds for the flash-lag, Fröhlich, and control task pairs.

A) Correlation (left) and bootstrap analyses (right) revealed virtually zero correlation between the flash-lag and Fröhlich illusion PSE. This indicates that the magnitude of one illusion is not predictive of the magnitude of the other. B) No correlation was found between Fröhlich PSE and contrast thresholds. C) An unexpected medium-sized positive correlation was observed between flash-lag PSE and contrast threshold, indicating that an individual capable of discriminating a small change in contrast has a smaller magnitude flash-lag effect. We speculate that this may be due to the very brief flash used in our display (8ms), accurate perception of which may be aided by a lower contrast threshold. Lines of best fit are shown in grey and Spearman rho values with 95% bootstrap CI are provided.

A Bayesian analysis (Dienes, 2014) that quantified the likelihood of the data belonging to the null hypothesis (H0) of no correlation versus the alternative hypothesis (H1) of a positive correlation (a weak version of the theory), indicated that the data are 5.56 times

more likely to have been generated under the null ($BF_{U(0, 0.9),0} = 0.179$). Using a hard version of the theory to model H1, according to which the two PSEs are equal, resulted in a $BF_{HN(0, 0.5),0} = 0.419$, indicating that the null is 2.38 times more likely than the alternative. Thus, depending on the exact implementation of the theory, the data are approximately 2 to 5 times more likely under the null.

Next, we tested for associations between contrast discrimination thresholds and PSEs in each illusion task. As shown in Figure 3C, contrast thresholds were positively correlated with flash-lag PSEs (*rho*(22) = 0.42, *p* = 0.04, 95% bootstrap CI = [-0.03, 0.72]), indicating that individuals capable of discriminating smaller differences in contrast had smaller flash-lag illusions. (We speculate on the reason behind this correlation in the discussion.) No correlation was observed between contrast thresholds and the Fröhlich PSE (*rho*(22) = -0.08, *p* = 0.71, 95% bootstrap CI = [-0.51, 0.35]). Because contrast thresholds unexpectedly explained variance in the flash-lag effect, we sought to test if an effect of Fröhlich PSE on flash-lag PSE emerged when controlling for the influence of contrast discrimination. However, a multiple regression model that predicted individual differences in the flash-lag PSE using the Fröhlich PSE and contrast thresholds (as a covariate) did not reveal an association between the two illusions (β = 0.07, SE = 0.15, *t*(22) = 0.45, *p* = 0.66), consistent with the results from the main correlation analysis.

For completeness, we also analyzed correlations between the slope of the psychometric functions from each task. Whereas the PSE in the illusion tasks capture the magnitude of each illusion (and is therefore the quantity of interest for the theory under consideration), the slope of the psychometric function reflects the general reliability or sensitivity of an individual's perceptual system as it captures the degree to which changes in the stimulus value translate to changes in behavior. We found a medium sized positive

correlation between the flash-lag and Fröhlich slopes ($rho(22) = 0.41$, $p = 0.05$), indicating that an individual who is more sensitive to changes in offset in the flash-lag illusion is also more sensitive to changes in offset in the Fröhlich illusion. It is possible the correlation between slopes could be due to a shared mechanism underlying the sensitivity of illusory percepts, such as rhythmic sampling.

Discussion

This study assessed the theory that the same mechanism of discrete perceptual sampling - oscillations at a given frequency - could explain the flash-lag and Fröhlich illusions. We induced illusory percepts in both the flash-lag and Fröhlich displays, yet the correlation between illusion sizes was virtually zero. A Bayesian analysis allowed us to determine the likelihood of our data being obtained from the hypothesized distribution according to alpha-based sampling theory. The BF indicated that responses to the flash-lag and Fröhlich illusion tasks were between 2.4-5.5 times more likely to come from the null distribution than various theory-derived alternatives. While additional research using EEG or MEG is needed to further support these conclusions, our current data suggest it is unlikely that a single oscillator, assumed to vary in frequency across subjects, is underlying individual variations in the flash-lag and Fröhlich effects, as this should drive a correlation between illusory percepts across tasks.

Although we observed moderate evidence for a null effect, there are several underlying reasons for obtaining null results. It could still be that discrete sampling theory is true and is neurally instantiated via oscillations, but that these two illusions rely on different frequencies which are themselves uncorrelated. A large body of work has linked alpha-band oscillations to temporal windows of processing (Cecere et al., 2015; Coffin & Ganz, 1977; Cooke et al., 2019; Grabot et al., 2017; Gray & Emmanouil, 2020; Kristofferson, 1967b;

Minami & Amano, 2017; Samaha & Postle, 2015; Shen et al., 2019; Valera et al., 1981; Wutz et al., 2018) and even specifically to the flash-lag illusion (Chakravarthi & VanRullen, 2012; Chota & VanRullen, 2019). On the other hand, lower-frequency oscillations in the theta range are also often implicated in establishing temporal windows of perception (Nakayama et al., 2018; Wutz et al., 2016; for review see VanRullen, 2016). Indeed, even different tasks within the same subjects can reveal different frequencies related to the temporal parsing of visual stimuli (Ronconi et al., 2017), indicating that multiple and task-dependent rhythms may underlie the perceptual moment. Consistent with these variations in temporal parsing of visual stimuli is the problem of "multiple temporal resolutions", as outlined by Herzog et al. (2020). Different perceptual phenomena attributed to discrete sampling have been explained by appealing to window sizes ranging from 3ms up to 450ms depending on the processing demands elicited from the particular visual features (Drissi-Daoudi et al., 2019; Holcombe, 2009). One possibility is that differential top-down attentional control is allocated during perception of the different tasks/stimuli, resulting in variations in duration of temporal integration windows. Our results are compatible with a model according to which the flash-lag and Fröhlich effect are driven by discrete sampling but at different frequencies or temporal sampling rates. However, on this theory, our finding that the two illusions were of very similar magnitude (Figure 1) may still require further explanation, as different neural frequencies or sampling rates underlying the two different illusions would likely result in different magnitudes of illusions even at the group level.

A second possible interpretation of our null effect is that these illusions do not rely on discrete sampling at all, contra Schneider (2018). Other viable accounts of the flash-lag and Fröhlich effects have been put forth and recently defended. Regarding the flash-lag, a recent review argues that motion extrapolation is currently the best account (Hogendoorn, 2020).

Motion extrapolation refers to the prediction of a moving object's trajectory based on its recent past. This is distinct from discrete sampling (or the related post-diction account of the flash-lag) in that the motion percept is not reconstructed after the fact, but is instead based on a prediction about where the stimulus will be. Motion extrapolation mechanisms have been observed as early as the retina (in some species) and could therefore begin very early after motion onset to produce a percept of the motion stimulus that is advanced with respect to a stationary flash (Hogendoorn, 2020). Regarding the Fröhlich effect, it has been argued that metacontrast masking plays a crucial role (Kerzel, 2010). In metacontrast masking, the mask and target do not overlap and stimulus onset asynchronies between 40-100ms between target presentation and mask presentation create strongest masking effects (Kerzel, 2010). It has been proposed that metacontrast masking suppresses the initial trajectory of the moving stimulus, thus creating the illusion that it begins farther ahead than its true starting location (Piéron, 1935). Because the moving dot is already along its trajectory when the flash appears in the flash-lag effect, this masking effect of the beginning trajectory would not affect perception in the flash-lag illusion. Thus, it remains an open possibility that these two illusions are based on different mechanisms, either one of which may not be discrete sampling.

A third possibility is that our stimulus design was suboptimal for detecting a true relationship. For instance, an unexpected correlation was found between PSEs in the flash-lag illusion and the contrast discrimination task. The control task was primarily administered to rule out the possibility that any observed correlation between the two illusion PSEs was a trivial reflection of any two tasks being correlated across individuals. Although this point is moot since no correlation was observed between the two illusion tasks, we speculate that the observed correlation between contrast thresholds and the flash-lag PSE might have occurred

since the flash in our flash-lag display was very brief (8ms) and perhaps having a lower contrast threshold could translate to more veridical flash localization and a smaller flash-lag effect. A longer flash should reduce variance in flash-lag estimates due to individual differences in contrast perception. However, a multiple regression model of our data that included contrast discrimination thresholds as a covariate still failed to find any relationship between the two illusions. Future studies should consider increasing the flash duration to facilitate perception of the flash, while also keeping in mind how the speed and proximity of the moving dot may interact with a longer flash and impact illusory effects. An additional stimulus consideration that may affect both the flash-lag and the Fröhlich effect is the interaction of each illusion with low-level motion processing. The flash-drag effect suggests that moving stimuli may distort the surrounding visual space and, thus, would affect perception of any nearby stationary stimuli (Whitney & Cavanagh, 2000). Moving the bars farther away from the horizontal trajectory of the dot in both illusion tasks could help to mitigate any distortion caused by low-level motion processing.

Lastly, a lack of variation in individual sampling rates or illusion magnitudes could also produce no correlation between PSEs. That is, no correlation would be expected if for every subject the true magnitude of each illusion were the same and variability in PSEs were due solely to response bias or some other factor. However, this account would also violate the hypothesis that individual differences in peak alpha frequency are modulating individual differences in visual sampling rates, since the distribution of peak oscillation frequencies in a random sample of the population is known to vary (Grandy et al., 2013; Haegens et al., 2014), and the same should be expected of our sample. Additionally, the split-half reliabilities of our PSE estimates were each very large (>0.9), making it unlikely that random variation in PSE estimation was masking any true cross-task correlation.

Although it can be difficult to know the source of a null effect, even if evidence in support of the null can be shown (as with our Bayesian analysis), our data can inform future studies. The task parameters used in this study produced the expected illusory effects of the flash-lag and Fröhlich illusions on average (though not significantly for several subjects) and such parameters could be used to test other perceptual phenomena or mechanisms related to discrete sampling theory. Alternatively, adjusting these task parameters or comparing the PSE across additional tasks could provide further insight into how individuals sample visual information, or more specifically, what stimulus designs might better capture the hypothesized "perceptual moments". Although our current data do not support the hypothesis that individual differences in perceptual moments are driving these two visual illusions, these findings are not sufficient to rule out discrete sampling theory altogether. They are also not sufficient to rule out the role of alpha oscillations or other frequencies in perceptual sampling in the two illusions in different ways. However, it should be noted that the correlation between psychometric function slopes lends more support to the rhythmic sampling theory, which suggests that alpha oscillations modulate the strength of percepts and may explain why some participants show more sensitivity or seemingly have more precision in their perceptual experience of both illusions. Future studies would benefit from measuring oscillatory activity during both tasks to further explore the underlying perceptual mechanisms.

CHAPTER 3: Individual Alpha Frequency Appears Unrelated to the Timing of Early Visual Responses

Published in Frontiers in Neuroscience as Morrow, Dou, and Samaha (2023)

Brain dynamics in the alpha-band (7-14 Hz) have been shown to predict various aspects of visual perception, such as the probability of target detection as well as temporal properties of perception. Although there is much evidence to support the involvement of alpha *power* in the suppression of neural activity and perceptual reports (reviewed in Samaha et al., 2020) as well as growing evidence regarding the relevance of alpha phase (VanRullen, 2016), it is less clear how alpha frequency may be involved in shaping visual information processing. Two theories have been proposed for how alpha-band frequency dynamics may relate to variations in visual perception: the rhythmic perception account and the discrete perception account (VanRullen, 2016). The rhythmic perception account proposes that alpha oscillations reflect phasic changes in neuronal excitability which principally modulate the intensity of perception and/or sensory responses. On the other hand, the discrete perception account suggests that alpha oscillations are involved in the timing and discretization of sensory events. According to these accounts, an individual's alpha frequency would either be related to the frequency and duration of excitability changes (rhythmic perception) or the discretization rate of perception (discrete perception). As recent reviews (Kasten & Herrmann, 2022; Menétrey et al., 2022) and experiments (Morrow & Samaha, 2022) have pointed out, current evidence does not clearly support one account over the other.

Studies have demonstrated a relationship between an individual's peak alpha frequency (IAF) and temporal properties of their perception but have not necessarily disentangled rhythmic from discrete perception. For example, several studies have linked variation in IAF to the temporal resolution of visual (Baumgarten et al., 2018; Coffin & Ganz, 1977; Gray & Emmanouil, 2020; Samaha & Postle, 2015) and multisensory perception

(Cecere et al., 2015; Cooke et al., 2019; Migliorati et al., 2020; Noguchi, 2022; but see Buergers & Noppeney, 2022), typically finding that higher alpha frequencies correspond to shorter windows of integration. These experiments, however, do not rule out intensity-based accounts whereby IAF is related to the duration of the period of excitation and inhibition. For instance, according to the rhythmic perception account, one of the stimuli in each trial (or the gap between stimuli) may be more likely to be missed (rather than integrated) due to a longer integration window (Fan, 2018). This account would be consistent with a growing body of literature demonstrating that alpha-band phase modulates perceptual detection (Ai & Ro, 2014; Alexander et al., 2020; Busch et al., 2009; Dugué et al., 2011; Mathewson et al., 2009; Samaha et al., 2015, 2017) and neuronal responses (Dou et al., 2022; Dougherty et al., 2017; Haegens et al., 2011; Spaak et al., 2014).

Here, we sought neural evidence for the hypothesis that IAF modulates the timing of sensory processes, which would be consistent with the discrete perception account. Specifically, we examined whether individual differences in alpha frequency predict the timing of early visual responses with a focus on the striate and extrastriate visual evoked potentials. We examined data from two studies that used high-contrast checkerboard stimuli, which are known to elicit large C1 event-related potential (ERP) responses. We extracted IAF from a prestimulus window in order to assess whether the frequency of prestimulus alpha-band activity modulates the onset and peak latency of early visual-evoked potentials. If alpha frequency is related to the discretization of visual perception, then we might expect higher frequencies to be associated with earlier onset sensory responses (i.e., quicker perceptual updates).

Method

Task-Irrelevant Viewing Paradigm

Two electroencephalogram (EEG) datasets were analyzed in this study due to the comparable stimuli used across the two experimental designs. The first dataset comes from a study conducted by Iemi et al. (2019) and is available for download at https://osf.io/yn6gb/. The data were collected from 27 participants (M_{age} = 26.33, *SEM* = 0.616; 14 female) with normal or corrected vision, although three participants' data were excluded from the analysis because they either did not finish the experiment or did not exhibit the C1 component in the lower visual field (LVF). In the original experiment, a pair of task-irrelevant, full-contrast checkerboard wedges were presented for 100ms in either the upper (UVF) or LVF (Figure 4). These wedges were designed with spatial frequency, location, and size characteristics that should activate the primary visual cortex in both hemispheres and produce a constructive summation of electrical fields, resulting in robust C1 responses (Figure 5). Participants were presented with an arrow at fixation indicating leftward or rightward direction while the task-irrelevant checkerboard stimuli were presented in UVF or LVF with equal probability. Participants were tasked with reporting the direction of the central arrow using the "<" or ">" key for left or right, respectively, while ignoring the checkerboards. Experimental blocks were 90 trials each with 60 stimulus-present trials and 30 stimulus-absent trials randomly distributed. Participants completed 9 blocks, totaling 810 trials. This dataset was collected from 64 channels arranged according to the International 10-10 system using a BioSemi ActiveTwo system with a 1024 Hz sampling rate. All channels were referenced online to the CMS-DRL ground electrodes. More detail of experimental procedures can be found in the original study (Iemi et al., 2019).

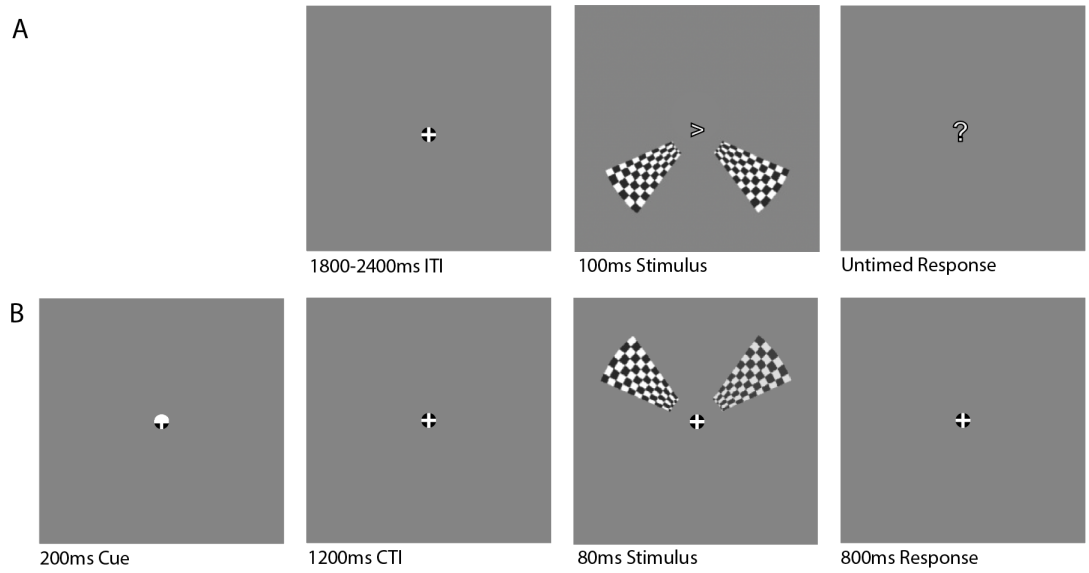

Figure 4: Stimulus Design for the task-irrelevant viewing and covert attention paradigms.

Data sets were analyzed from two different experimental designs that both presented large checkerboard wedge stimuli to either the upper or lower visual field to evoke a large C1 component response. A) In the task-irrelevant viewing paradigm, a fixation was presented for a variable inter-trial interval (ITI) and then two full contrast checkerboard wedges were presented for 100ms to either the upper or lower (pictured) visual field. A question mark then appeared to signal to the participant to push a button with their dominant hand to indicate which direction a fixation arrow had pointed during the stimulus presentation. B) In the spatial attention task, a cue highlighted either the upper or lower half of the fixation for 200ms and indicated to participants to covertly shift their attention to the upper or lower visual field. After a 1200ms cue-target interval (CTI), the same two checkerboard wedges were presented for 80ms, except the right wedge varied in contrast between 60-100% while the left wedge was held at 80% contrast. Participants were then asked to indicate which wedge had a greater level of contrast via button press ("<" or ">" for left or right, respectively).

Covert-Attention Paradigm

The second dataset comes from a cued spatial attention experiment that was conducted in our lab which has not yet been published. This study was approved by the Institutional Review Board of University of California Santa Cruz (UCSC). Twenty-one participants from the UCSC community completed the experiment (M_{age} = 22; *SEM* = 0.941; 15 female, 4 male, 1 non-binary, and 1 undisclosed). Three participants were excluded from the analysis for either poor task accuracy (1 participant) or the lack of a clear C1 ERP

response (2 participants). All participants had normal or corrected-to-normal vision and were compensated with course credit and a $20 gift card. Data and task scripts can be found at https://osf.io/5egkp/.

This cued attention experiment used an adapted version of the checkerboard stimuli for a covert-attention cued contrast discrimination task. This task also presented the two checkerboard wedges to either the upper or lower visual field, but participants were instructed to attend to the cued visual field and report which wedge had a greater contrast. The right wedge was fixed at 80% contrast while the left wedge varied between 60-100% contrast. On each trial, a fixation consisting of a white cross centered within a black circle of 0.5 degrees of visual angle (DVA) on a 50% gray background was present on the screen for the duration of the experiment. The top or bottom of the fixation circle turned white for 200ms to indicate for participants to shift their attention to the cued visual field. After a cue-target interval of 1200ms, the two bilateral checkerboard wedges were presented to either the upper or lower visual field. The stimulus code was copied from Iemi et al. (2019) and consisted of wedge segments taken from a radial checkerboard pattern with 15 circles and 68 radial lines, with the first, inner circle beginning 3 DVA from central fixation and the final, outer circle ending 10 DVA from central fixation. The wedges were presented for 80ms, and participants had 800ms to respond with "<" or ">" button press according to whether they perceived the left or right wedge to have a great amount of contrast, respectively. The right edge was always presented at 80% contrast and the left wedge varied in contrast such that it was randomly presented at either 60%, 100% or one of eight linearly-spaced contrast levels between 74% and 86% contrast. Participants completed 10 blocks of 100 trials each, within which the cue was valid 80% of the time. This second dataset was recorded from 64 electrodes corresponding to the International 10–10 system using an actiCHamp EEG system with a

1000 Hz sampling rate. All channels were referenced online to channel Cz. The stimulus presentation was controlled by Psychtoolbox 3 (Kleiner, 2007; Pelli, 1997) running in the MATLAB environment on an Ubuntu operating system.

EEG Preprocessing

Raw data from both datasets were preprocessed in the same way using custom Matlab scripts in conjunction with EEGLAB toolbox functions (Delorme & Makeig, 2004). Datasets were high-pass filtered at 0.1 Hz and low-pass filtered at 40 Hz using a zero-phase Hamming-windowed sinc FIR filter, downsampled to 500Hz, and epoched to include trial data from 2s before through 2s after stimulus onset. The data were manually inspected to remove trials and channels with artifacts such as muscle movement or eye blinks that overlapped with stimulus presentation. Noisy channels were interpolated and an independent components analysis using the INFOMAX algorithm (EEGLAB function binica.m) was used to remove ocular artifacts. For the task-irrelevant viewing dataset, an average of .58 electrodes were interpolated using spherical spline interpolation and an average of 30.46 trials were rejected for each participant. For the covert attention dataset an average of 3.4 electrodes were interpolated using spherical spline interpolation and an average of 164.6 trials were rejected for each participant. Data were then re-referenced to the average of all channels and baseline corrected using a 200ms prestimulus baseline window.

Analysis

The goal of our study was to extract the IAF for each subject along with the timing of their early sensory responses (with a focus on the C1 component). To this end, we first identified the electrode for each subject that had the largest C1 amplitudes for upper and lower visual fields. For 73% of subjects, POz was the best C1 electrode, 9% had PO4, 7% had PO3, 7% Pz, 2% P1, and 2% Oz. These electrodes were used for all subsequent analyses.

Individual Alpha Frequency Computation (IAF)

IAF was computed from data from a 500ms prestimulus window. Each trial was zero-padded (frequency resolution 0.15 Hz), tapered with a Hamming window, and linearly detrended before performing an FFT (Samaha & Postle, 2015). Single-trial power estimates were log10 transformed and IAF was computed as the local maximum in the trial-averaged spectrum within a frequency range from 7 to 14 Hz (Figure 5).

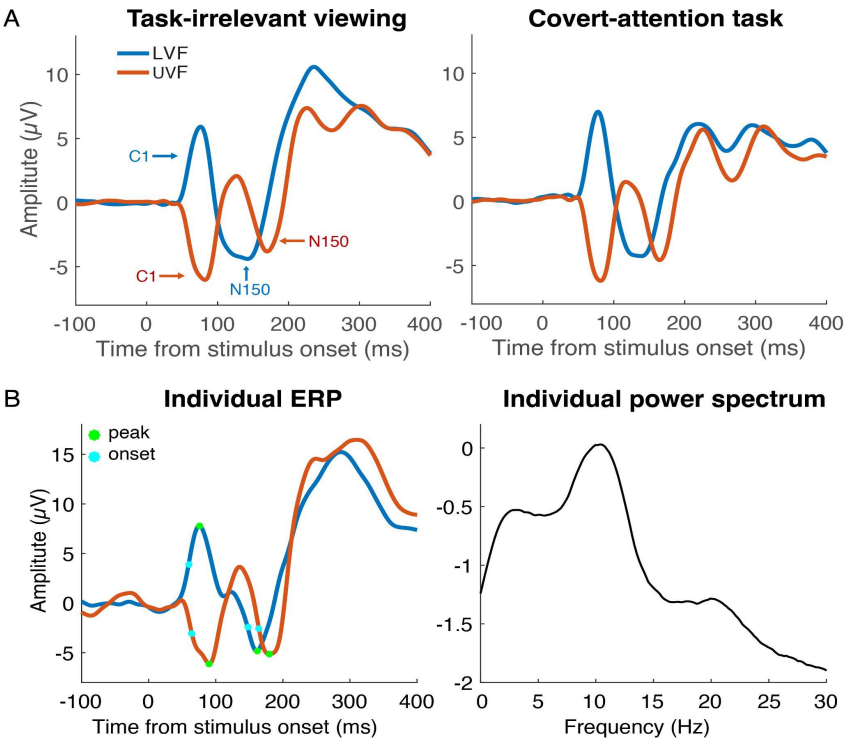

Figure 5: The C1 and N150 Event-Related Potentials (ERPs) and an individual power spectrum.

A) Average ERPs of LVF (blue line) and UVF (red line) stimuli in the task-irrelevant viewing dataset (left) and the covert-attention task (right). ERPs were recorded from the individual electrode with the largest C1 component. The C1 peaked around 90ms and the N150 peaked within the time window of 100ms to 200ms. B) Average ERPs (left) of one individual participant with points showing the onset time (light blue dots) and peak time (green dots) of the C1 and N150 components. The same participant's power spectrum from prestimulus data is shown in the right panel. Peak frequency was defined as the frequency with largest amplitude in the range form 7-14 Hz.

ERP Latency Measures

We used two different approaches to compute the latency of the early sensory responses (the C1 component and the subsequent N150 component). First, we identified the peak latency of the C1 and N150. C1 peaks were identified by recording the timing of the local maximum (LVF stimulus) or minimum (UVF stimulus) ERP voltage in a 40-96ms window after stimulus onset. Due to the large C1 peaks overlapping and influencing the later N150 component, a different window was used for the UVF and LVF N150 peaks. N150 peaks in the LVF were identified from within a 96-230ms window, and N150 peaks in the UVF from within a 120-230ms window. Because the peak latency is an arbitrary waveform feature and possibly contaminated with noise, we additionally computed the *onset latency* of each component, measured as the 50% fractional latency (Luck, 2005). Onset latency was computed as the timepoint at which each ERP reached 50% of its peak amplitude value relative to 0μV. For analyses involving the N150 onset measures, two participants were left out from the attention task and four participants were left out from the task-irrelevant viewing dataset due to positive N150 peak amplitudes. Lastly, we also computed difference scores between the C1 and N150 component latencies to derive a measure of the relative timing between ERP components. Specifically, we subtracted C1 peak latencies from N150 peak latencies and C1 onset latencies from N150 onset latencies separately for UVF and LVF. These difference scores were used to capture the possibility that IAF was related not to the absolute latency of the responses but to the relative latency with which the responses were generated in the visual system. Thus, we derived a total of 12 latency metrics: C1 peak and onset, N150 peak and onset, and C1-N150 peak and onset difference, each for upper and lower visual field stimuli.

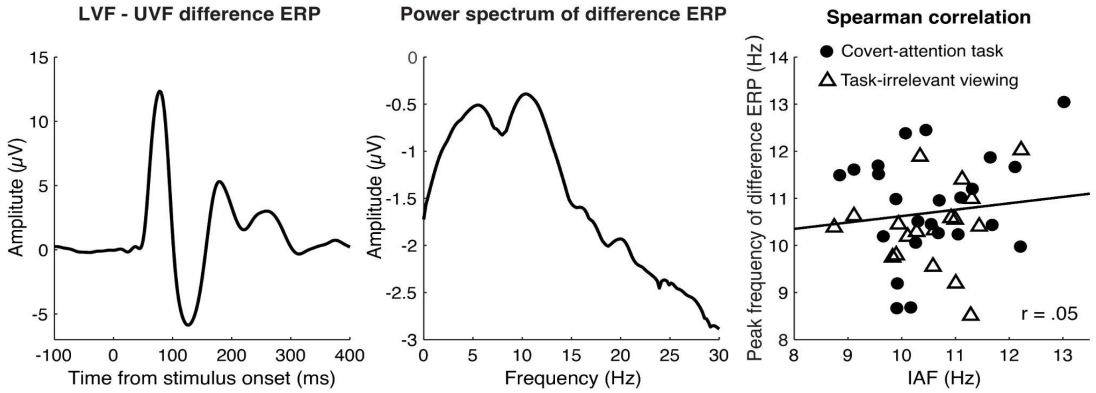

Figure 6: Peak frequency of the difference ERP for the combined tasks and the correlation between task-irrelevant viewing and covert attention paradigm peak frequencies.

The left panel shows the grand average difference ERP (LVF-UVF), which captures spatially-specific activity and boosts the signal-to-noise ratio in our data. The middle panel shows the grand averaged power spectrum of the difference ERP within the post-stimulus time window of 0ms to 500ms, revealing a clear alpha peak. The right panel illustrates the relationship between peak frequency of difference ERP (computed between 7 and 14 Hz) and IAF. Dots represent individual participants from the task-irrelevant viewing dataset and triangles represent participants from the covert attention task. The black lines represent the least-squares fit. A Spearman correlation showed no significant relationship between these two peak frequencies for the aggregated data nor when each task was analyzed separately.

Peak Frequency of the ERP

Because the detection of ERP components uses some arbitrary waveform features (e.g., peak, or 50% latency) and because the N150 component was difficult to identify clearly for all subjects and visual field locations (see Results), we supplemented our main analysis with the following more agnostic, data driven approach. Based on the fact that the difference between the UVF and LVF stimuli reflect spatially specific responses, we computed the LVF minus UVF difference ERP. This has the added benefit of increasing the signal-to-noise (since the first few deflections in the ERPs have opposing polarities) and also has spectral energy with a peak in the alpha-range (see Figure 6). Thus, we also computed the peaks from the FFT of the difference ERP (0-500ms post-stimulus) as a more general measure of spatially-specific neural response latencies, as higher frequency ERPs correspond to smaller delays between peaks. We searched for peaks between 7 and 14 Hz at the best C1 electrode,

in keeping with all prior analyses. This approach also has the benefit of summarizing the frequency of an individual's visual ERP in a single metric (since it collapses across visual fields, and we do not need to hand-pick different components and time windows).

Statistical Analysis

Our primary analysis involved correlating IAF with each measure of component latency using Spearman correlations and data pooled across both studies. We supplemented this analysis with separate Spearman correlations run each task separately. We additionally checked for correlations of latency metrics between upper and lower visual fields as an internal consistency check. Lastly, we compared C1, N150, and the differences in latency metrics (N150 - C1) across the two tasks using independent-samples t-tests to assess any differences in component timing between the two datasets.

Results

As shown in Figure 5, despite being collected in different labs and with different monitors, stimulus timing, and EEG systems, the ERPs were highly similar. In order to assess any differences in component timings across the two datasets, we ran an independent-samples t-test comparing the various components of interest across the two tasks. Regarding the C1 component, we found no significant task difference for the UVF C1 peak latencies ($t(40) = -1.05$, $p = .30$), but we did find a significant task difference for the LVF C1 peak latencies ($t(40) = -2.12$, $p = .04$). An opposite pattern was seen for C1 onset latency such that there *was* a significant task difference for UVF C1 onset latencies ($t(40) = -3.16$, $p < .01$) but there was *not* a significant task difference for LVF C1 onset latencies ($t(40) = -1.88$, $p = .07$). This indicates that C1 onset latencies tended to be earlier for the attention task, although this was not replicated across visual fields or latency metrics (e.g., onset versus peak). Regarding N150 latencies, there was a significant task difference in UVF N150 peak latencies ($t(40) =$

2.74, $p < .01$), but no significant task difference in UVF N150 onset latencies ($t(34) = 1.72$, $p = .09$). We found no significant differences for either LVF N150 latency measure across tasks (peak: $t(40) = -0.94$, $p = .36$; onset: $t(34) = -0.99$, $p = .33$). This indicates that the attention task was associated with earlier onset N150, although only for the UVF and for one latency metric. Regarding the difference in ERP component latencies (N150-C1) across tasks, results showed a significant task difference for the UVF (peak: $t(40) = 3.33$, $p < .01$; onset: $t(34) = 2.80$, $p < .01$), but not in the LVF (peak: $t(40) = -0.32$, $p = .75$; onset: $t(34) = -0.60$, $p = .55$). Again, these task differences were confined to the UVF. Finally, there was no significant difference in peak alpha frequencies between the two datasets ($t(40) = 0.08$, $p = 0.94$).

We speculate that any differences in ERP component timing across the experiments could be due to the different recording environments and equipment. Specifically, the task-irrelevant viewing paradigm used a CRT monitor which tends to have lower absolute luminance outputs which would affect the absolute contrast of the stimuli. Because our focus is on the C1 component, which is generally not very sensitive to task differences, and because any overall difference in component timing should not preclude observing an effect of individual differences, we aggregated data across the two studies for our main analysis. However, we also report correlations for each task separately to assess any task-related differences.

As a sanity check before our main analysis, we examined correlations between the UVF and LVF ERP component timings across subjects, as we would expect the timing of these events to be related. We combined datasets for this analysis, given that we were comparing across subjects. Indeed, the UVF and LVF C1 peak and onset latencies were significantly correlated across visual fields (peak: $r(40) = .39$, $p = .01$; onset: $r(40) = .36$, $p = .02$). There was no significant correlation for the UVF or LVF N150 peak or onset latencies

(peak: $r(40) = .21$, $p = .18$; onset: $r(34) = .29$ $p = .09$), although the relationships were both positive. We expect more variation in the latency of N150 measures as they are affected differently by the overlap of the polarity-reversing C1 responses for UVF and LVF. As a result, we also see no significant relationship between C1 and N150 peak and onset latency differences (peak: $r(40) = .15$, $p = .35$; onset: $r(34) = .18$, $p = .29$). This result confirms that the C1 shows reasonable within-subject consistency in timing across the two visual field locations.

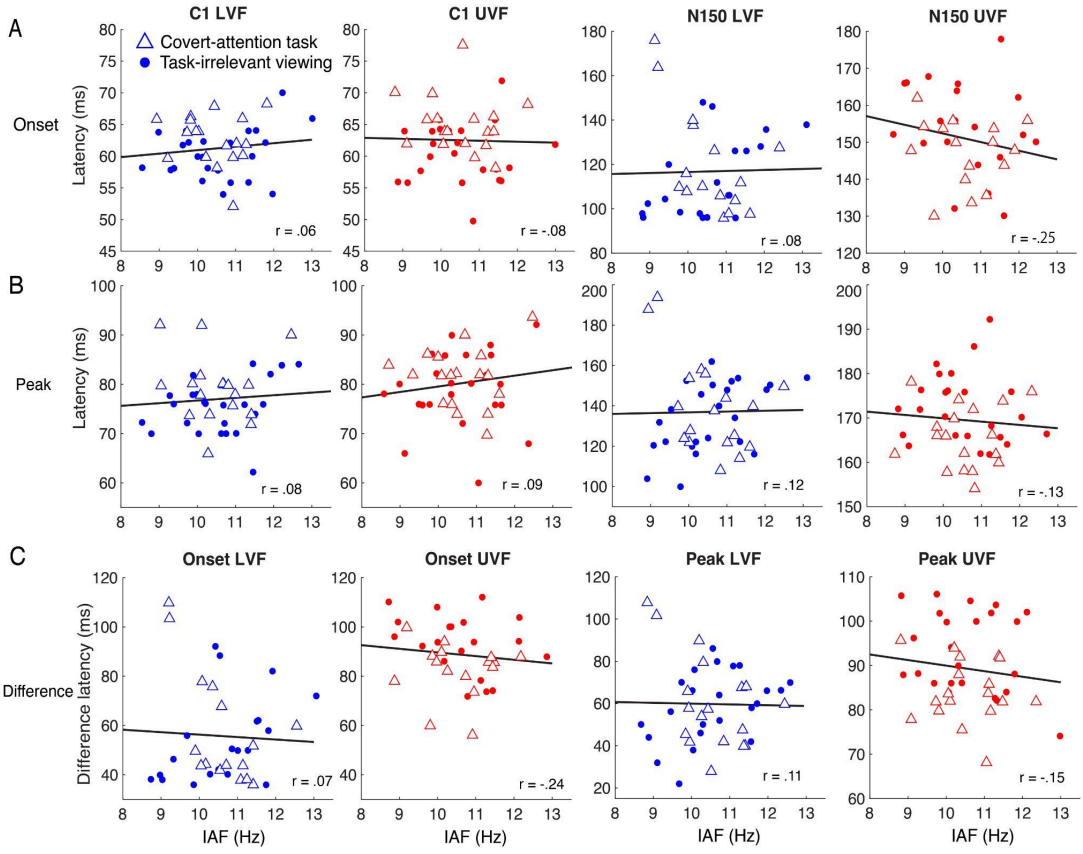

Figure 7: Relationships between IAF and the latencies of ERP components.

The LVF (blue shapes) and UVF (red shapes) stimulus correlations between peak, onset, and difference latencies. Dots represent individual participants from the task-irrelevant viewing dataset and triangles represent participants from the covert attention task. The black lines represent the least-squares fit describing how the onset and peak latencies of C1 and N150 change as IAF changes. A) There were no significant Spearman correlations between IAF

and C1 onset latency (left two columns) and N150 onset latency (right two columns). B) There were no significant Spearman correlations between IAF and C1 peak latency (left two columns) and N150 peak latency (right two columns). C) No significant Spearman correlations were found between IAF and the difference in onset latency (left two columns) and peak latency (right two columns).

Our main analysis evaluated the relationship between IAF and C1 latency measures pooling data across tasks (Figure 7). We found no significant correlation between IAF and C1 peak latency for either visual field (UVF: $r(40) = .09$, $p = .59$; LVF: $r(40) = .08$, $p = .61$) or C1 onset latency for either visual field (UVF: $r(40) = -.08$, $p = .62$; LVF: $r(40) = .06$, $p = .69$). Additionally, there was no significant correlation between N150 peak latency and IAF for either visual field (UVF: $r(40) = -.13$, $p = .41$; LVF: $r(40) = .12$, $p = .45$), or between N150 onset latency and IAF (UVF: $r(34) = -.25$, $p = .15$; LVF: $r(34) = .10$, $p = .51$). Similarly, there was no significant correlation between the differences in peak latencies and IAF for either visual field (UVF: $r(40) = -.25$, $p = .15$; LVF: $r(40) = .08$, $p = .65$), or the differences in onset latencies and IAF (UVF: $r(34) = -.24.$, $p = .16$; LVF: $r(34) = .07$, $p = .68$).

To determine whether participants within each task showed any different effects, we also report correlations separated by task. For the task-irrelevant viewing paradigm, there were no significant correlations between IAF and any of the ERP components or the latency differences between components in the UVF (Table 1). Additionally, there were no significant correlations between C1 peak latency or C1 onset latency for the LVF (Table 1), but there were significant positive correlations between IAF and N150 peak latency ($r(22) = .52$, $p < .01$), and N150 onset latency ($r(18) = .47$, $p = .04$), and subsequently, the difference in peak and onset latencies between the components in the LVF (peak: $r(22) = .43$, $p = .03$; onset: $r(18) = .50$, $p = .02$). For the covert-attention task paradigm, there were also no significant correlations between IAF and any of the ERP components or the latency

differences between components in the UVF (Table 1), although a negative correlation between IAF and the C1 peak latency was marginally significant ($r(16) = -.45$, $p = .06$). For the LVF, no significant correlation was found between IAF and either C1 components, the N150 peak latency, or the difference in latency between component peaks (Table 1). There was a significant negative correlation between IAF and N150 onset latency for the LVF stimuli ($r(16) = -.53$, $p = .03$) as well as between IAF and the difference in latency between component onsets ($r(14) = -.53$, $p = .04$).

	Task-irrelevant viewing				Covert-attention task			
	Upper Visual Field		Lower Visual Field		Upper Visual Field		Lower Visual Field	
	r	*p*	*r*	*p*	*r*	*p*	*r*	*p*
C1 peak latency	.15	.47	.27	.19	-.44	.06	-.25	.31
C1 onset latency	-.02	.92	.08	.73	-.38	.12	-.10	.69
N150 peak latency	-.16	.46	.52	.009*	-.03	.90	-.41	.09
N150 onset latency	-.33	.15	.47	.04*	-.11	.69	-.53	.03*
Peak latency difference	-.17	.43	.43	.03*	-.25	.32	-.37	.13
Onset latency difference	-.30	.20	.50	.02*	.05	.87	-.53	.04*

Table 1: Correlations between Individual Alpha Frequency (IAF) and sensory ERP peak and onset latencies.

IAF was correlated with C1 and N150 ERP peak and onset latencies, as well as the differences between component peak and onset latencies, using a Spearman correlation. For the N150 onset latency and onset latency difference measures, two participants were removed from the covert-attention task and four were removed from the task-irrelevant viewing paradigm. The full dataset was used for all other correlations. Asterisks indicate significant correlations ($p < .05$).

Lastly, as a data-driven approach to estimating the relative latency of each participant's evoked response, we considered the correlation between IAF and the peak frequency of the ERP difference wave (LVF-UVF; see Method). We found no significant relationship between IAF and peak frequency of the difference ERP waveform for either task (task-irrelevant viewing: $r(22) = .06$, $p = .77$; covert-attention task: $r(16) = .12$, $p = .64$), or for the two tasks combined ($r(40) = .05$, $p = .73$).

Discussion

Our main analysis found no significant correlations between IAF and any of the ERP peak, onset, or latency difference measures when collapsing across tasks. While we did find a few significant correlations when examining tasks separately, specifically driven by the N150 ERP, these relationships were only seen in one visual field (LVF), and were in different directions for the different tasks, making the results difficult to interpret according to either discrete or rhythmic perception account. We thus interpret these specific and opposing significant correlations as likely reflecting noise (i.e., type 1 error given that many correlations were computed and a Bonferoni correction for the number of comparisons would result in no significant correlations). Our main focus was on the C1 ERP was the component since our stimuli were designed to elicit this response, subjects had clear C1 components, and it is the first visual-evoked response, potentially being most susceptible to modulation by alpha frequency given putative generators in the visual thalamus and primary visual cortex (Dougherty et al., 2017; Hughes & Crunelli, 2005; Lőrincz et al., 2009). However, the lack of a relationship between IAF and C1 peak or onset latency in the main and task-specific analyses suggests that the frequency of alpha is unrelated to the timing with which visual responses first arrive in the primary visual cortex.

We also found that IAF was not reliably predictive of N150 latency, nor the

difference between C1 and N150 latency metrics in any of our pooled analysis. However, we did find significant positive correlations between IAF and N150 onset latency and IAF and onset latency differences in the LVF for the task-irrelevant viewing paradigm, meaning that as IAF increased across participants, N150 onsets occurred later in time and the difference between C1 onset and N150 onset increased. However, we found significant negative correlations between IAF and these same components in the LVF for the covert-attention task. In other words, as IAF increased across participants, the N150 onset occurred earlier in time and the difference between C1 onset and N150 onset decreased. It is unclear what theory would predict a different direction of correlation under different task demands, or what theory would predict a correlation between IAF and ERPs in only one visual field; given the lack of a clear theoretical explanation, the fact that the results would not survive a correction for multiple comparisons, and that the results are based on smaller sample sizes, we do not put much weight on these results.

Overall, our findings suggest that alpha frequency does not modulate the timing of neural responses associated with early perceptual processing, an effect we would expect to see if alpha oscillations were indeed responsible for discretizing perceptual events as theorized by the discrete perception account. While it is true that these results do not rule out discrete perception, they suggest that any discretization of percepts that may manifest in behavior likely results from later perceptual processing, as opposed to through these early sensory ERP components. Thus, there is little evidence to suggest that alpha oscillations are responsible for driving changes in the latency of neural events, as suggested by the discrete perception account. However, the prediction that alpha oscillations modulate the strength of sensory responses is supported by prior work (Dou et al., 2022)

The lack of a relationship between IAF and the peak frequency of the ERP difference

waveform (Figure 7) also supports the lack of a relationship between alpha frequency and neural response latencies. One reason for the null effect could be related to the stimulus used here. A seminal study by VanRullen and Macdonald (2012) showed that, when participants viewed a stimulus that randomly modulated in luminance at 160 Hz over a 6 second period, there was a cross-correlation between the EEG signal over occipital electrodes and the luminance values that lasted up to 1 second and which, importantly, fluctuated at an alpha frequency (so-called alpha "echoes"). This implies that a unit change in luminance causes a long-lasting reverberation in the alpha frequency. Interestingly, the frequency of an individual's alpha echo was found to strongly correlate with their resting IAF (VanRullen & Macdonald, 2012), which would imply that the timing of neural responses to a luminance change is related to IAF.

We suggest two possible interpretations of our null results in light of the VanRullen & Macdonald (2012) finding. First, our stimuli were defined by their contrast rather than their luminance (each increase in brightness was canceled out by a decrease in brightness elsewhere in the stimulus). Thus, it remains possible that the timing of luminance responses is perhaps related to alpha frequency in a way that contrast responses are not. Second, we measured ERP onset metrics, not alpha echoes. ERPs likely reflect a mixture of some steady-state response (as in the alpha echo) and various onset and offset responses caused by the sudden appearance and disappearance of the stimulus. Thus, it remains possible that only the steady-state component of the visual response is related to alpha frequency, but not the onset or offset transients. This would imply that the alpha echo approach measures a qualitatively different aspect of visual processing than ERPs.

Our results also have implications for the idea that visual ERP components are generated by a phase-rest of ongoing oscillations (Gruber et al., 2005; Klimesch et al., 2007).

Although our conclusions are restricted to the alpha-band, the lack of correlation speaks against the idea that stimulus onset resets ongoing alpha oscillations and that this is what produces (or contributes) to ERP generation. If the C1 or N150 were generated by a phase reset, we would expect a strong correlation between the frequency of the oscillations being reset and the timing of the ERP components, which was not found. Instead, it is likely that these early visual components reflect additive neural activity that sums with ongoing or background neural oscillations (Iemi et al., 2019).

Future research could further assess whether IAF is related to the latency of other early sensory responses, such as the P1 and N1, as these ERPs were not clear in our datasets due to the high-amplitude C1 response. It is possible that there may be instances where discrete perception occurs and different ways that discrete perception may manifest. However, given that alpha frequency was not related to the latency of the earliest visual ERP (C1), our findings are inconsistent with the notion that alpha is modulating the timing of afferent visual responses.

CHAPTER 4: Prestimulus Alpha Phase Modulates the Strength of Early Visual Responses

Published in NeuroImage as Dou, Morrow, Iemi, and Samaha (2022)

Visual perception depends not only on physical stimulus properties, but also on intrinsic neural dynamics at the moment a stimulus is presented. Several experiments have demonstrated that the phase of prestimulus alpha-band (7-14 Hz) oscillations is associated with fluctuations in subsequent perceptual reports (Alexander et al., 2020; Busch et al., 2009; Busch & VanRullen, 2010; Harris et al., 2018; Mathewson et al., 2009; Samaha et al., 2015, 2017). However, the neurophysiological locus of phasic alpha inhibition is difficult to infer from perceptual reports alone. Specifically, the functional role that alpha oscillations play in perception has largely been attributed to two contrasting hypotheses, with human evidence in favor of either (or both or neither) remaining sparse. On the one hand, alpha generators have been observed in relay sectors of the visual thalamus and are postulated to phasically inhibit afferent visual input in a feedforward manner (Hughes et al., 2011; Hughes & Crunelli, 2005; Lörincz et al., 2008; Lőrincz et al., 2009). On the other hand, evidence also suggests that the direction of influence of alpha activity propagates backwards along the visual hierarchy, reflecting a feedback influence upon the visual cortex (Bastos et al., 2015; Buffalo et al., 2011; Halgren et al., 2019; Rassi et al., 2019; van Kerkoerle et al., 2014).

Perceptual reports could, in theory, be modulated either by feedforward or feedback alpha activity. Thus, although these two hypotheses are not mutually exclusive, human evidence supporting either one is lacking. Here, we tested whether there was a relationship between prestimulus alpha phase and the earliest visual-evoked response in the human electroencephalogram (EEG), which could provide evidence for a feedforward account given some further assumptions.

In the current dataset, human subjects passively viewed large, high-contrast

checkerboard wedges in the upper and lower visual field (U/LVF). The visual stimuli used here can elicit robust C1 event-related potentials (ERP), which peak between 70-80 milliseconds post-stimulus (Clark et al., 1994; Di Russo et al., 2002, 2003; Kelly et al., 2008). According to the cruciform model of primary visual cortex, folding patterns in the cortical sheet of primary visual cortex (V1; but not V2 or V3) (Clark et al., 1994; Jeffreys & Axford, 1972; Kelly et al., 2013) are such that UVF stimuli produce a negative-going C1 ERP and LVF stimuli produce a positive-going C1 (when using an average or mastoid reference) with a scalp focus over central parieto-occipital electrodes (Di Russo et al., 2002, 2003; Vanegas et al., 2013). Specifically, when the upper visual field is stimulated, the visual information is transmitted from the retina to the lateral geniculate nucleus (LGN), which projects this input onto the lower bank of the calcarine sulcus of V1. This produces a negative C1 component on the scalp, owing to the orientation of pyramidal neurons in the lower bank. When the lower visual field is stimulated, the visual information is projected on the upper bank of the calcarine sulcus of V1 through the LGN, producing a positive C1. As the polarity of the C1 is closely related to retinal location, it has been thought to reflect afferent V1 input (Clark et al., 1994; Di Russo et al., 2003, 2002; Kelly et al., 2008). Therefore, we hypothesized that if alpha arises from visual thalamus (LGN), and phasically gates afferent cortical input, then alpha oscillations should modulate the initial stimulus-evoked response in V1. We found that the phase of ongoing alpha oscillations modulates the global field power (GFP) of the EEG during this first volley of stimulus processing (the C1 time window). On the standard assumption (Buzsáki et al., 2012; Cohen, 2017; Jackson & Bolger, 2014) that this early activity reflects postsynaptic potentials relayed to visual cortex from the thalamus, our results suggest that alpha phase gates visual responses during the first feed-forward sweep of processing.

Method

The EEG Dataset

The EEG dataset was originally collected by Iemi and colleagues (2019) and is described in more detail in the original manuscript or the Method section of Chapter 2. In the original study, prior analyses focused on the relationship between prestimulus alpha power and C1 responses, but not on alpha phase. In short, 27 participants (mean age: 26.33, SEM = 0.616; 14 female, 13 male; three left-handed) with normal or corrected vision were presented with a pair of task-irrelevant, full-contrast checkerboard wedges for 100ms either in the upper (UVF) or lower visual field (LVF) with equal probability. The C1 component can be consistently elicited by checkerboard stimuli on these stimulation trials. To ensure central fixation, the fixation mark turned into either one of two equally probable targets (‘>’ or ‘<’) for the duration of stimulus presentation. In 33% of trials, only this small central fixation change occurred (FIX trials), giving us a control condition where no C1-eliciting stimulus was presented. The inter-trial interval between stimuli was uniformly selected between 1.8 and 2.4 s. Each subject underwent 810 trials.

The EEG was recorded from 64 electrodes corresponding to the extended International 10–10 system using a BioSemi ActiveTwo system at a sampling rate of 1024 Hz. All channels were referenced online to the CMS-DRL ground electrodes. One participant did not complete the experiment. We excluded one participant from the analysis because their C1 component was not detected in the LVF after preprocessing. A total of 25 participants were included in the analysis.

EEG Preprocessing

Raw data were preprocessed using custom MATLAB scripts (version R2019b) and the EEGLAB toolbox (Delorme & Makeig, 2004). Continuous recordings were high-pass filtered at 0.1 Hz using a zero-phase Hamming-windowed sinc FIR filter (as implemented in

the EEGLAB function “pop_eegfiltnew.m”). EEG data were then downsampled to 500 Hz and segmented into epochs centered on stimulus onset using a time window of -2000ms to 2000ms. Individual trials containing eye-blinks and other artifacts during stimulus presentation were inspected visually and removed from data (M = 34.96, SEM = 6.14). Noisy channels were spherically interpolated (M = 0.46, SEM = 0.25) and independent components analysis implemented with the INFOMAX algorithm (EEGLAB function “binica.m”) was used to remove components reflecting ocular artifacts (M = 1.08, SEM = 0.05). Data were re-referenced offline to the mean of all electrodes and a prestimulus baseline of -200ms to 0ms was subtracted from each trial.

Stimulus-Evoked Responses

To rectify the polarity of the EEG during the C1, which is reversed for UVF compared to LVF stimuli (Figure 8) and to provide a global measure of the visual-evoked response during the early sweep of cortical activation, we computed the global field power (GFP) of the EEG during the C1 time window. The GFP has been used in prior literature to examine prestimulus phase effects on stimulus-evoked responses rather than analyzing the event-related potential (ERP) directly, since the ERP may trivially sum or cancel with the phase of ongoing oscillations (Busch & VanRullen, 2010). For the single-trial circular-linear association analysis (wITPC; see below), we computed GFP on single trials by taking the spatial standard deviation of voltage averaged over a 20ms window centered on each participant's C1 peak (defined at the electrode with the largest difference between UVF and LVF stimuli in the time window between 50 to 96ms post-stimulus; see Figure 8). For the alpha phase binning analysis (FFT; see below), we first computed the ERP for each alpha phase bin and visual field location and then computed the GFP as the spatial standard deviation of each ERP (sometimes referred to as the global mean field power). Then we

averaged GFP over a 20ms window centered on each participant's peak GFP response, found by searching within the same time window as the C1 (50-96ms).

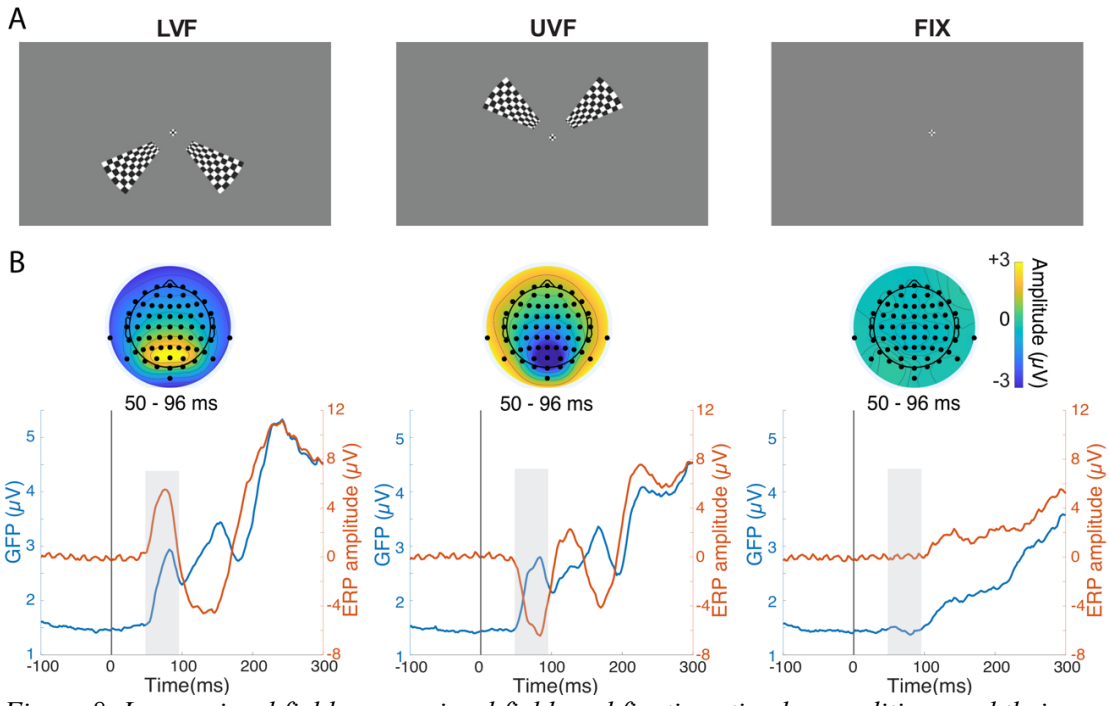

Figure 8: Lower visual field, upper visual field, and fixation stimulus conditions and their stimulus-evoked responses.

A) The stimuli were task-irrelevant, bilateral, full-contrast checkerboard wedges designed to elicit a robust C1 component. The stimuli were presented in the lower visual field (left column, LVF), upper visual field (middle column, UVF), or were absent (right column, FIX) with equal probability. B) ERPs (red line) were computed for the subject-specific electrodes with the largest C1 activity. Shaded time windows indicate the time range of the C1 component. The polarity of the C1 reversed across fields of stimulation (LVF versus UVF) in a manner consistent with striate generation. The C1 was absent on FIX trials. Topographical plots show ERP averaged across 50-96ms. The GFP (blue line) was calculated by taking the spatial standard deviation of voltage averaged over a 20ms window centered on each participant's C1 peak within 50-96ms. GFP provides a global measure of neural response magnitude that also rectifies the polarity reversal of the C1.

Single-Trial Circular-Linear Association (wITPC)

We took two complementary analysis approaches to study the influence of prestimulus phase on GFP amplitudes during the C1 time window. We first compute the weighted intertrial phase coherence (wITPC; Cohen, 2014; Cohen & Voytek, 2013; Samaha et al., 2017) as a means of exploring circular-linear associations between single-trial phase

and GFP across a range of frequencies and time points. wITPC is computed as the resultant vector length, or inter-trial phase clustering (also called the phase-locking factor or inter-trial coherence), of phase angles across trials once the length of each vector has been weighted by the linear variable of interest (here GFP). Note that oscillation amplitude information in this analysis is ignored. wITPC was computed separately for each subject, visual field location, time-frequency point, and electrode. Phase was extracted via complex Morlet wavelet convolution at integer frequencies between 3 and 30Hz, with wavelet cycles increasing linearly from 3 to 8 as a function of frequency. A post-wavelet downsampling factor of 5 was applied to speed up subsequent analyses.

Permutation-based statistics were used for both trial-level and group-level analysis. At the trial level, the wITPC value for each condition, time-point, frequency, electrode, and subject was converted to a z-score relative to a null distribution obtained by recomputing wITPC across 1,000 sets of randomly re-ordered trials. Thus, a positive z-score indicates that trials with large GFP values tend to cluster around a specific phase angle more so than would be expected under a randomized association. These wITPC (z) values were then tested against zero at the group level using a one-tailed, repeated-measures t-test (since negative wITPC (z) is difficult to interpret), with an alpha of 0.01. Only the electrode with largest C1 for each subject was used in the group level analysis, though Figure 9 displays the topography of average wITPC (z) across all electrodes. For 80% of subjects, this electrode was POz, 12% PO4, 4% PO3, and 4% Oz. The result of this t-test produced a map of significant time-frequency pixels for each visual field location (i.e., Figure 9). A cluster-based permutation test was conducted to control for the number of comparisons across times and frequencies using the cluster size statistic (Cohen, 2014). On each of 10,000 permutations, a random half the subject's wITPC (z) values were multiplied by -1 and a one-

tailed t-test with alpha set to 0.01 was conducted on this permuted data. The size of the largest significant cluster in the null map was recorded, building a distribution of significant cluster sizes expected under the null hypothesis of no phase-GFP coupling. Only significant clusters in the real data that exceeded the 95th percentile of the distribution of null hypothesis cluster sizes was considered significant. Lastly, to visualize wITPC (z) across frequencies during the prestimulus period, wITPC (z) was averaged across the time window -300 to 0ms relative to stimulus onset and plotted as a function of the phase-providing frequency (see Figure 9, right panel).

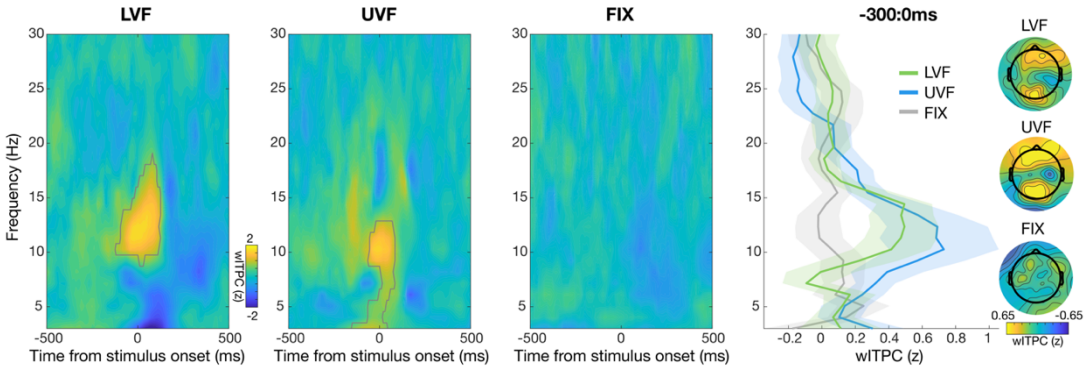

Figure 9: Single-trial time-frequency circular-linear association between phase and Global Field Power (GFP).

Pseudo-color plots show subject-averaged wITPC(z), which describes the normalized coupling strength between phase across times and frequencies and GPF during each individual's C1 time window. The phase-providing electrode was chosen for each individual based on the largest C1 amplitude, but the distribution of wITPC(z) across the scalp from -300 to 0ms and 7-14 Hz is shown in the topographical plots in the right-hand panel. Significant (cluster-corrected) time-frequency points are delimited with a gray line and reveal a modulation of GFP by alpha-band phase (and some adjacent frequencies) just prior to and during stimulus onset for both LVF and UVF stimuli. The effect was absent on FIX trials, when no C1-eliciting stimulus was presented. The right-hand panel shows the wITPC(z) across frequencies for the period from -300 to 0ms relative to stimulus onset. A peak in coupling is noticeable in the 7-14 Hz range. Shaded bands indicate ±1 SEM across subjects.

Prestimulus Alpha-Band Phase Binning (FFT)

To complement the mass-univariate results obtained via wITPC with a more hypothesis-driven analysis of alpha, we conducted a Fast Fourier Transform (FFT) of 500ms

of prestimulus data only and sorted GFP in the C1 time window into different bins of prestimulus alpha phase. This analysis allowed us to 1) better characterize the effect size of prestimulus alpha phase in terms of GFP amplitude modulation, 2) tailor the analysis to each individual's peak alpha frequency, and 3) rule out any contamination of the results by post-stimulus data since only a prestimulus window was extracted for phase sorting.

Prestimulus data were extracted from the same set of subject-specific electrodes with the largest C1 response and just from -500 to 0ms relative to stimulus onset for each trial. Prestimulus phase was extracted from single-trials by first linearly detrending each data segment, multiplying the data with a Hamming window, performing an FFT, and extracting the phase angle from the complex Fourier coefficients. Alpha band phase was extracted at each participant's peak alpha frequency within the range 7-14 Hz, taken from the power spectrum of the same prestimulus data. Single trials of LVF, UVF and FIX conditions were then separately sorted into 7 equally-spaced bins between -180° to 180°. Following prior work (Busch & VanRullen, 2010; Harris et al., 2018), to account for potential individual differences in the specific phase of GFP coupling (related to anatomical differences in how the oscillation field projects to the scalp or differences in V1 conductance latencies), phase bins were circularly-shifted to align the phase bin with the largest GFP amplitude at 0°. This phase bin was then removed from statistical analysis and visualization to remove bias.

For statistical analysis, we conducted a 2 × 7 repeated measures ANOVA with visual field (UVF or LVF) and phase level (1:7, non-shifted) as the within-subject factors. For the GFP in the circularly-shifted phase bins, a 2 × 6 repeated measures ANOVA was conducted with factors, visual field and shifted phase level (excluding the center phase bin used for aligning). Statistical tests were reported for both the shifted and non-shifted data. Lastly, we examined whether any effect of alpha phase on GFP depended on the power of prestimulus

alpha by additionally sorting trials according to visual field, phase, and high versus low prestimulus alpha power using a median split of power averaged over a 4 Hz window centered on each participant's IAF. We conducted the same ANOVAs as above but with the additional factor power (high or low) and an interaction term between phase and power.

Results

We quantified early visual cortical input in response to task-irrelevant, bilateral, full-contrast radial checkerboard patterns presented in UVF and LVF in separate trials. The stimuli used in this experiment (originally reported in Iemi et al., 2019) produced robust C1 responses with polarities, topographies, and timings consistent with striate genesis (Figure 8). The mean amplitude of the C1 component at subject-specific electrodes were 5.26 μV (SEM = 0.61) for LVF and -6.11 μV (SEM = 0.56) for UVF and the average C1 peak latencies were 75.12ms (SEM = 1.27) and 79.36ms (SEM = 1.27) for LVF and UVF respectively. Note that bilateral stimulation (likely producing constructive signal interference across left and right V1) gave rise to C1 amplitudes two to three times larger than the typical C1 (Di Russo et al., 2002, 2003; Kelly et al., 2008; Vanegas et al., 2013), giving us a strong signal to analyze with respect to the ongoing alpha phase. We used the GFP during the C1 time window as a metric of early V1 input in order to rectify the polarity of the C1 (making larger responses always positive; Figure 8) and because voltage at a single electrode may simply cancel/sum with the phase of ongoing oscillations recorded at that same electrode. For these reasons, GFP has been used in previous research to link prestimulus phase to post-stimulus EEG responses, where, for instance, it was found that ~7 Hz phase modulates GFP to near-threshold stimuli around 450ms post-stimulus (Busch & VanRullen, 2010). As a control, to ensure that alpha phase was not trivially related to post-stimulus GFP in the C1 time window, we also analyzed a subset of trials (~33%) which contained only a small change at fixation (FIX trials), but no

C1-producing stimuli. Following the C1 component, we observed a negative going component peaking between 100ms and 200ms relative to stimulus onset (N150) and a positive going component between 200ms and 300ms relative to stimulus onset (P250) for both LVF and UVF. The GFP of N150 (within the time window of 120ms to 200ms) and P250 (within the time window of 200ms to 280ms) were also computed in the following analysis in order to test the specificity of any effect found in the C1 time window.

We computed circular-linear associations using the weighted inter-trial phase coherence (wITPC; Cohen, 2014; Cohen & Voytek, 2013; Samaha et al., 2017) to describe the relationship between single-trial GFP amplitudes (averaged over a 20ms window centered on the C1 peak for each subject) and oscillatory phase across a range of time and frequency points surrounding stimulus onset (extracted via Morlet wavelet convolution). When normalized with respect to the mean and standard deviation of a permuted wITPC distribution, this metric takes on *z* units that reflect the strength of phasic coupling between the linear variable (GFP) and circular variable (phase) relative to a null hypothesis distribution. As seen in Figure 9, significant (cluster-corrected) wITPC was found between GFP in the C1 time window and prestimulus phase for both LVF and UVF trials, but not on FIX trials. For LVF stimuli, GFP was predicted by phase in a cluster of time-frequency points spanning 9-18 Hz and -130 to 120ms from stimulus onset, with a maximum wITPC (z) = 1.74 at 12.35 Hz and 0ms. For UVF stimuli, GFP was predicted by phase in a cluster spanning 3 to 13 Hz and -150 to 85ms with a maximum wITPC (z) = 1.65 at 10 Hz and -10ms. We suspect that differences in the frequency range of clustering across visual fields partly reflects contamination of phase estimates by the ERP, as the first few peaks in the ERP waveforms occur at lower frequencies for LVF compared to UVF stimuli (see Figure 8B). No significant phase-GFP coupling was observed on FIX trials (where only a small fixation change

occurred) suggesting that the positive effects on L/UVF trials are not a trivial result of phase predicting GFP at any post-stimulus window but instead depend on the presence of a C1 component.

Scalp topographies from prestimulus time points (Figure 9, right panel) indicate an occipital and frontal distribution, consistent with the scalp distribution of the effects of alpha-band phase on visual cortex excitability inferred from TMS-EEG experiments (Dugué et al., 2011; Samaha et al., 2017). To understand whether this frontal component of the topography reflects the phase of an additional frontal alpha source, or the opposing phases of a single dipole located intermediate between visual and frontal sensors, we computed the difference in the phase angle of coupling between prestimulus (-300 to 0ms) alpha (10 Hz) and C1 GFP at occipital electrode POz and at frontal electrode AFz, which captures the topography in Figure 9. If the frontal and occipital components represent two ends of a dipole, then the phase of maximal coupling (defined as the phase angle of wITPC) should be 180 degrees out-of-sync (e.g., the alpha phase predictive of GFP is near the trough over visual electrodes, but the peak over occipital electrodes). A circular V-test (as implemented in the circ-stats toolbox for MATLAB), which tests for clustering around a specific direction confirms that the differences in phase coupling between frontal and occipital channels is significantly clustered around 180 deg for UVF, LVF, and FIX trials ($Vs > 10.80$, $ps < .001$), but not at 0 deg for all conditions ($Vs < -10.80$, $ps > .10$). This suggests that the frontal component is likely just one side of a dipole possibly originating from a central source projecting to both occipital and frontal channels.

Although a phase effect is expected to be maximal immediately prior to and during stimulus processing and to decay as a function of time before stimulus onset, as has recently been confirmed empirically (Alexander et al., 2020), it is nevertheless important to confirm

that any prestimulus phase effect is not confounded by post-stimulus data, which can occur when using a sliding window analysis as done here with wavelets. To this end, we ran an additional analysis using a fast-Fourier transform (FFT) of the 500ms preceding stimulus onset to exclude any post-stimulus contamination. The FFT approach has the further advantage of allowing us to extract phase at each participant's IAF to complement our mass-univariate wavelet-based approach with a more hypothesis-driven analysis focused on alpha-band oscillations. We sorted post-stimulus GFP in the C1 time window by 7 levels of prestimulus alpha-band phase. A 2 × 7 repeated measures ANOVA on post-stimulus GFP with visual field (UVF or LVF) and phase level (1:7, non-shifted) as factors revealed a significant main effect of phase level ($F(6, 144) = 3.57$, $p < .01$). No significant main effect of visual field ($F(1, 24) = 1.12$, $p = .30$) or an interaction effect ($F(6, 144) = .91$, $p = .49$) were found. We conducted a one-way ANOVA on the GFP on FIX trials with phase level (non-shifted) as within-subjects factor and found no main effect of phase level ($F(6, 144) = .41$, $p = .87$).

To account for potential individual differences in phase effects (Busch et al., 2009; Busch & VanRullen, 2010; Harris et al., 2018), we re-ran the above analyses after circularly shifting alpha phase for each subject such that the phase with peak GFP became the center phase, which was then removed before statistical testing (Figure 10A). We used 2 × 6 repeated measures ANOVA on the GFP, with factors visual field and shifted phase level (excluding the center phase bin used for aligning). The effect of visual field ($F(1, 24) = 1.14$, $p = .30$) and the interaction between visual field and shifted phase level ($F(5, 120) = .60$, $p = .70$) were not significant. However, as shown in Figure 10B, there was a significant main effect of shifted phase level ($F(5, 120) = 5.41$, $p < .001$). For both LVF and UVF, GFP amplitude decreased as prestimulus alpha phase deviated from the central phase bin,

indicating that prestimulus alpha oscillations influenced the early sensory response to the U/LVF stimuli. In addition, the effect of shifted phase level on the GFP on FIX trials was not evident ($F(5, 120) = .73$, $p = .60$) from a one-way ANOVA. This was in line with the results of the wITPC analysis, confirming that the phasic effect relies on the presence of a C1 component.

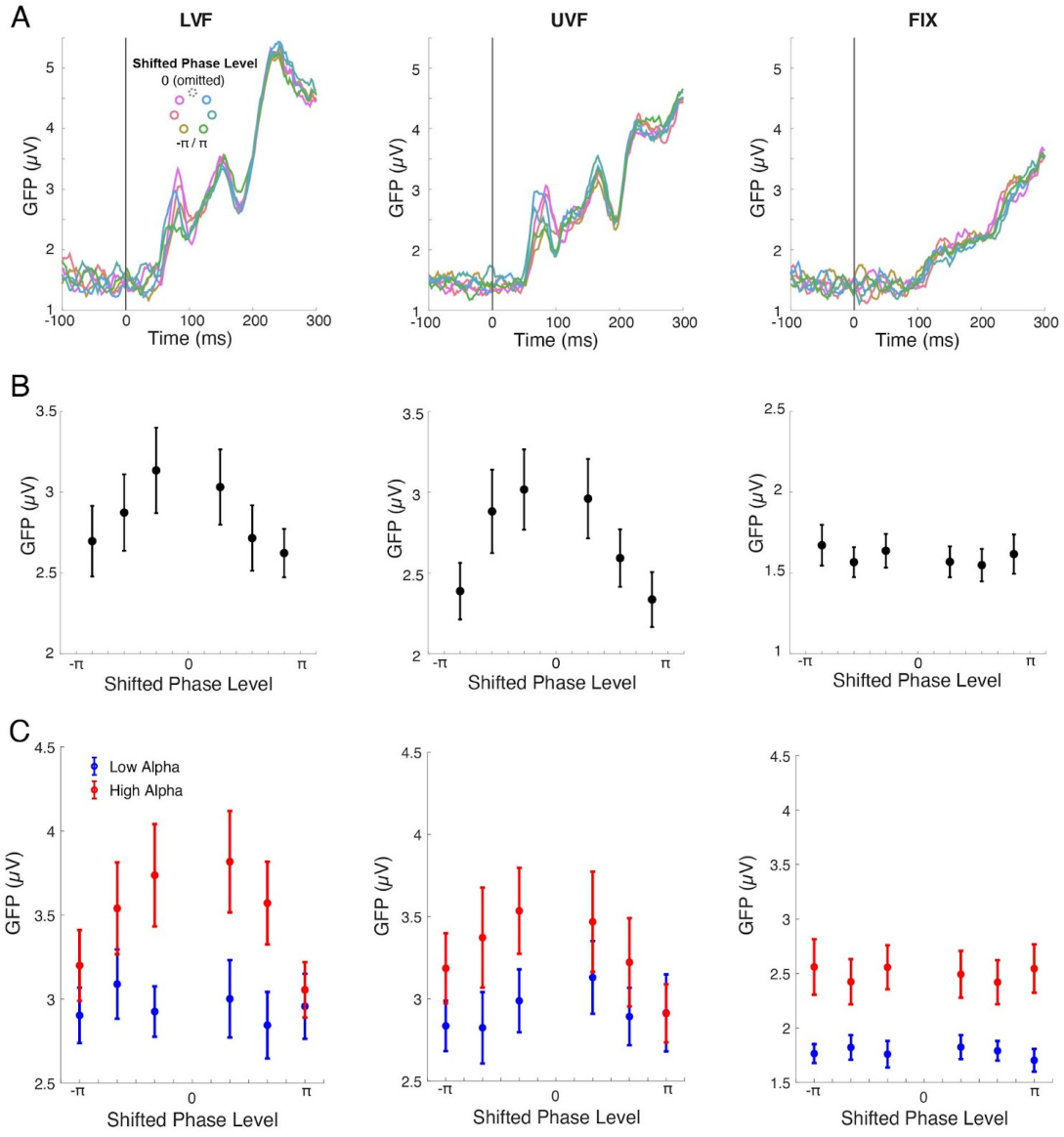

Figure 10: Global Field Power (GFP) as a function of prestimulus alpha phase estimated via FFT.

A) To rule out post-stimulus contamination of phase estimates, single trials were sorted into 7 equally-spaced phase bins between -180° to 180° determined from an FFT using only prestimulus data (-500 to 0ms). The phase bins were circularly-shifted to align the phase bin with the largest post-stimulus GFP in the C1 time window to 0°. This central bin was then left out from plotting and statistical tests. Time courses show the prestimulus alpha phase modulates GFP for both LVF and UVF trials. No obvious GFP response or modulation by alpha phase was observed within the C1 time window on FIX trials (right). B) Averaged GFP over a 20ms window centered on each participant's peak GFP response within the C1 time window decreases monotonically as the shifted phase bins deviate from the removed central bin for both LVF and UVF stimuli. This indicates a phasic effect of prestimulus alpha which was absent on FIX trials. Error bars represent ±1 SEM across subjects. C) Same convention as panel B but broken down by high and low prestimulus alpha power (median split). Note that higher alpha power is associated with higher GFP regardless of the presence of the C1-eliciting stimulus simply because larger amplitude alpha implies more spatial variance (which is the basis of GFP). Importantly, alpha phase interacts with amplitude in predicting GFP only on U/LVF trials, not on FIX trials. Error bars represent ±1 SEM across subjects.

Theoretically, the effects of alpha phase may depend on alpha power (Jensen & Mazaheri, 2010; Klimesch et al., 2007; Mathewson et al., 2011). To test this, we separately classified single trials of LVF, UVF and FIX conditions into high and low power relative to the median power and then sorted trials into 7 equally-spaced phase bins for each power level. GFP was averaged over a 20ms window centered on the GFP peak in each power and phase level. As shown in Figure 10C, after circularly shifting alpha phase and removing the center phase bin for each subject, a 2 (visual field) × 2 (power level) × 6 (shifted phase bin) ANOVA revealed significant main effect of prestimulus alpha power ($F(1, 24) = 12.33$, $p < .01$) and shifted phase ($F(5, 120) = 3.78$, $p < .01$). The interaction effect between prestimulus alpha power and shifted phase was also significant ($F(5, 120) = 3.53$, $p < .01$), indicating that prestimulus alpha phase effect was stronger with strong prestimulus alpha power. Only the power effect was significant on FIX trials ($F(1, 24) = 12.33$, $p < .01$). It might seem surprising that high prestimulus power was associated with higher C1 GFP given previous results showing an inhibitory role of alpha power on C1 ERP amplitude (Iemi et al., 2019). Recall, however, that GFP is computed as the standard deviation across electrodes and when alpha power is high, there is, all else being equal, more variability in the signal across the

scalp. Thus, this rather trivial effect shows up even in the absence of any C1 component, as seen in FIX trials (Figure 10C). Importantly, though, the phase effect (and its interaction with power) is only found in U/LVF trials.

To test whether prestimulus alpha phase influences only the initial stimulus-evoked response in V1 (GFP during C1 time window) rather than later components, the same FFT analysis was applied to examine the alpha phase dependency for subsequent peaks in the GFP (i.e.,~150ms and 250ms). The post-stimulus GFP surrounding the 150ms peak and 250ms peak were separately sorted into 7 equally spaced bins based on prestimulus alpha-band phase. Two 2 × 7 repeated measures ANOVAs on post-stimulus GFP with visual field (UVF or LVF) and phase level (1:7, non-shifted) as factors were conducted. For the 150ms GFP peak, no significant main effects of the phase level ($F(6, 144) = .47$, $p = .83$) and visual field ($F(1, 24) = 1.74$, $p = .20$) and no significant interaction effect ($F(6, 144) = .73$, $p = .62$) were found. For the 250ms GFP peak, only the main effect of visual field was significant ($F(1, 24) = 36.83$, $p < .001$), and the main effect of phase level ($F(6, 144) = .52$, $p = .79$) and the interaction effect ($F(6, 144) = 1.08$, $p = .38$) were not significant.

After circularly shifting alpha phase for each subject such that the phase with largest C1 GFP became the center phase, we used a 2 × 6 repeated measures ANOVA on the GFP for the 150ms and 250ms peaks separately, with factors visual field and shifted phase level (excluding the center phase bin used for aligning). For the 150ms GFP peak, the main effects of the phase level ($F(5, 120) = 1.58$, $p = .17$) and visual field ($F(1, 24) = 2.8$, $p = .11$) were not significant. There was a significant interaction effect between phase level and visual field ($F(5, 120) = 2.69$, $p < .05$). For the 250ms GFP peak, the main effect of visual field was significant ($F(1, 24) = 34.20$, $p < .001$), whereas the main effect of shifted phase level ($F(5, 120) = 1.65$, $p = .15$) and the interaction effect ($F(5, 120) = .10$, $p = .99$) were not significant.

One limitation of shifting the phase bin based on the C1 GFP for the 150ms and 250ms GFP peaks is that the phase dependences for those two later components may be at different phase angles compared to C1 GFP. To address it, we then circularly shifted alpha phase for each subject centering on the bin with the largest 150ms GFP peak and 250ms GFP peak separately. The center bins were removed from following statistical testing. The same 2 × 6 repeated measures ANOVAs described above were conducted for both peaks. We did not observe any significant effects (*ps* > .17) from this analysis. Taken together, these results show prestimulus alpha phase fails to shape the components during later time windows of sensory processing, which may reflect a greater mixture of top-down and bottom-up processing, or may simply be further removed in time from the prestimulus data used to sort responses.

Discussion

We investigated the influence of alpha oscillations on visual responses by testing the relationship between prestimulus alpha phase and post-stimulus GFP measured at the time of the earliest visual-evoked potential in V1, corresponding to the C1 ERP component. According to the "standard model" of EEG genesis, scalp voltage is thought to primarily reflect the postsynaptic potentials of pyramidal neurons (Cohen, 2017; Di Russo et al., 2002), meaning the C1 is potentially generated by afferent synaptic input onto V1 from the thalamus. Indeed, a monkey experiment looking at the likely homologue of the C1 component suggests a contribution from layer 4 thalamocortical afferents (Tenke et al., 1993), although intralaminar synaptic activity within V1 likely also contributes to the C1 (Foxe et al., 2008). Using single-trial circular-linear associations between prestimulus phase and post-stimulus GFP, we found a significant effect within the frequency ranges of 9-18 Hz for LVF and 3-13 Hz for UVF, with maximum effects of alpha in both cases. An additional

analysis using an FFT ruled out the potential smear of post-stimulus responses into the prestimulus window and confirmed the significant modulation of prestimulus alpha phase on GFP during the C1 time window. Analysis of FIX trials, with no C1-producing stimulus, strongly suggest that the effect on U/LVF trials are not a trivial result of pre-and post-stimulus signal autocorrelation. Thus, our results demonstrate that prestimulus alpha phase is predictive of sensory responses in the early stages of visual processing.

What is the biological mechanism underlying alpha oscillations that accounts for these findings? The LGN plays a key role in generating the alpha band (7–14 Hz) oscillation measured over visual cortex (Bollimunta et al., 2011; Hughes et al., 2011; Hughes & Crunelli, 2005; Lopes da Silva et al., 1973; Lörincz et al., 2008; Lőrincz et al., 2009). Of particular relevance for explaining the current finding is the model of Lőrincz et al (2009), which is based on a combination of in vivo and in vitro recordings of the cat LGN that demonstrated the existence of a specialized subset of LGN neurons that are intrinsically bursting, and which synchronize at alpha frequencies via gap junctions (Hughes et al., 2011). These thalamic bursting neurons were found to drive the local field potential in the LGN and the concurrent scalp EEG at an alpha rhythm that phasically inhibited, via interneurons, the relay mode LGN neurons that carry the afferent visual signals to V1. This model seems well suited to explain the phasic modulation of early visual responses in humans that we observed. Assuming that EEG signals principally reflect postsynaptic electrical potentials (Buzsáki et al., 2012; Cohen, 2017; Jackson and Bolger, 2014), and activity in the C1 time window reflects from afferent input to V1, a simple model that can explain our findings is that alpha is gating the output of neurons that are leaving the LGN (optic radiations), as shown in Figure 11. The optic radiations release excitatory neurotransmitters to the postsynaptic terminal in V1, generating an excitatory postsynaptic potential (EPSP) putatively underling the C1 (or at

least parts of the C1 waveform). Therefore, oscillatory gating in the thalamus could explain the phasic modulation of the C1 GFP that we observe, consistent with the model of Lőrincz et al (2009). Note also that a previous analysis of these same data focused on spontaneous alpha amplitude fluctuations and found that prestimulus alpha amplitude modulates C1 amplitude (Iemi et al., 2019).

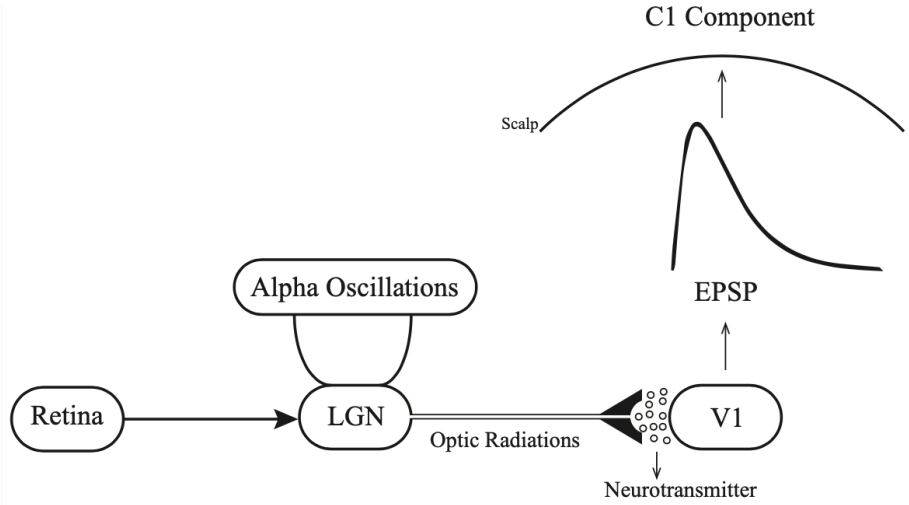

Figure 11: Possible neural circuit for the modulation of the C1 component by alpha oscillations.

Assuming that EEG is primarily sensitive to postsynaptic potentials, then afferent input onto V1, putatively generating the C1 component, could be modulated by ongoing oscillations in the thalamus.

One could argue that alpha observed at the scalp level is a mixture of many different components as we could not measure alpha at the thalamus directly. Speculatively, however, our results showed an occipital and frontal distribution of the effect of alpha-band phase with an opposing phase relationship consistent with a dipole originating at a more central source, possibly near the thalamus. However, our suggestion of a thalamic origin comes not from having source-localized alpha, but by observing an effect of prestimulus alpha on putatively afferent V1 input. Although this early feedforward inhibitory model of alpha could explain the present findings, we certainly do not intend to downplay the possibility that alpha oscillations also influence the visual cortex from higher- to lower-order cortex in a feedback

manner, as has been argued from both monkey and human data (Bastos et al., 2015; Buffalo et al., 2011; Halgren et al., 2019; van Kerkoerle et al., 2014). These two accounts of alpha are not mutually exclusive. Additionally, if the C1 is generated, in part, by intralaminar activity within V1, then there is the possibility that alpha activity feeding back into V1 impacts the C1. Either way our results constrain the modulation of visual-evoked responses by alpha phase to early visual cortex, whether via feedback or feedforward phasic inhibition.

Several experiments in humans have highlighted a relationship between prestimulus alpha phase and different aspects of visual performance in near-threshold detection or discrimination tasks (Busch et al., 2009; Busch & VanRullen, 2010; Mathewson et al., 2009; Ronconi et al., 2017; Samaha et al., 2015, 2017; Sherman et al., 2016), but see (Benwell et al., 2017; Ruzzoli et al., 2019). Given our results suggesting an impact of alpha phase on early visual responses, a reasonable hypothesis is that the gating of early visual responses may underlie the effect of alpha phase on behavior, yet no study has directly linked early sensory responses, alpha phase, and psychophysical performance. Behavior in psychophysical tasks may also be altered by phasic effects of feedback alpha activity, however, sufficient models have not yet been developed that would predict different behavior effects of top-down versus bottom-up alpha effects in visual cortex. As our experiment was designed to study spontaneous alpha, it also remains possible that effects of prestimulus phase on sensory responses differs under conditions where stimuli are predictable or task-relevant. For instance, there is discrepancy in the literature as to whether the impact of alpha phase on perception does (Busch & VanRullen, 2010), or does not (Harris et al., 2018) depend on top-down attention. Resolving this debate may also shed light on the feedforward and feedback contributions to phasic effects of alpha on perception. Moreover, the precise effect of alpha phase on behavior is itself still not clear, as one report has found effects of

alpha phase on response criterion, rather than detection sensitivity (Sherman et al., 2016), another paper found effects on discrimination accuracy (putatively reflecting sensitivity changes; Samaha et al., 2015), and most other studies have only analyzed hit rates (Alexander et al., 2020; Busch et al., 2009; Busch and VanRullen, 2010; Dugué et al., 2011; Harris et al., 2018; Samaha et al., 2017), which are ambiguous between a change in sensitivity or criterion (Samaha et al., 2020). Moreover, several studies have reported no phase effects on stimulus detection/discrimination (Benwell et al., 2017; Chaumon and Busch, 2014; Ruzzoli et al., 2019), though a recent experiment, optimized in many ways to detect an effect, found a rather large change in detection rates of ~20% between stimuli presented during the peak versus trough of occipital alpha (Alexander et al., 2020). Model-based approaches (Zazio et al., 2020), as have recently been applied to the study of oscillatory amplitude dynamics (Samaha et al., 2020), may serve well to better understand the link between oscillatory phase, sensory responses, and perceptual behavior.

CHAPTER 5: Sensitivity in Duration Perception is Related to an Individual's Alpha Frequency

Time perception can take many forms, from the sensory perception of sub-second-long stimuli to the cognitive processing involved in perceiving the passage of minutes- or hours-long events. Despite the seemingly simple nature of perceiving the duration of brief events, the neural mechanisms underlying this process are not well understood. Specifically, it remains unclear how information about the timing or duration of a sensory event is being processed at the neural level and what, if any, is the role that neural oscillations play. One potential explanation for how the brain processes timing information is through frequency channels that facilitate the maintenance and spread of stimulus information from sensory areas to other brain areas (Ayhan et al., 2009, 2011; Bruno et al., 2010, 2013; Bruno & Cicchini, 2016). Generally, oscillatory activity in the alpha-band range (7-14 Hz) has been shown to be related to the strength and speed of visual processing.

An individual's alpha frequency (IAF) has been found to be related to temporal discriminability of visual stimuli (Battaglini et al., 2020; Drewes et al., 2022; Samaha & Postle, 2015) and temporal aspects of cross-modal binding (Baumgarten et al., 2018; Cecere et al., 2015; Keil & Senkowski, 2017), suggesting a relationship between alpha frequency and the duration of temporal binding windows in perception. Additionally, support for the rhythmic sampling theory suggests that alpha oscillations play a role in the strength of our sensory representations (Keitel et al., 2022; VanRullen, 2016). This may explain why individuals with faster IAF, or more frequent increases in sensory representation strength, are more sensitive at discriminating visual and multisensory stimuli. While the rhythmic sampling theory is typically evaluated through measures of the strength of sensory-evoked responses (Dou et al., 2022; Jensen & Mazaheri, 2010), or temporal binding phenomena occurring around the duration of a single alpha cycle (~100ms; see Samaha & Romei, 2024

for a review), the theory could also apply to the processing and representation of stimuli over time. Individual differences in duration perception of sensory events, particularly on the order of hundreds of milliseconds (ms), may be driven by the number of alpha cycles involved in stimulus processing. There is a wealth of behavioral research on the perception of peri-second sensory durations, but current evidence directly assessing the role of alpha frequency in duration perception is limited and conflicting.

Duration perception has been studied using a variety of tasks and, while it has been evaluated in different sensory modalities and even in multimodal contexts, duration perception is often studied in the visual modality. In a series of foundational studies, Efron (1970) demonstrated that there seems to be a minimum perceptible (visual) duration. In these studies, two flashes were presented with varying degrees of overlap and with either the first or second flash changing in duration while the other was held at 500ms. Participants tended to perceive the two flashes as simultaneous up to an average gap of 105ms between onsets, which, interestingly, is roughly the length of the average alpha cycle. Additionally, the slope of performance changed markedly once the first flash exceeded roughly 120-130ms in duration, while the duration of the second flash did not significantly alter gap perception. These findings were thought to highlight the minimum perceptible stimulus duration for each participant. Perception scaled in a graded fashion such that as stimuli became increasingly longer than these minimum perceptible durations, shorter gaps between stimuli were able to be perceived. Taken together, these findings suggest that the minimum perceptible duration may vary based on the type of stimulus that is perceived (a flash or a gap between flashes) and these percepts vary across individuals.

It is important to note that Efron's (1970) study was severely underpowered, with a sample size of two participants, but additional studies have found 100ms to be a critical

window for perceptual processing (Grondin, 1993; Jazayeri & Shadlen, 2015). This 100ms-window is critical in determining whether multisensory events are bound together or not, and the specific length of the binding window varies based on an individual's alpha frequency (IAF; Migliorati et al., 2020; Stevenson et al., 2012; Venskus & Hughes, 2021) and with the manipulation of alpha frequency via non-invasive brain stimulation methods (Venskus et al., 2021). Efron (1970) also found individual differences in the duration of the minimum percept, and similar individual differences in duration perception have been supported by subsequent research (Ivry & Schlerf, 2008; Williams et al., 2019). This critical window of duration perception not only has provided a framework for future studies in selecting appropriate ranges for stimulus durations, but also highlights a possible link between duration perception and the alpha frequency, which has a cycle-length of around 100ms.

Given the behavioral research and the considerable amount of research linking an individual's IAF to their ability to temporally discriminate visual and multisensory events (Cecere et al., 2015; Migliorati et al., 2020; Samaha & Postle, 2015; see Chapter 1 for additional details), it is reasonable to hypothesize that visual alpha oscillations are involved in duration perception, at least for visual events, if not also for multisensory events. In fact, it has long been proposed that alpha oscillations may be used as a clocking mechanism and contribute to the timing of psychological processing, such that alpha cycles at roughly 100ms were thought to define psychological moments (Ellingson, 1956; White, 1963). Some early research suggested a link between alpha and individual variation in temporal estimates at intervals between 2-8s (Legg, 1968), and temporal productions of 10s intervals (Ross, 1968). However, other research found weak or no evidence linking intra- or inter-individual fluctuations in alpha, respectively, to estimates of 10s-time intervals (Surwillo, 1966). Other methods of duration perception were examined by Cahoon (1969), who found a positive

relationship between endogenous alpha (driven by internal processes), but not exogenous alpha (driven by external stimulation), on verbal timing estimates and the timing of motor tapping, but not on reproductions of temporal intervals. It was concluded that Cahoon's (1969) findings aligned with the theory of alpha as an internal clock mechanism, yet subsequent evidence supporting the theory is still limited.

Since the wave of research in the '60s, there have been very few studies looking at how alpha oscillations relate to time perception. Two studies have specifically examined the role of alpha frequency in duration perception, but the results are inconclusive and somewhat conflicting. In one study, participants engaged in a two-alternative forced-choice (2AFC) temporal judgment task where they were asked to report whether the second interval was longer or shorter than the first interval (Milton & Pleydell-Pearce, 2017). The trial consisted of four 10ms flashes presented both above and below fixation to indicate (1) the start of the trial, (2) the onset of the first interval, (3) the offset of the first interval/onset of the second interval, and (4) the offset of the second interval. The first interval was always 400ms and the second interval varied according to participant performance on a staircase task which began with intervals at 200 and 600ms. Alpha phase at the onset of each interval and IAF were examined. The proportion of trials where participants reported that the second interval was longer varied significantly by alpha phase bins (Milton & Pleydell-Pearce, 2017). The point of subjective equality (PSE, or the interval duration at which participants were equally likely to say the second interval was longer or shorter than the first), was significantly correlated with IAF. However, IAF was not related to the slope of individual psychometric functions, suggesting alpha frequency did not modulate sensitivity in discriminating interval durations.

Another study used tACS at participants' IAF or IAF +/- 2 Hz while participants engaged in a temporal generalization task (Mioni et al., 2020). In this task, participants

compared target intervals to a learned 600ms standard and responded according to whether the target interval was equal or different in duration. The target intervals could be between 300-900ms in duration in 100ms steps. All stimuli were black circles presented centrally on a gray background. This study found that manipulating alpha frequency had a significant effect on perceived duration, such that speeding up alpha frequency led to more over-estimation of durations, while slowing down alpha frequency led to more under-estimation of durations. These changes did not relate to increases or decreases in precision of duration estimation, indicating the involvement of alpha oscillations in duration perception but not temporal variability (Mioni et al., 2020). These studies both found no relationship between alpha frequency and duration perception sensitivity, despite prior work suggesting alpha frequency's role in visual and multisensory sampling. Both studies also found that alpha oscillations play a role in some form of bias in duration perception (a shift in PSE or tendency to over-/under-estimate) but link these biases to different characteristics of alpha (phase angle or exogenous frequency).

Across both studies we see design considerations that make the results difficult to compare and interpret. First, the design in Mioni et al. (2020) introduces a training block where participants practice estimating the duration of the standard interval. Training on multisensory integration tasks can lead to changes in the width of the temporal binding window (Navarra et al., 2005; Powers et al., 2009; Stevenson et al., 2013), a measure often associated with IAF (Cecere et al., 2015; Venskus & Hughes, 2021). Mioni and colleagues (2020) were not looking at multisensory integration and are manipulating IAF with tACS during the target interval presentations (as opposed to during the training of the standard intervals), making it important to consider how training may interact with comparisons between these stimuli in the control tACS condition. Second, Milton & Pleydell-Pearce

(2017) use empty intervals that share a very brief (10ms) onset-offset marker to indicate when the first interval is ending, and the second interval is beginning. It seems likely that participants were still estimating their perception of the first interval's duration while they were simultaneously being presented and asked to track the duration of the second interval, making it potentially difficult for participants to process these intervals accurately or even as two separate intervals. Third, while both studies used a relatively short standard interval (either 400 or 600ms), the interval did not capture durations around the alpha cycle (100ms) or longer durations (around 1s) that would have been comparable to prior work from the 60's. Additionally, the presentation order for these standard intervals was not counterbalanced with the target intervals in Milton & Pleydell-Pearce's (2017) 2AFC task. The temporal order effect (TOE) also suggests that participants show bias for perceiving one interval as longer when intervals are subsequently presented (Grondin, 2010), making counterbalancing in these temporal discrimination tasks critical.

The goal of the current study was to use a comprehensive set of tasks and stimuli to more rigorously evaluate the role of alpha frequency in duration perception. Participants performed duration discrimination tasks that expanded on work by Milton and Pleydell-Pearce (2017) and Mioni et al. (2020) by including short, medium, and long standard interval durations, counterbalancing the presentation of standard and comparison stimuli, and introducing a "filled" interval type. The experiment also included a duration estimation task similar to early temporal estimation tasks by Cahoon (1969) and Legg (1968). It was expected that IAF would relate to sensitivity in discriminating durations, but perhaps to different extents for the different stimulus lengths, and a bias to over- or under-estimate durations.

Method

Participants

This study was approved by the University of California Santa Cruz Institutional Review Board. Fifty-five participants with a mean age of 21.46 (SD = 5.16) were recruited from UCSC's SONA systems, the online psychology research pool, as well as from the Samaha Lab. The study consisted of two days of testing; the first day of testing took no more than 1.5 hours and involved the completion of questionnaires and behavioral tasks. Participants received 1.5 SONA research credits and a $10 Amazon gift card. The second day of testing, which had to be completed within 1-12 days of the first, took no more than 3.5 hours and involved the completion of behavioral tasks with simultaneous EEG recording. Participants were rewarded with 3.5 SONA research credits and a $30 Amazon gift card. The sample consisted of 68.52% of participants who identified as female, 24.07% who identified as male, and 7.41% who identified as non-binary. The participant sample was 45.45% White/Caucasian, 25.45% Asian (35.71% did not specify, but of those who did specify, Indian-identifying participants made up 14.29% and those who identified as either Chinese, Cambodian, Filipino, Japanese, Persian, Taiwanese, or Vietnamese each made up 7.14%), 20% Hispanic/Latino, and 9.09% multiracial (20% Black/Southeast Asian, 20% White/Indian, 20% White/Filipino, 20% White/Taiwanese, and 20% White/Chinese). Participants all had normal or corrected-to-normal vision.

Procedure

Each day, participants signed a written consent form and filled out some basic questions about their state that day (e.g. tiredness, hours since they last ate, etc.) before completing additional tasks. On day one, participants answered demographic questions and completed the Comprehensive Autistic Trait Inventory (CATI; English et al., 2021) and the

Prodromal Questionnaire-Brief (PQ-B; Loewy et al., 2005). Participants then completed a short task to estimate their critical flicker frequency (CFF; Wells et al., 2001), which they did on both testing days prior to the duration perception tasks. Participants then did at least two practice blocks of each task (more if their performance was low or participants reported having difficulty with the task) and then one experimental block of each task where there was no feedback. On day two, participants were fitted with the EEG cap and then completed one practice block and two experimental blocks of the duration estimation task. Participants then completed one practice block and five experimental blocks of each duration discrimination task, with the static and dynamic conditions counterbalanced. Finally, participants sat with their eyes closed for two minutes in order to collect resting state data at the end of the session. Participants were allowed to take breaks between blocks, as needed, and were welcome to quit the experiment at any time should they no longer be interested in participating.

Questionnaires

Participants were asked to complete two questionnaires, the CATI and the PQ-B, so that we could assess the extent to which autistic and prodromal traits in a normal healthy population relate to variations in IAF and duration perception. Cognitive impairments can vary widely in the Autism Spectrum Disorder (ASD) population and may be linked to variations in IAF (Dickinson et al., 2018). Research indicates that individuals with ASD have atypical sensory processing, characterized by improved perception of local features, or detail, and impaired perception of global structure, or contextual information (for reviews see Chung & Son, 2020 and Dakin & Frith, 2005). However, there is conflicting evidence around whether individuals with ASD have normal or enhanced processing of time intervals (Poole et al., 2022; Wallace & Happé, 2008). Individuals with schizophrenia and schizotypal disorders, on the other hand, tend to have impairments in visual perception and visual

working memory (Tek et al., 2002), which are thought to underlie difficulties in temporal processing and time perception (Roy et al., 2012), and have lower IAF on average (Ramsay et al., 2021; Sponheim et al., 2023; Trajkovic et al., 2021). Particularly, a meta-analysis suggests that individuals with schizophrenia are less accurate at discriminating durations and have the tendency to overestimate durations (Thoenes & Oberfeld, 2017). Thus, we wanted to explore varying amounts of autistic and schizotypal traits in the normal population related to variations in temporal perception.

To measure autistic traits in the neurotypical population, we used the CATI (English et al., 2021), a 42-item inventory that asks participants to rate how much they agree with statements associated with traits typically seen in the ASD population. Responses are given via a 5-point scale ranging from "Definitely Disagree" to "Definitely Agree". The items come from one of six main categories of traits (Social Interactions, Communication, Social Camouflage, Cognitive Rigidity, Repetitive Behavior, and Sensory Sensitivity) and include statements like, "Metaphors or 'figures of speech' often confuse me," and "I feel discomfort when prevented from completing a particular routine." Answers for each of the items were totaled for each participant, providing a score between 42-210.

The PQ-B (Loewy et al., 2005) was used to measure schizotypal or prodromal traits in the neurotypical population, an inventory consisting of 21 items asking about thoughts, feelings, and experiences within the past month. Items were responded to with a "yes" or "no" and included statements such as, "Do familiar surroundings sometimes seem strange, confusing, threatening or unreal to you?" and "Have you felt that you are not in control of your own ideas or thoughts?". If the participant responded "yes", a follow-up distress scale item asked whether the experience caused the participant to feel "frightened, concerned, or it causes problems" on a 5-point scale ranging from "Strongly Disagree" to "Strongly Agree".

Participant scores were computed in two ways: 1) by totaling the number of "yes" responses to get a score between 0-21, and 2) by totaling the values of the distress scale responses to get a score between 21-105. We were primarily interested in the first score which provided a numerical range of the prodromal experiences across individuals.

Critical Flicker Frequency (CFF)

The CFF was used as a marker of an individual's temporal resolution in their vision (Cass et al., 2011; Eisen-Enosh et al., 2017). Temporal resolution is an aspect of visual processing that is strongly correlated with IAF in related tasks such as the two-flash fusion illusion (Drewes et al., 2022; Samaha & Postle, 2015). Individual differences in CFF are also related to IAF in clinical populations with hepatic encephalopathy (Baumgarten et al., 2018; Butz et al., 2013; Esmat et al., 2017; May et al., 2014). We thus hypothesized that performance on the CFF task might relate to duration perception, and administered this task across both days of testing to provide a baseline measure of temporal discrimination abilities that can be compared against performance on duration perception. We used the Flicker-Fusion system by Lafayette Instruments, which is designed to provide a clear measure of an individual's CFF or, more specifically, the rate at which participants perceive a flickering stimulus as opposed to a continuous stimulus presentation. Participants viewed a flashing light through a viewing chamber and reported whether they perceived the light as flashing or continuous. The light was presented binocularly at the same rate to each eye and the rate of presentation adaptively changed according to participant responses. Initial changes were on the magnitude of +/-5 Hz, with final changes on the magnitude of +/- 0.1 Hz, and participants performed the task until the Flicker-Fusion system had identified the participant's CFF, which took just a few minutes of testing.

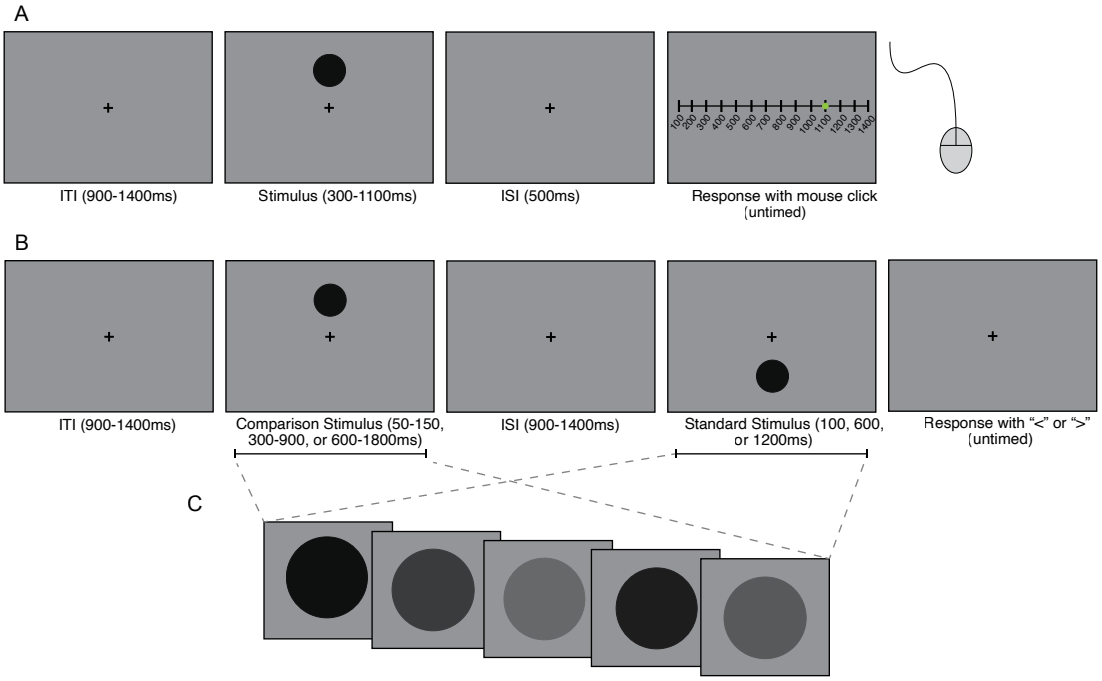

Figure 12: Diagram of duration perception tasks.

A) Duration estimation task. Participants were presented a dot either above or below the central fixation and asked to report how long they perceived the dot to be. Responses were recorded with a mouse click along a slider of possible durations. B) Duration discrimination task. Participants were presented a dot above fixation, followed by a dot below fixation, or vice versa (dot presentation alternated by block) and were asked to report which dot they perceived as being longer in duration. Responses were recorded with a button press of "<" to indicate the first dot was longer or ">" to indicate that the second dot was longer. C) A cartoon of the dynamic stimulus. The luminance value of the stimuli in the dynamic duration discrimination task condition randomly modulated with every screen refresh (120 Hz) throughout the stimulus presentation, ranging from 0-0.5 or black to gray.

Duration Estimation Task

Participants performed a duration estimation task in which they were asked to provide an estimate of the duration of a visual event (Figure 12A). In both the practice and experimental blocks, participants observed a dark gray dot presented on a medium gray background either 3 degrees of visual angle (DVA) above or below the central fixation. The dots could be between 300-1100ms in 100ms intervals and were presented for a pseudo-randomly selected duration such that each duration was presented an equal number of times

during the block. Participants were provided a slider that appeared along the horizontal meridian of the response screen and displayed a number line of possible interval durations, ranging from 100-1400ms in 100ms intervals. The slider provided numbers outside of the range of actual durations to reduce bias when reporting the shortest and longest possible durations. Participants selected the perceived duration of the dot by increasing or decreasing the value on the slider bar by moving the mouse right or left, respectively, and clicking to record their response. The current value was displayed on the screen in numerical values and was represented on the slider by a green dot which appeared at a random starting location on each trial. The inter-trial interval (ITI) ranged between 1.2-1.8s after the response was input. This long ITI was intended to ensure participants had enough time to refocus on the central fixation after the response screen is removed. The practice block was 48 trials long and provided feedback displaying the actual stimulus duration if participants were incorrect in their estimate or "Correct!" if participants were correct. The experimental blocks were 90 trials long with each possible duration presented 10 times, totaling 180 trials.

Duration Discrimination Task

The duration discrimination task was a two-interval forced choice (2IFC) task in which participants were asked to report which of two visual stimuli they perceived to be longer in duration (Figure 12B-C). This task had two conditions: a "static" condition, where the stimulus was the same gray dot as presented in the duration estimation, and a novel "dynamic" condition where the dot varied randomly in luminance values between medium gray (0.5 luminance) to black (0 luminance) on every screen refresh of the monitor (120 Hz). There is evidence that unit changes in luminance are cross correlated with the broadband EEG signal in a manner related to the participant's IAF (VanRullen & Macdonald, 2012), suggesting that our dynamically modulating stimulus should elicit a strong response at the

alpha frequency and allow for a robust evaluation of the role of IAF in duration discrimination. To make the dynamically modulating stimulus, we created random luminance sequences for each dot presentation on each trial, and then normalized the sequences using an inverse discrete Fourier transform to ensure the dot had equal energies at all frequencies. Besides the introduction of a flickering dot, the dynamic task was identical to the static task. The order of these conditions was counterbalanced across experimental sessions.

In both duration discrimination conditions, participants observed the first dot either 3 DVA above or below the central fixation, and then a second target on the opposite side of fixation, with the presentation order counterbalanced across blocks so that participants could always expect the location of the first dot as well as the second dot. In other words, whether the first stimulus was presented above or below fixation alternated from block to block but was held constant across the block. For all blocks, one target (the "standard") was presented for a standard duration of 100, 600, or 1200ms, and the other target (the "comparison") was presented for a fraction of the standard duration (either 50%, 70%, 90%, 110%, 130%, or 150% of the standard duration). In this way, the comparison was always proportional to the standard, allowing for more variability in comparison durations at the longer durations and less at the shorter durations (Haigh et al., 2021). There were six presentations of each standard and comparison pair, resulting in 30 trials for each standard duration and 108 trials for each block. The practice blocks used comparison durations that were 50%, 80%, 120%, and 150% to give participants exposure to some of the easier discriminations and allow them to learn the task, as well as some discriminations of medium difficulty as practice for the experimental block. There were 48 trials total, again with equal presentation of each standard and comparison pair. For all blocks, the presentation order of the standard and comparison varied each trial. Participants will respond with a button press to indicate whether the first

(“<”) or the second (“>”) target was longer in duration.

EEG Preprocessing

All EEG data that was collected was high pass filtered at 0.1 Hz, downsampled to 500 Hz, and re-referenced using a median reference. Trials were epoched based on the onset time of the stimulus (the first stimulus for the discrimination task) to include 500ms of pre- and post-stimulus data based on the longest possible stimulus duration(s) for each task. We also epoched the eyes-closed data into 105 1s-long “trials” prior to manual inspection. All task data was then manually inspected to identify trials with muscular artifacts within a -500 prestimulus to -500 post-stimulus window or eye-blinks overlapping the stimulus presentations and channels with consistent or excessive line noise. After removing selected trials (estimation task: M = 14.62, SD = 19.83; discrimination task: M = 67.30, SD = 54.98) and interpolating selected channels (estimation task: M = 2.71, SD = 1.76; discrimination task: M = 3.56, SD = 1.86) using spherical interpolation, an independent components analysis (ICA) was conducted, and ocular artifact components removed (M = 1.71, SD = 0.72). Eyes-closed data was manually inspected for noisy channels (M = 2.13, SD = 1.42) and trials (M = 5.46, SD = 7.09) to be interpolated and rejected, respectively, but no ICA was run for this data. Finally, all data was average re-referenced again and task data was baseline corrected using a 200ms prestimulus baseline window.

A fast-Fourier transform (FFT) was used to identify peak alpha frequency for each individual (Figure 13). The 500ms prestimulus window from each trial, or the entire 1s trial from the eyes-closed data, was zero-padded, linearly detrended, and tapered using a Hamming window. The FFT was performed across the length of the prestimulus window for each epoch. Power was then averaged across trials using the electrodes with the highest alpha power (O1, O2, PO7, and PO8) to identify the frequency within the alpha-band range (7-14

Hz) that had the most power for each participant, resulting in their IAF. If participants did not have a clear alpha peak, they were assigned a peak of 10 Hz. Only one participant did not have a clear peak in the eyes-closed data, providing the best estimate of IAF across participants (there were 3, 3, and 2 participants without peaks in the EEG data for the estimation, static discrimination, and dynamic discrimination tasks, respectively). The eyes-closed alpha peaks were therefore used in analyses comparing task performance to IAF, and the task EEG data was used only in single trial analyses of alpha frequency.

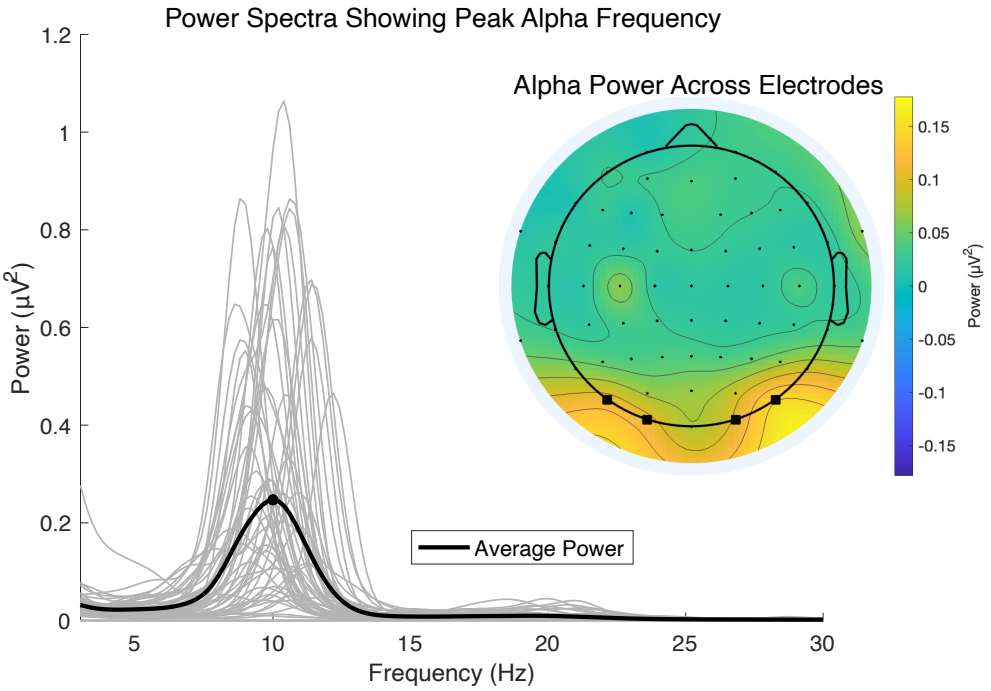

Figure 13: Topoplot of alpha power and power spectra for eyes-closed resting state data. The average power spectrum (black line) shows the average peak alpha frequency (black dot) is at 10 Hz. Colored lines are power spectra for individual subjects and emphasize the variability in peak frequencies. The inset topoplot demonstrates electrode locations (from left to right: PO7, O1, O2, PO8) with the highest alpha power during eyes-closed recording, which were used in the FFT to determine each individual's peak alpha frequency.

A frequency sliding approach based on equations from Cohen (2014) was used to extract instantaneous alpha frequency at the trial level (the dotheslide.m script can be found at

https://samahalab.ucsc.edu/resources). We computed the instantaneous frequency for each trial and electrode using a sliding window across -600 to -200ms prestimulus range and an alpha band range centered around each participant's IAF +/- 2 Hz. For the discrimination task data, we found the instantaneous frequency from before each stimulus presentation, organized by whether the stimulus was the standard or comparison ("stimulus frequency"). This allowed us to evaluate differences in stimulus processing that may be driven by instantaneous alpha frequency. We also averaged the standard and comparison prestimulus alpha frequencies to assess how this related to potential trial-to-trial changes in performance ("trial frequency").

Behavioral Data

For the duration estimation task, we explored measures of estimation accuracy and error. More specifically, we calculated participant's average estimates at each possible duration and their coefficient of variance (CV) in estimates at each possible duration and averaged each of these across durations to have a single value of estimates and CV of estimates for each participant. The CV provided an unbiased measure of the variance in estimates, as it corrects for the larger variance inherent in estimates of longer durations. This measure can be interpreted as a precision measure (as variation in estimates decreases, precision inherently increases). To further evaluate performance, we also calculated participant's average error, absolute average error, and the SD of error at each possible duration and then averaged each of these values across durations.

Participant performance on the discrimination tasks was modeled by fitting a logistic psychometric function (Palamedes toolbox version 1.10.4) to the proportion of times participants chose the comparison stimulus as "longer" for each of the possible comparison durations. This was done separately for each standard duration and each condition. Additionally, separate psychometric functions were fit to high and low frequency trials

median split by instantaneous trial frequency for each participant, and to trials based on whether the prestimulus instantaneous frequency was higher or lower for the comparison stimulus than the standard stimulus. For all data fitting, alpha was set to the range of comparison values, β was set to -10 to 100 to capture the expected positive slope, and the lambda and gamma values were fixed at .05 to denote the lower and upper bounds. Slopes were not normally distributed, so we applied a log10 transformation to all slope data. We used the slope parameter output as a measure of sensitivity for each condition (100ms, 600ms, and 1200ms standards, static and dynamic conditions) and then averaged the slopes by the main effects of interest (standard durations and stimulus types). In other words, to analyze each the average performance at each standard duration, we averaged the static and dynamic conditions, and to analyze the average performance of each task condition, we averaged across all standard durations.

Statistical Analyses

The main goal was to evaluate the role of IAF in duration perception across individuals. We used Spearman correlations to examine the relationship between IAF and several duration estimation measures: mean estimates, CV of estimates, mean error, absolute mean error, and SD of error. As an additional test of the main duration estimation effects of interest, we ran t-tests on the mean estimates and CV comparing participants with high and low IAF, median split. For the duration discrimination task, we also used Pearson correlations to assess the relationship between IAF and the slopes for each of the conditions and the mean slopes across conditions. Mean duration discrimination performance (slope grand mean) was moderately correlated with age ($rho(53) = .28$, $p = .04$), and thus we performed all of the aforementioned correlations after correcting for age in each measure of performance using a linear model (both age-corrected and non-age corrected results can be found in Table 2).

Finally, given the number of variables in question in the duration discrimination task and their potential relationships, we used a mixed effects model to predict duration discrimination slopes using the interactions between IAF and standard duration, IAF and task condition, each of their main effects, and participant age.

It is also possible that duration perception changes with moment-to-moment changes in alpha frequency and so we performed within-subjects analyses on the instantaneous frequency measures extracted from each trial. For the duration estimation task, we binned mean estimates and CV of estimates using a median split of instantaneous trial frequency. We then performed t-tests to evaluate mean estimates and CV of estimates in high versus low frequency trials. We also binned the slopes of psychometric fits from the duration discrimination task by trials with high versus low instantaneous trial frequency as well as for trials with high versus low comparison stimulus frequency. We then performed t-tests comparing average slopes for high and low instantaneous alpha frequency at the stimulus level and trial level.

We were also curious about the extent to which CFF, CATI, and PQ-B scores related to IAF and duration perception sensitivity, as well as how the sensitivity measures across tasks related to one another. Given the non-normal distribution of CFF, CATI, and PQ-B scores, we computed separate Spearman correlations between IAF and each of these variables. We also used a Spearman correlation to explore the relationship between the CATI and PQ-B scores and participants' mean estimates, CV of estimates, and duration discrimination slope values. Additionally, we wanted to compare our main measures of interest across tasks to see how duration estimation related to duration discrimination. We computed a Spearman correlation between the mean slope of the duration discrimination task (taken across all conditions) and the CV of estimates as well as between the mean slope of the

duration discrimination task and the gran mean of estimates from the duration estimation task. Lastly, we checked whether the CV of estimates and grand mean of estimates were correlated using a Spearman correlation.

Results

Duration Estimation

Generally, participants performed as expected on the duration estimation task (Figure 14). Average estimates were near veridical for medium durations (600-800ms) and beginning to decrease for longer durations (90-1100ms) as predicted by prior research (Wearden et al., 2007), although average estimates for shorter durations (300-500ms) tended to be higher than the actual durations. We were primarily interested in looking at participants' average estimates at each duration, to get a measure of bias, and their variation around those estimates, to get a measure of precision. We found that average estimates (Figure 14) were not significantly related to IAF ($rho(52) = .08$, $p = .57$), nor were they significantly different when median split by IAF ($t(54) = .50$, $p = .62$). However, the CV of estimates (Figure 14) was significantly negatively correlated with IAF ($rho(52) = -.30$, $p = .03$), such that faster IAF was associated with a lower CV, or a lower amount of variance in their estimates. Additionally, the CV was significantly different for groups with high IAF compared to low IAF, median split ($t(54) = -2.63$, $p = .01$), such that individuals with faster IAF had significantly lower CV of their estimates. We also explored whether IAF was related to participant error in estimates and the deviation of those errors, to get additional measures of bias and precision. There was no significant correlation between any of the residual error measures (mean error, absolute mean error, and SD of error) and IAF (see Table 2). Finally, we split trials based on each participant's trial alpha frequency median split to explore trial-to-trial variability in estimate. We found no significant difference between high and low trial

frequency and average estimates ($t(54) = -.95$, $p = .35$) or CV of estimates ($t(54) = 1.32$, $p = .19$).

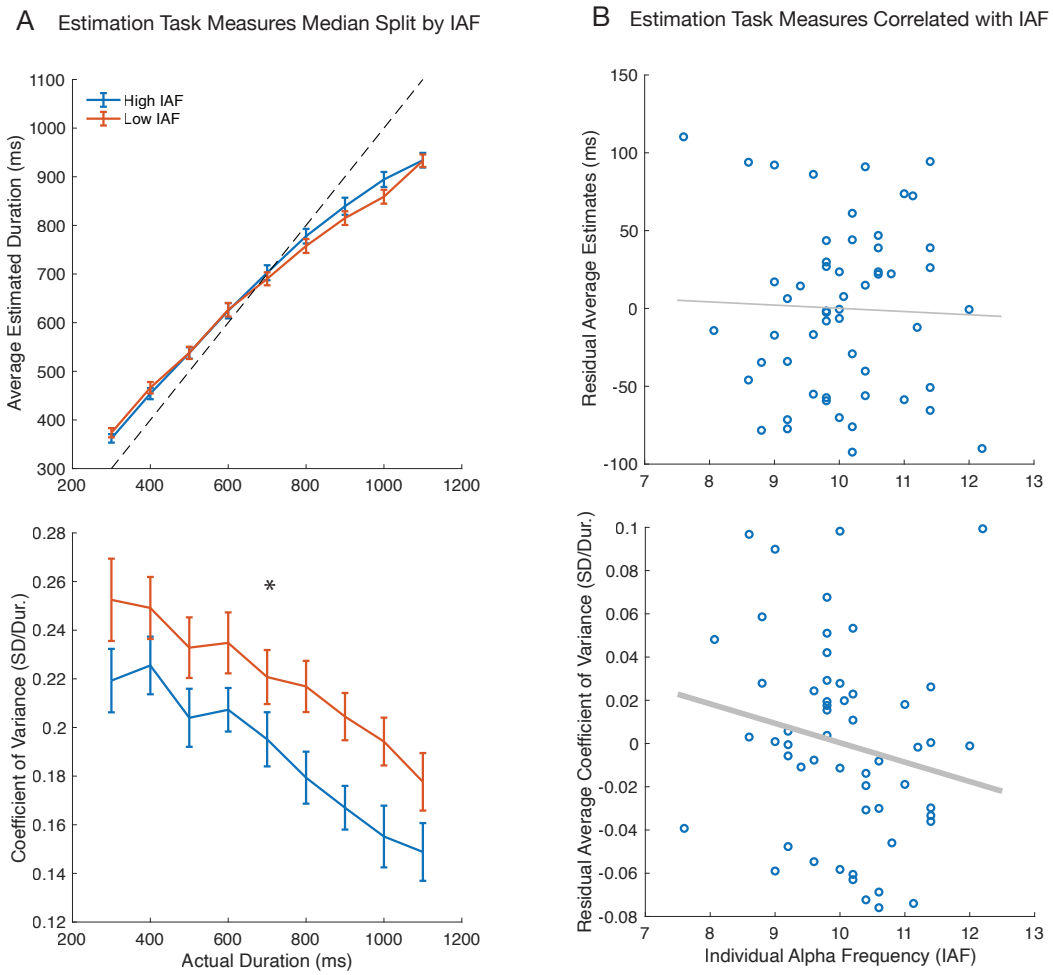

Figure 14: Duration estimation task measures correlated with IAF and median split by IAF.

Mean estimates are plotted in the top row and the coefficient of variance (CV) of estimates are plotted in the bottom row. A) Participants were split by the median IAF, and their mean estimates and CV of estimates are plotted for every actual duration that was presented in the duration estimation task. Participants with high IAF are shown in blue and participants with low IAF are shown in red (error bars are SEM). Asterisks indicate significance ($p < .05$) B) Mean estimates and CVs of estimates were averaged across all durations and corrected for age. Plots show the correlation between IAF and the residuals for mean estimates and CV of estimates, where each blue dot indicates an individual participant. Bolded fit lines indicate significance ($p < .05$).

Duration Discrimination

Performance across the different standard durations in the discrimination task seemed

to improve as durations became longer (Figure 15A), despite the comparison durations being proportionally matched, thus satisfying Weber's law (Haigh et al., 2021). However, we also found that individual differences in slopes across all durations were generally moderately positively correlated to one another (ranging from *rho*(52) of .30-.59; see Figure 15B). Psychometric functions fit the duration discrimination data well for all participants and tasks except one participant who did not have a fit for the 1200ms dynamic condition. Given the correlation among slopes from the different tasks, we imputed this missing data by averaging the participant's 1200ms static slope and 600ms dynamic slope to be used in the following results. The correlations between IAF and the residual psychometric function slopes (after correcting for age) for each of the averaged conditions are shown in Figure 16.

	Age-corrected		Non-age-corrected	
	Estimate	*Standard Error*	*t(323)*	*p*
Duration Estimation Measures				
Mean Estimates	.08	.57	.05	.72
CV of Estimates	-.30*	.03*	-.28*	.04*
Mean Error	.13	.36	.03	.84
Absolute Mean Error	-.18	.20	-.07	.61
SD of Error	-.18	.20	-.08	.55
Duration Discrimination Measures				
Mean Slope	.29*	.03*	.21	.12
Mean Static Slope	.37*	.005*	.31*	.02*
Mean Dynamic Slope	.13	.35	.09	.52
Mean 100ms Slope	.30*	.02*	.26	.05
Mean 600ms Slope	.26	.05	.18	.19
Mean 1200ms Slope	.17	.22	.07	.63

Table 2: Age-corrected and non-age-corrected statistical results of duration estimation and duration discrimination analyses.

Each measure was corrected for age using a linear model to account for the amount of variance explained in the performance measure by participant age. These measures were used in the main correlation analyses described in Chapter 5. Non-age-corrected correlations were also performed and are provided in the final two columns of the table. Asterisks indicate significant correlations ($p < .05$).

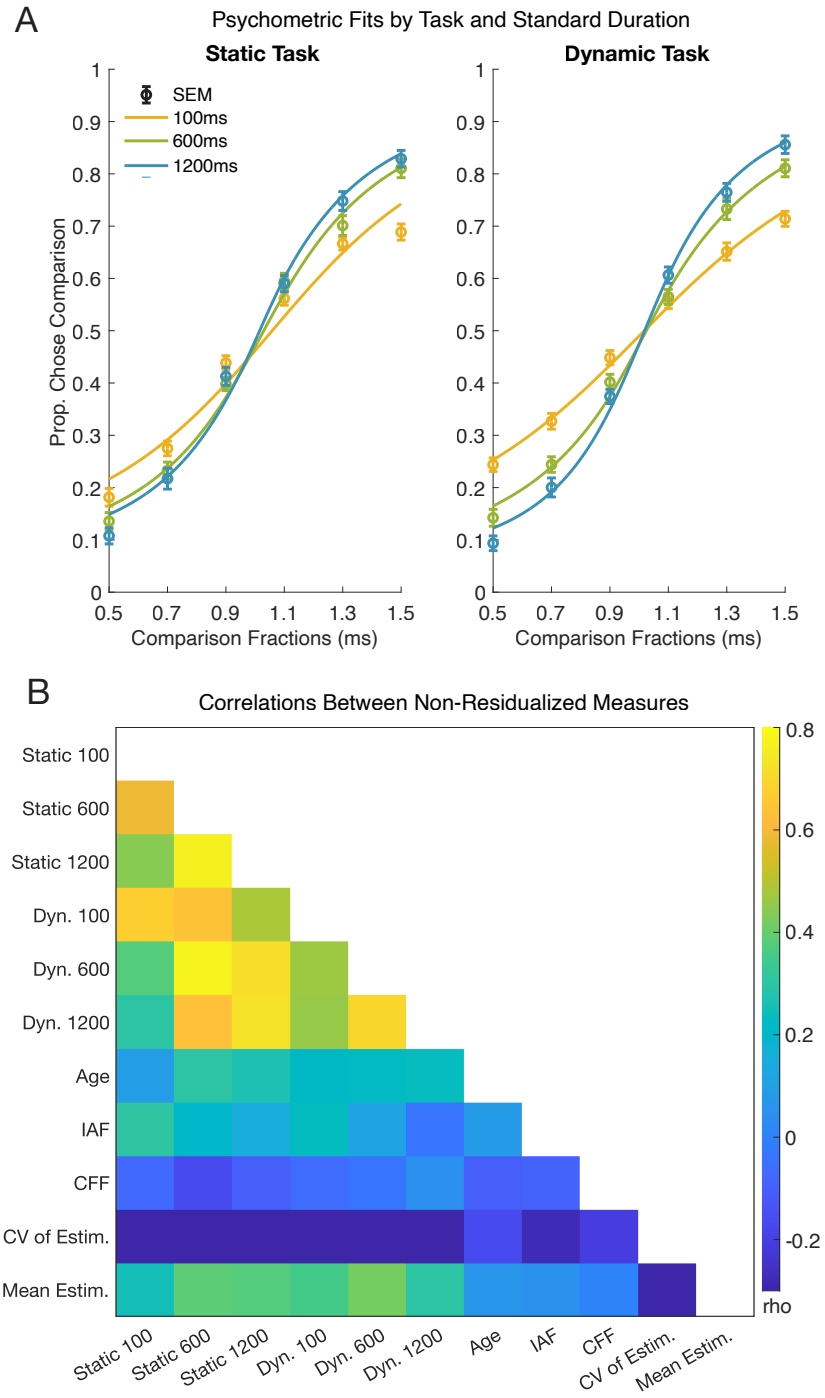

Figure 15: Psychometric function fits for the duration discrimination task by conditions, and a correlation matrix of key measures.

A) The proportion of times participants chose the comparison stimulus as being "longer" than the standard stimulus is plotted against what fraction the comparison duration was relative to the standard stimulus. Psychometric function fits (lines) are shown alongside actual data (dots with SEM error bars). High IAF participants are plotted in blue and low IAF participants are plotted in red for the 100ms standards (top row), 600ms standards (middle row), and 1200ms standards (bottom row) for the static (left column) and dynamic (right column) conditions. B) A correlation matrix showing the Spearman correlation strength between each duration discrimination condition (from top to bottom, or left to right: static 100ms, static 600ms, static 1200ms, dynamic 100ms, dynamic 600ms, dynamic 1200ms), age, IAF, CFF, and the CV of estimates (the sensitivity measure in the duration estimation task), and the mean estimate (the bias measure in the duration estimation task).

First, we wanted to evaluate whether IAF was related to duration discrimination sensitivity overall. We found that sensitivity (slope), when averaged across all conditions, was significantly correlated with IAF ($rho(52) = .29$, $p = .03$). Exploring this relationship further, we found a significant correlation between IAF and the average slope for the static condition ($rho(52) = .37$, $p < .01$), but not for the dynamic condition ($rho(52) = .13$, $p = .35$). Finally, we were interested in understanding how duration discrimination performance changed across the different standards. There was a significant correlation between IAF and sensitivity discriminating 100ms standards ($rho(52) = .30$, $p = .02$) and a moderate correlation between IAF and sensitivity discriminating 600ms standards ($rho(52) = .26$, $p = .05$). No significant relationship was found between IAF and sensitivity discriminating 1200ms standards ($rho(52) = .17$, $p = .22$).

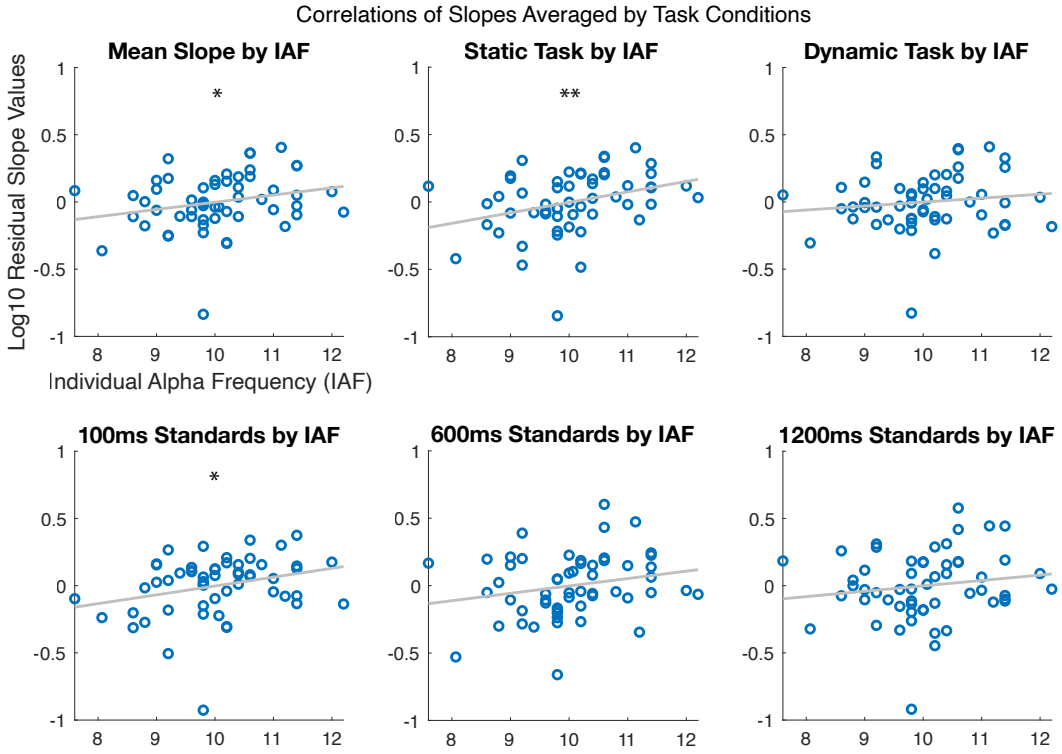

Figure 16: Correlations between IAF and slopes for all duration discrimination task conditions.

Plots show the correlation between IAF and residual duration discrimination slopes, which have been corrected for age and averaged across duration discrimination task conditions of interest. The average slope across all conditions is plotted in the top left, with task types plotted in the top rightmost plots (from left to right: static condition, dynamic condition), and standard duration conditions are plotted in the bottom row (from left to right: 100ms, 600ms, 1200ms) and). Each blue dot indicates an individual participant. Asterisks indicate significance of $p < .05$ (*) and $p < .01$ (**).

Our linear mixed effects model captured the relationship between IAF and all of the variables in the duration discrimination task. We found that participant performance (non-age-corrected slopes) could be predicted using IAF, age, standard duration, and stimulus type (static or dynamic) as predictor variables ($R^2 = .72$). Specifically, age ($\beta = 0.02$, SE = 0.005, $t(323) = 3.06$, $p = .002$), IAF ($\beta = 0.10$, SE = 0.03, $t(323) = 2.83$, $p = .005$), and standard duration ($\beta < 0.001$, SE < 0.001, $t(323) = 13.52$, $p < .001$) were significant predictors of slope as a measure of task performance. While stimulus type was not a significant predictor of

performance, it significantly interacted with IAF to predict performance ($\beta < -0.05$, SE = 0.02, $t(323) = -2.42$, $p = .02$), indicating that the relation between the duration discrimination sensitivity and IAF was, somewhat surprisingly, stronger for static compared to dynamic stimuli. There was no significant interaction between IAF and duration as a predictor variable, suggesting that the IAF relation to duration discrimination sensitivity was not strongly dependent on overall stimulus duration.

The within-subjects analysis for the duration discrimination task looked at high and low instantaneous alpha frequency at both the stimulus frequency level (where trials were sorted by whether the comparison stimulus had higher or lower prestimulus alpha frequency than the standard stimulus) and trial frequency level (where trials were sorted by whether the average prestimulus frequency before each stimulus was higher or lower than the median frequency). Given the reduced number of trials, several psychometric functions did not have good fits. Out of the 165 slopes fit for each analysis, there were a total of 11 slopes for the stimulus frequency analysis and 5 slopes for the trial frequency analysis that needed to be imputed. To do so, we averaged those same participants' data from the two most similar conditions. Slope, averaged across all conditions, was not significantly different for trials with higher frequency compared to trials with lower frequency ($t(54) = -.13$, $p = .89$). Slope, on average, was also not significantly different on trials where the comparison stimulus had a higher frequency compared to trials where the standard stimulus had a higher frequency ($t(54) = 1.69$, $p = .10$). However, given the somewhat larger difference between trials in the stimulus frequency analysis, we explored additional effects. In the static condition, we see a similarly small difference such that on trials where the comparison stimulus had a higher frequency, the slopes are slightly (though not significantly) steeper ($t(54) = 1.75$, $p = .09$). We do not see any difference in the dynamic condition ($t(54) = 0.87$, $p = .39$). When

exploring the effect across standard durations, there is no difference at the 100ms standard ($t(54) = 1.09$, $p = .28$), the 600ms standard ($t(54) = 1.37$, $p = .18$), or the 1200ms standard ($t(54) = -0.27$, $p = .79$).

Exploratory Measures

We were interested in evaluating whether IAF or duration perception performance related to the magnitude of trait-like scores across participants (Figure 17A). No significant correlation was found between IAF and individual's CATI scores or PQ-B scores. The CATI and PQ-B scores also did not significantly relate to any of the main performance measures of interest (mean estimates, CV of estimates, and duration discrimination slopes). Given the relationship between CFF and IAF in clinical populations, we compared CFF to various measures. First, we explored potential correlations between IAF with the CFF averaged across days as well as the CFF from only the second day, the same testing session where we measured IAF. Neither CFF score was significantly correlated with IAF (average CFF: $rho(53) = -.09$, $p = .51$; day 2 CFF: $rho(53) = -.15$, $p = .26$). We also evaluated whether the CFF from the first day, the testing session where participants completed the trait questionnaires, was correlated with either questionnaire score (Figure 17B). We found a moderately weak, non-significant, correlation between CFF and CATI scores ($rho(53) = .24$, $p = .08$) and PQ-B scores ($rho(53) = .23$, $p = .09$). We also looked at whether the different performance measures for the different duration perception tasks were related. We found that the average CV of estimates and the average slopes of the psychometric fits were significantly negatively correlated across participants ($rho(53) = -.56$, $p < .001$). Interestingly, we also found that participant's average overall estimates correlated significantly with the average slopes of the psychometric fits ($rho(53) = .41$, $p < .01$). Finally, the average CV of estimates and the average overall estimates were significantly negatively correlated ($rho(53)$

= -.43, $p < .01$).

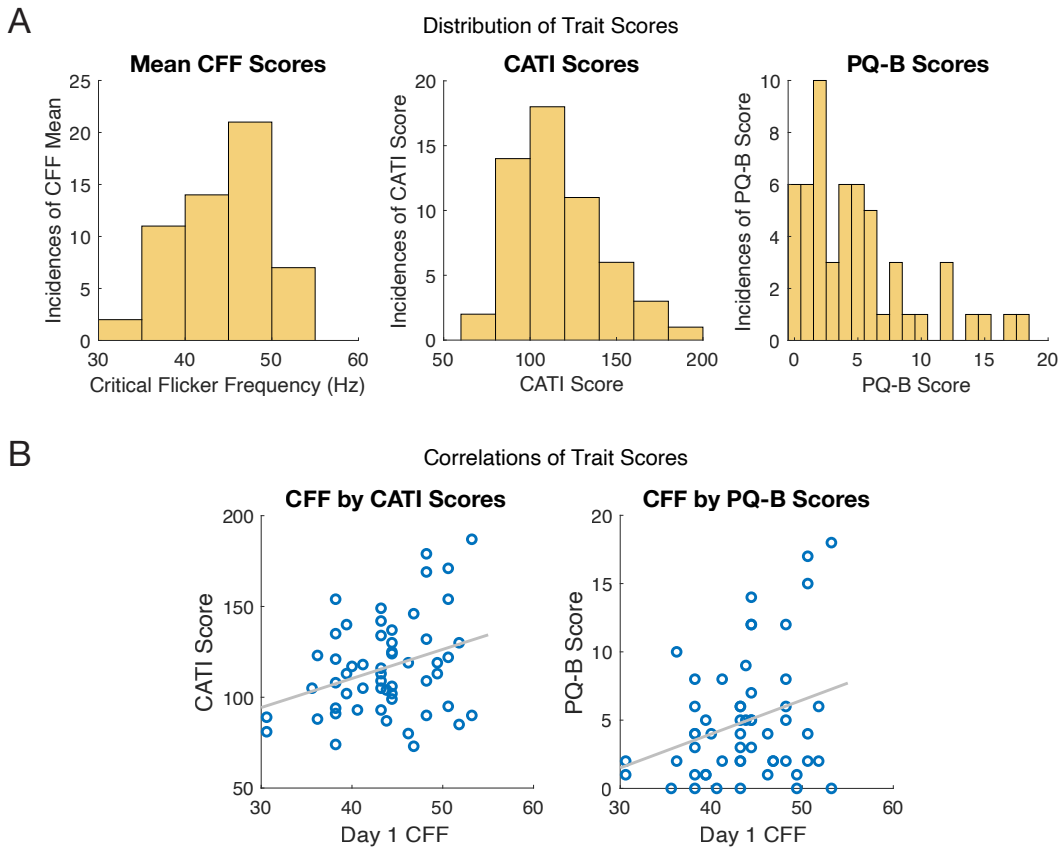

›

Figure 17: Distribution of CFF, CATI, and PQ-B scores across the sample, and correlations between Day 1 CFF and the CATI and PQ-B scores.

A) Histograms demonstrate the number of participants with each trait-like score that was measured in the experiment: critical flicker frequency (CFF), Comprehensive Autistic Trait Inventory (CATI) and the Prodromal Questionnaire (PQ-B). B) A Spearman correlation was computed between the Day 1 CFF scores and the CATI scores (left) and PQ-B scores (right) as an exploratory measure of the relationship between traits that were expected to, but did not relate to, IAF. Neither correlation reached statistical significance.

Discussion

This study highlights the relationship between IAF and individual variation in duration perception, particularly around duration perception sensitivity. IAF did not relate to a bias or tendency to over- or under-estimate durations, but instead related to the precision of visual duration estimates and the sensitivity with which participants discriminated visual

durations. In other words, participants with faster IAF did not demonstrate an overall bias or shift in their average estimates, nor were they more accurate in their estimates, as measured by the absolute error of estimates, but they did show greater precision in their estimates, as measured by the CV of estimates. Participants with faster IAF were also more sensitive at discriminating two similar durations, as measured by the slope of their psychometric functions, than participants with slower IAF. Importantly, these two measures were related: less variance in estimates (greater precision) was associated with a steeper slope (better discriminability). Our duration discrimination findings are consistent with, and expand upon, the vast literature supporting the role of IAF in sensitivity discriminating quick successive visual stimuli and multisensory stimuli (Cecere et al., 2015; Cooke et al., 2019; Di Gregorio et al., 2022; Migliorati et al., 2020; Noguchi, 2022; Samaha & Postle, 2015; Venskus et al. 2021), and our duration estimation findings provide novel evidence that the sensitivity driven by IAF also plays a role in overall precision of estimating the duration of visual events.

We explored performance on the duration discrimination task and how it related to IAF and found that the relationship changed with stimulus type and duration, though the latter variable was not a significant predictor of performance in the mixed effects model. We found that the relationship between IAF and sensitivity was strongest for short standard durations (100ms; Figure 16), regardless of whether the stimulus was static or dynamic (see Figure 15 correlation matrix), but that relationship decayed as the length of the stimulus increased. There was a low to moderate correlation at medium standard durations (600ms), and a weak to no correlation at long standard durations (1200ms). These findings reinforce the idea that the alpha cycle characterizes the minimum perceptible duration, and other percepts are built up of multiples of these cycles. The 100ms standard is roughly the average alpha cycle, and thus discrimination around this standard (where comparisons ranged from 50-150ms) should

most prominently highlight the differences in duration discrimination across individuals as IAF varies. The 600ms standard also captured this range, given that the closest comparisons were 60ms above or below the standard, and while still significant, the strength of correlation between performance and IAF is decreased at this standard duration. The correlation was no longer significant between performance and IAF at the 1200ms standard duration, where the nearest comparisons were 120ms above or below the standard, which is nearly outside of the alpha cycle range except for those individuals at the lower end of the alpha-band range (8.3 Hz or less). In our mixed effect model, the standard duration was a significant predictor in performance on the task (performance improved for longer durations), but it did not significantly interact with IAF as a predictor. In other words, the improved performance on longer durations was likely unrelated to IAF. A possible explanation for the role of IAF in short duration discrimination is that these shorter durations rely more on sensory mechanisms, comparable to the research on temporal resolution and temporal binding of stimuli. Meanwhile, longer durations may begin to recruit additional cognitive processes and rely more heavily on visual working memory than sensory perception for the comparison of durations.

The role of IAF in duration discrimination was specific to the static condition. We found a significant relationship between IAF and the average sensitivity on trials where participants observed a static stimulus but found no relationship on trials where participants observed a dynamically modulating stimulus. This finding was supported by our mixed effects model that indicated the stimulus type alone did not significantly predict performance but did significantly interact with IAF to predict performance. In other words, participants performed similarly, on average, across the task conditions, but the relationship between IAF and task conditions differed enough to significantly affect the prediction of performance in

the model. The dynamic stimulus was modulating randomly in luminance but with equal energy at all frequencies, and thus was not designed to entrain alpha. However, these types of random luminance changes are known to cross-correlate with EEG activity in the alpha-band range for up to 1s (VanRullen & Macdonald, 2012). Although the luminance changes are typically correlated with alpha activity at the participant's IAF, it is possible that the long-lasting activity generated while observing these stimuli may have interfered with participants' spontaneous ongoing alpha rhythms. If IAF was modulated at all during stimulus processing, it may have affected the observed relationship between participants eyes-closed IAF and duration discrimination performance without necessarily affecting overall performance on the task. Alternatively, these stimuli may have simply been more cognitively-demanding for participants to observe and duration perception in this task may have recruited more cognitive mechanisms, as opposed to sensory mechanisms where IAF would have played a greater role. Anecdotally, participants reported using different strategies for the different conditions, and even attempted to "count" the flickers, despite the fact that individual luminance changes were imperceptible to participants, given that they occurred at 120 Hz. Likely participants were counting the number of large, perceptible, luminance changes in the stimulus, which may not have always been aligned with stimulus duration. Overall, it seems the role of IAF may be heavily dependent on the type of stimulus being tracked, and future research should further explore what stimulus properties engage IAF for duration perception.

We performed single-trial analyses to explore within-subject changes in alpha frequency and how that related to performance on duration perception tasks. There was no effect of trial frequency on either bias (mean estimates) or precision (CV of estimates) measures in the duration estimation task, or on sensitivity (slope) in the duration discrimination task. Despite IAF modulating precision and sensitivity in these tasks at the

subject level, it seems that duration perception may be relatively stable within an individual despite spontaneous changes in alpha frequency. This finding is supported by theories of time perception that suggest it is an inherent process modulated by an internal clock mechanism (Karmarkar & Buonomano, 2007; Surwillo, 1966; Treisman, 1963; Treisman et al., 1990). Assuming this temporal clock is modulated by an individual's IAF, minute changes in alpha frequency might be taken into consideration and temporal judgments may be interpreted relative to the individual's typical clock speed. This internal clock theory may also explain why we did not find a difference in sensitivity on trials where the frequency was faster for the comparison stimulus versus trials where the frequency was faster for the standard stimulus. While bias did not seem to be affected by alpha frequency in duration estimates at the subject level, nor does the point-of-subjective-equality (the point at which participants are equally likely to choose the standard and comparison as being "longer") visually appear different across these trials, it still may be pertinent to statistically evaluate bias in duration discrimination at the single-trial level. It could also be interesting to group trials by performance (over- or under-estimates or correct or incorrect discriminations), and then evaluate whether alpha frequency is significantly different on those trials. The first pass of single-trial analyses, however, does not indicate that moment-to-moment changes in alpha frequency relate to participant sensitivity in duration estimation or discrimination.

The final analyses examining IAF's relationship to the CFF and CATI and PQ-B scores and CATI and PQ-B scores to task performance were somewhat exploratory in nature, and we failed to find any significant relationships across the measures. Research on patients with hepatic encephalopathy shows that IAF correlates with CFF (Baumgarten et al., 2018; Butz et al., 2013; Esmat et al., 2017; May et al., 2014). However, it is likely that CFF and IAF are uniquely correlated in these clinical populations, perhaps due to other underlying

mechanisms that drive these patients to have lower IAF on average compared to healthy controls (Butz et al., 2013; Götz et al., 2013; May et al., 2014). Similarly, IAF varies in populations with ASD (Dickinson et al., 2018) and schizotypal disorders (Ramsay et al., 2021; Sponheim et al., 2023; Trajkovic et al., 2021), and duration perception varies in populations with ASD (Poole et al., 2022; Wallace & Happé, 2008) and schizotypal disorders (Roy et al., 2012; Tek et al., 2002; Thoenes & Oberfeld, 2017). Thus, it was hypothesized if variations in IAF are underlying the distortions in duration perception in both of these populations, we might expect that as the magnitude of these traits varies in normal healthy adults, so would IAF. However, there were no significant correlations between IAF and ASD traits (CATI) or schizotypal traits (PB-Q), perhaps due to the non-normal distribution of trait scores whereby individuals tended to score low in both of these traits (see Figure 17A). While we found lower IAF to be associated with reduced duration perception sensitivity, it is likely not driven by the magnitude of ASD or schizotypal traits in those individuals.

Our main results contradict some recent literature exploring the role of IAF in duration perception, which found evidence that IAF relates to bias, but not sensitivity (Mioni et al., 2020). However, it is likely that this effect is driven by the manipulation of IAF with tACS, where +/- 2 Hz changes in alpha frequency were induced in participants. Mioni et al. (2020) asked participants to learn a 600ms standard and then, after receiving tACS, observe stimuli of varying durations and report whether they were the same as or different from the learned standard. The research showed that speeding up or slowing down alpha frequency led to more over- or under-estimations of comparison durations, respectively. In our study, we found no relationship between IAF and this type of estimation bias, either at the subject or trial level, though our within-subject analysis examined endogenous, trial-to-trial changes in alpha frequency. While we did find a relationship between IAF and duration discrimination

sensitivity overall, unlike Mioni et al. (2020), the results from our dynamic duration discrimination condition might relate to their null sensitivity findings. We found no relationship between IAF and sensitivity for the dynamic condition of the duration discrimination task, which induced an ongoing alpha rhythm reflective of the luminance changes in the stimulus. It is possible that, if duration perception is driven by one's endogenous alpha rhythms, performance could change and introduce a bias when alpha is manipulated to be outside of the participant's alpha frequency range. The stimuli being compared in the Mioni et al. (2020) study were presented either at the participant's IAF (standard) or when their alpha frequency was stimulated to be faster or slower (comparison). It is interesting to note that their study also did not find a within-subjects difference in sensitivity and provides additional motivation to explore potential bias in our single-trial analysis of prestimulus alpha frequency. Given the evidence, however, it seems likely that endogenous changes in alpha frequency are not sufficient to induce a bias in duration perception if they fall within the typical internal clock range.

Overall, the rhythmic sampling theory could explain our main findings, as the theory would suggest that individuals with faster IAF have a more frequent strengthening of their visual perception, which is suggested to occur with each alpha cycle. This larger accumulation of strong sensory representations over a duration could provide an overall more accurate representation of that duration, particularly when comparing two similar durations. Further supporting this theory and interpretation of our findings is the fact that the sensitivity measures (CV of estimates and slope in discriminations) were significantly negatively correlated across tasks; as discrimination sensitivity increased, the amount of variance in estimates decreased. While this correlation is not sufficient to conclude that these processes are supported by the same underlying mechanism, it is a necessary relationship to observe if

IAF is indeed the mechanism driving the magnitude of sensitivity across participants in both tasks. This study highlights the role of IAF in duration perception, specifically by supporting improved duration discrimination sensitivity for short durations and static stimuli. Given that IAF was also related to precision – albeit not accuracy – in duration estimates, our pattern of findings lends further support to the rhythmic sampling theory of visual perception by means of alpha frequency.

As a final analysis, we were also able to look at correlations between different measures of task performance and duration perception, a comparison that – to the authors' knowledge – has not been done before. First, the two main duration estimation measures were significantly negatively correlated, such that as average estimates increased, the variation of estimates decreased, meaning those participants with higher estimates were more precise. While we did not expect our measure of bias (average estimates) to be related to our precision measure (CV of estimates), both could be explained by the rhythmic sampling account. Perceptual strengthening (and weakening) would be occurring more often for individuals with faster IAF, but not to the extent that it would induce as strong of a bias in estimates as we would expect if those participants were perceiving additional visual samples, as suggested by the discrete sampling account. Importantly, there was not sufficient difference in average estimates across participants in a way that meaningfully related to IAF. We also compared duration discrimination sensitivity (slope) to the duration estimation task and found that as precision in duration estimates increased, so did discriminability (which also related to IAF). Taken together, these results indicate a specific relationship between alpha frequency and the specificity of visual percepts. However, we also found that average estimates related to discrimination sensitivity. It is difficult to explain why the tendency to estimate durations as longer would relate to duration discrimination sensitivity, and additional research should

these measures in different duration perception tasks to see how they relate. As a whole, these somewhat exploratory findings provide novel evidence of the relationship between performance measures on these rather different duration perception tasks.

Additional duration perception tasks and stimulus types should be explored in the context of IAF to better understand the mechanisms underlying temporal processing and duration perception. A large sample size, such as that used in this study, is critical for analyzing individual differences in IAF and temporal perception (Samaha & Romei, 2024). Several results from both the duration estimation and duration discrimination tasks should be explored further. For example, given the somewhat unintuitive relationship between average duration estimates and other duration perception measures, future studies should test different duration estimation designs. Previous duration estimation tasks have used interval reproduction methods, whereby participants use a button press or saccade to recreate the stimulus observed on each trial (Grondin, 2010; Jazayeri & Shadlen, 2015; van Wassenhove et al., 2019). An interval reproduction design could yield better measures of accuracy and error than our design, which asked participants to report the perceived duration in a more forced-choice manner by using a set scale of possible durations separated by 100ms intervals. This could be especially helpful for capturing estimates of shorter durations, which are likely recruiting more sensory mechanisms than longer durations which potentially rely on more cognitive mechanisms. Additionally, according to the duration discrimination task, the role of IAF in duration perception seems to vary with interval length, and this could provide a more nuanced view of duration estimation at shorter intervals.

Future studies should also examine how different duration discrimination task designs relate to IAF. It was hypothesized that introducing a dynamic and visually-stimulating condition would engage participants in a way that recruited IAF more, being that

IAF is so strongly related to visual perception. Instead, we found that IAF was only related to static duration discrimination, and the lack of a relationship with dynamic duration discrimination could have been driven by the features of our dynamic stimulus. To maintain a dynamic stimulus design but reduce visual stimulation and the possibility that the flickering stimulus induced non-spontaneous alpha activity, future research could change the stimulus luminance or color slowly over the stimulus duration, varying the rate on each trial. This would also reduce participants' ability to attempt to "track" the dynamic changes, as occurred with our stimulus design. However, our current results seem to indicate that the mechanisms for which IAF is helpful in duration perception may rely less on visual cues than expected. Thus, another important future direction is to evaluate the role of IAF in filled versus empty intervals, as has often been done in behavioral duration perception studies (Buffardi, 1971; Hasuo et al., 2014; Wearden et al., 2007; Williams et al., 2019). Introducing an empty versus filled paradigm would allow researchers to see whether IAF plays a unique role in perceiving static filled intervals or is also recruited for perceiving empty intervals. It also seems that IAF plays a greater role in facilitating the discrimination of short durations (around 100ms), seeing as we did not observe a correlation between IAF and discrimination of 600ms standards (though this could, in part, be due to the inclusion of the dynamic condition in the analysis) or 1200ms standards. Future research should compare the relationship between IAF and performance across multiple short standard durations (for example, 100-500ms standards, in 100ms intervals) to see where the role of IAF in duration discrimination begins to break down.

Finally, we did not find significant results at the single-trial level, which could be explained by the small number of trials in the analyses when broken down by both condition and instantaneous frequency. Future research that aims to explore trial-to-trial differences in

alpha activity should consider including a greater number of trials in their experiment to get at the more nuanced role that alpha frequency may play in duration perception within an individual. Implementing these design considerations would further our understanding of how alpha frequency supports temporal perception.

References

Ai, L., & Ro, T. (2014). The phase of prestimulus alpha oscillations affects tactile perception. *Journal of Neurophysiology*, *111*(6), 1300–1307. https://doi.org/10.1152/jn.00125.2013

Alexander, K. E., Estepp, J. R., & Elbasiouny, S. M. (2020). Effects of Neuronic Shutter Observed in the EEG Alpha Rhythm. *eNeuro*, *7*(5). https://doi.org/10.1523/ENEURO.0171-20.2020

Anliker, J. (1963). Variations in Alpha Voltage of the Electroencephalogram and Time Perception. *Science*, *140*(3573), 1307–1309.

Ayhan, I., Bruno, A., Nishida, S., & Johnston, A. (2009). The spatial tuning of adaptation-based time compression. *Journal of Vision*, *9*(11), 2–2. https://doi.org/10.1167/9.11.2

Ayhan, I., Bruno, A., Nishida, S., & Johnston, A. (2011). Effect of the luminance signal on adaptation-based time compression. *Journal of Vision*, *11*(7), 22–22. https://doi.org/10.1167/11.7.22

Barnett, M. W., & Larkman, P. M. (2007). The action potential. *Practical Neurology*, *7*(3), 192–197.

Bastos, A. M., Vezoli, J., Bosman, C. A., Schoffelen, J.-M., Oostenveld, R., Dowdall, J. R., De Weerd, P., Kennedy, H., & Fries, P. (2015). Visual Areas Exert Feedforward and Feedback Influences through Distinct Frequency Channels. *Neuron*, *85*(2), 390–401. https://doi.org/10.1016/j.neuron.2014.12.018

Battaglini, L., Mena, F., Ghiani, A., Casco, C., Melcher, D., & Ronconi, L. (2020).

The Effect of Alpha tACS on the Temporal Resolution of Visual Perception. *Frontiers in Psychology*, *11*, 1765. https://doi.org/10.3389/fpsyg.2020.01765

Baumgarten, T. J., Neugebauer, J., Oeltzschner, G., Füllenbach, N.-D., Kircheis, G., Häussinger, D., Lange, J., Wittsack, H.-J., Butz, M., & Schnitzler, A. (2018). Connecting occipital alpha band peak frequency, visual temporal resolution, and occipital GABA levels in healthy participants and hepatic encephalopathy patients. *NeuroImage: Clinical*, *20*, 347–356. https://doi.org/10.1016/j.nicl.2018.08.013

Benwell, C. S. Y., Tagliabue, C. F., Veniero, D., Cecere, R., Savazzi, S., & Thut, G. (2017). Prestimulus EEG Power Predicts Conscious Awareness But Not Objective Visual Performance. *eNeuro*, *4*(6). https://doi.org/10.1523/ENEURO.0182-17.2017

Bodenmann, S., Rusterholz, T., Dürr, R., Stoll, C., Bachmann, V., Geissler, E., Jaggi-Schwarz, K., & Landolt, H.-P. (2009). The Functional Val158Met Polymorphism of COMT Predicts Interindividual Differences in Brain α Oscillations in Young Men. *Journal of Neuroscience*, *29*(35), 10855–10862. https://doi.org/10.1523/JNEUROSCI.1427-09.2009

Bollimunta, A., Mo, J., Schroeder, C. E., & Ding, M. (2011). Neuronal Mechanisms and Attentional Modulation of Corticothalamic Alpha Oscillations. *Journal of Neuroscience*, *31*(13), 4935–4943. https://doi.org/10.1523/JNEUROSCI.5580-10.2011

Bruno, A., Ayhan, I., & Johnston, A. (2010). Retinotopic adaptation-based visual

duration compression. *Journal of Vision*, *10*(10), 30. https://doi.org/10.1167/10.10.30

Bruno, A., & Cicchini, G. M. (2016). Multiple channels of visual time perception. *Current Opinion in Behavioral Sciences*, *8*, 131–139. https://doi.org/10.1016/j.cobeha.2016.02.028

Bruno, A., Ng, E., & Johnston, A. (2013). Motion-direction specificity for adaptation-induced duration compression depends on temporal frequency. *Journal of Vision*, *13*(12), 19. https://doi.org/10.1167/13.12.19

Buergers, S., & Noppeney, U. (2022). The role of alpha oscillations in temporal binding within and across the senses. *Nature Human Behaviour*, 1–11. https://doi.org/10.1038/s41562-022-01294-x

Buffalo, E. A., Fries, P., Landman, R., Buschman, T. J., & Desimone, R. (2011). Laminar differences in gamma and alpha coherence in the ventral stream. *Proceedings of the National Academy of Sciences*, *108*(27), 11262–11267. https://doi.org/10.1073/pnas.1011284108

Buffardi, L. (1971). Factors affecting the filled-duration illusion in the auditory, tactual, and visual modalities. *Perception & Psychophysics*, *10*(4), 292–294. https://doi.org/10.3758/BF03212828

Busch, N. A., Dubois, J., & VanRullen, R. (2009). The Phase of Ongoing EEG Oscillations Predicts Visual Perception. *Journal of Neuroscience*, *29*(24), 7869–7876. https://doi.org/10.1523/JNEUROSCI.0113-09.2009

Busch, N. A., & VanRullen, R. (2010). Spontaneous EEG oscillations reveal periodic

sampling of visual attention. *Proceedings of the National Academy of Sciences*, *107*(37), 16048–16053. https://doi.org/10.1073/pnas.1004801107

Butz, M., May, E. S., Häussinger, D., & Schnitzler, A. (2013). The slowed brain: Cortical oscillatory activity in hepatic encephalopathy. *Archives of Biochemistry and Biophysics*, *536*(2), 197–203. https://doi.org/10.1016/j.abb.2013.04.004

Buzsáki, G., Anastassiou, C. A., & Koch, C. (2012). The origin of extracellular fields and currents—EEG, ECoG, LFP and spikes. *Nature Reviews Neuroscience*, *13*(6), 407–420. https://doi.org/10.1038/nrn3241

Cahoon, R. L. (1969). Physiological Arousal and Time Estimation. *Perceptual and Motor Skills*, *28*(1), 259–268. https://doi.org/10.2466/pms.1969.28.1.259

Cass, J., Van der Burg, E., & Alais, D. (2011). Finding Flicker: Critical Differences in Temporal Frequency Capture Attention. *Frontiers in Psychology*, *2*, 320. https://doi.org/10.3389/fpsyg.2011.00320

Cecere, R., Rees, G., & Romei, V. (2015). Individual Differences in Alpha Frequency Drive Crossmodal Illusory Perception. *Current Biology*, *25*(2), 231–235. https://doi.org/10.1016/j.cub.2014.11.034

Chakravarthi, R., & VanRullen, R. (2012). Conscious updating is a rhythmic process. *Proceedings of the National Academy of Sciences*, *109*(26), 10599–10604. https://doi.org/10.1073/pnas.1121622109

Chaumon, M., & Busch, N. A. (2014). Prestimulus Neural Oscillations Inhibit Visual Perception via Modulation of Response Gain. *Journal of Cognitive*

Neuroscience, *26*(11), 2514–2529. https://doi.org/10.1162/jocn_a_00653

Chota, S., & VanRullen, R. (2019). Visual Entrainment at 10 Hz Causes Periodic Modulation of the Flash Lag Illusion. *Frontiers in Neuroscience*, *13*. https://doi.org/10.3389/fnins.2019.00232

Chung, S., & Son, J.-W. (2020). Visual Perception in Autism Spectrum Disorder: A Review of Neuroimaging Studies. *Journal of the Korean Academy of Child and Adolescent Psychiatry*, *31*(3), 105–120. https://doi.org/10.5765/jkacap.200018

Clark, V. P., Fan, S., & Hillyard, S. A. (1994). Identification of early visual evoked potential generators by retinotopic and topographic analyses. *Human Brain Mapping*, *2*(3), 170–187. https://doi.org/10.1002/hbm.460020306

Clayton, M. S., Yeung, N., & Cohen Kadosh, R. (2018). The many characters of visual alpha oscillations. *European Journal of Neuroscience*, *48*(7), 2498–2508. https://doi.org/10.1111/ejn.13747

Coffin, S. (1977). Cortical EEG Frequency Composition and the Quality of Apparent Motion in Man. *Psychophysiology*, *14*(6), 586–589. https://doi.org/10.1111/j.1469-8986.1977.tb01205.x

Coffin, S., & Ganz, L. (1977). Perceptual correlates of variability in the duration of the cortical excitability cycle. *Neuropsychologia*, *15*(2), 231–241. https://doi.org/10.1016/0028-3932(77)90031-8

Cohen, M. X. (2014). Fluctuations in Oscillation Frequency Control Spike Timing and Coordinate Neural Networks. *Journal of Neuroscience*, *34*(27), 8988–

8998. https://doi.org/10.1523/JNEUROSCI.0261-14.2014

Cohen, M. X. (2017). Where Does EEG Come From and What Does It Mean? *Trends in Neurosciences*, *40*(4), 208–218. https://doi.org/10.1016/j.tins.2017.02.004

Cohen, M. X., & Voytek, B. (2013). Linking Nonlinear Neural Dynamics to Single-Trial Human Behavior. In M. (Meyer) Z. Pesenson (Ed.), *Multiscale Analysis and Nonlinear Dynamics* (1st ed., pp. 217–232). Wiley. https://doi.org/10.1002/9783527671632.ch09

Cooke, J., Poch, C., Gillmeister, H., Costantini, M., & Romei, V. (2019). Oscillatory Properties of Functional Connections Between Sensory Areas Mediate Cross-Modal Illusory Perception. *Journal of Neuroscience*, *39*(29), 5711–5718. https://doi.org/10.1523/JNEUROSCI.3184-18.2019

Cottier, T. V., Turner, W., Holcombe, A. O., & Hogendoorn, H. (2023). Exploring the extent to which shared mechanisms contribute to motion-position illusions. *Journal of Vision*, *23*(10), 8. https://doi.org/10.1167/jov.23.10.8

Dakin, S., & Frith, U. (2005). Vagaries of Visual Perception in Autism. *Neuron*, *48*(3), 497–507. https://doi.org/10.1016/j.neuron.2005.10.018

Delorme, A., & Makeig, S. (2004). EEGLAB: An open-source toolbox for analysis of single-trial EEG dynamics including independent component analysis. *Journal of Neuroscience Methods*, *134*(1), 9–21. https://doi.org/10.1016/j.jneumeth.2003.10.009

Di Gregorio, F., Trajkovic, J., Roperti, C., Marcantoni, E., Di Luzio, P., Avenanti, A., Thut, G., & Romei, V. (2022). Tuning alpha rhythms to shape conscious

visual perception. *Current Biology*, *32*(5), 988-998.e6. https://doi.org/10.1016/j.cub.2022.01.003

Di Russo, F., Martínez, A., & Hillyard, S. A. (2003). Source Analysis of Event-related Cortical Activity during Visuo-spatial Attention. *Cerebral Cortex*, *13*(5), 486–499. https://doi.org/10.1093/cercor/13.5.486

Di Russo, F., Martínez, A., Sereno, M. I., Pitzalis, S., & Hillyard, S. A. (2002). Cortical sources of the early components of the visual evoked potential. *Human Brain Mapping*, *15*(2), 95–111. https://doi.org/10.1002/hbm.10010

Dickinson, A., DiStefano, C., Senturk, D., & Jeste, S. S. (2018). Peak alpha frequency is a neural marker of cognitive function across the autism spectrum. *European Journal of Neuroscience*, *47*(6), 643–651. https://doi.org/10.1111/ejn.13645

Dienes, Z. (2014). Using Bayes to get the most out of non-significant results. *Frontiers in Psychology*, *5*. https://doi.org/10.3389/fpsyg.2014.00781

Dienes, Z. (2019). How Do I Know What My Theory Predicts? *Advances in Methods and Practices in Psychological Science*, *2*(4), 364–377. https://doi.org/10.1177/2515245919876960

Dockree, P. M., Kelly, S. P., Foxe, J. J., Reilly, R. B., & Robertson, I. H. (2007). Optimal sustained attention is linked to the spectral content of background EEG activity: Greater ongoing tonic alpha (∼10 Hz) power supports successful phasic goal activation. *European Journal of Neuroscience*, *25*(3), 900–907. https://doi.org/10.1111/j.1460-9568.2007.05324.x

Doerig, A., Scharnowski, F., & Herzog, M. H. (2019). Building perception block by

block: A response to Fekete et al. *Neuroscience of Consciousness*, *2019*(1). https://doi.org/10.1093/nc/niy012

Dou, W., Morrow, A., Iemi, L., & Samaha, J. (2022). Pre-stimulus alpha-band phase gates early visual cortex responses. *NeuroImage*, *253*, 119060. https://doi.org/10.1016/j.neuroimage.2022.119060

Dougherty, K., Cox, M. A., Ninomiya, T., Leopold, D. A., & Maier, A. (2017). Ongoing Alpha Activity in V1 Regulates Visually Driven Spiking Responses. *Cerebral Cortex*, *27*(2), 1113–1124. https://doi.org/10.1093/cercor/bhv304

Drewes, J., Muschter, E., Zhu, W., & Melcher, D. (2022). Individual resting-state alpha peak frequency and within-trial changes in alpha peak frequency both predict visual dual-pulse segregation performance. *Cerebral Cortex*, bhac026. https://doi.org/10.1093/cercor/bhac026

Drissi-Daoudi, L., Doerig, A., & Herzog, M. H. (2019). Feature integration within discrete time windows. *Nature Communications*, *10*(1), Article 1. https://doi.org/10.1038/s41467-019-12919-7

Dugué, L., Marque, P., & VanRullen, R. (2011). The Phase of Ongoing Oscillations Mediates the Causal Relation between Brain Excitation and Visual Perception. *Journal of Neuroscience*, *31*(33), 11889–11893. https://doi.org/10.1523/JNEUROSCI.1161-11.2011

Eagleman, D. M., & Sejnowski, T. J. (2007). Motion signals bias localization judgments: A unified explanation for the flash-lag, flash-drag, flash-jump, and Frohlich illusions. *Journal of Vision*, *7*(4), 3–3. https://doi.org/10.1167/7.4.3

Efron, R. (1970). The relationship between the duration of a stimulus and the duration of a perception. *Neuropsychologia*, *8*(1), 37–55.

Eisen-Enosh, A., Farah, N., Burgansky-Eliash, Z., Polat, U., & Mandel, Y. (2017). Evaluation of Critical Flicker-Fusion Frequency Measurement Methods for the Investigation of Visual Temporal Resolution. *Scientific Reports*, *7*(1), Article 1. https://doi.org/10.1038/s41598-017-15034-z

Eisinga, R., te Grotenhuis, M., & Pelzer, B. (2013). The reliability of a two-item scale: Pearson, Cronbach, or Spearman-Brown? *International Journal of Public Health*, *58*(4), 637–642. https://doi.org/10.1007/s00038-012-0416-3

Ellingson, R. J. (1956). Brain waves and problems of psychology. *Psychological Bulletin*, *53*(1), 1–34. https://doi.org/10.1037/h0042562

English, M. C. W., Gignac, G. E., Visser, T. A. W., Whitehouse, A. J. O., Enns, J. T., & Maybery, M. T. (2021). The Comprehensive Autistic Trait Inventory (CATI): Development and validation of a new measure of autistic traits in the general population. *Molecular Autism*, *12*(1), 37. https://doi.org/10.1186/s13229-021-00445-7

Ergenoglu, T., Demiralp, T., Bayraktaroglu, Z., Ergen, M., Beydagi, H., & Uresin, Y. (2004). Alpha rhythm of the EEG modulates visual detection performance in humans. *Cognitive Brain Research*, *20*(3), 376–383. https://doi.org/10.1016/j.cogbrainres.2004.03.009

Esmat, S., Garem, N. E., Raslan, H., Elfekki, M., & Sleem, G. A. (2017). Critical Flicker Frequency is Diagnostic of Minimal Hepatic Encephalopathy. *Journal*

of Investigative Medicine, *65*(8), 1131–1135. https://doi.org/10.1136/jim-2017-000428

Fan, Y. (2018). Alpha-Band Oscillation Mediates the Temporal Organization of Serially Presented Flashes. *The Journal of Neuroscience*, *38*(15), 3613–3615. https://doi.org/10.1523/JNEUROSCI.3633-17.2018

Faul, F., Erdfelder, E., Lang, A.-G., & Buchner, A. (2007). G*Power 3: A flexible statistical power analysis program for the social, behavioral, and biomedical sciences. *Behavior Research Methods*, *39*(2), 175–191. https://doi.org/10.3758/BF03193146

Fekete, T., Van de Cruys, S., Ekroll, V., & van Leeuwen, C. (2018). In the interest of saving time: A critique of discrete perception. *Neuroscience of Consciousness*, *2018*(niy003). https://doi.org/10.1093/nc/niy003

Foxe, J. J., & Snyder, A. C. (2011). The Role of Alpha-Band Brain Oscillations as a Sensory Suppression Mechanism during Selective Attention. *Frontiers in Psychology*, *2*. https://doi.org/10.3389/fpsyg.2011.00154

Foxe, J. J., Strugstad, E. C., Sehatpour, P., Molholm, S., Pasieka, W., Schroeder, C. E., & McCourt, M. E. (2008). Parvocellular and Magnocellular Contributions to the Initial Generators of the Visual Evoked Potential: High-Density Electrical Mapping of the "C1" Component. *Brain Topography*, *21*(1), 11–21. https://doi.org/10.1007/s10548-008-0063-4

Fröhlich, F. W. (1923). Über die Messung der Empfindungszeit. *Zeitschrift Für Sinnesphysiologie*, *54*, 58.

Fu, S., Greenwood, P. M., & Parasuraman, R. (2005). Brain mechanisms of involuntary visuospatial attention: An event-related potential study. *Human Brain Mapping*, *25*(4), 378–390. https://doi.org/10.1002/hbm.20108

Goldman, R. I., Stern, J. M., Engel, J., & Cohen, M. S. (2002). Simultaneous EEG and fMRI of the alpha rhythm. *Neuroreport*, *13*(18), 2487–2492. https://doi.org/10.1097/01.wnr.0000047685.08940.d0

Götz, T., Huonker, R., Kranczioch, C., Reuken, P., Witte, O. W., Günther, A., & Debener, S. (2013). Impaired evoked and resting-state brain oscillations in patients with liver cirrhosis as revealed by magnetoencephalography. *NeuroImage: Clinical*, *2*, 873–882. https://doi.org/10.1016/j.nicl.2013.06.003

Gould, I. C., Rushworth, M. F., & Nobre, A. C. (2011). Indexing the graded allocation of visuospatial attention using anticipatory alpha oscillations. *Journal of Neurophysiology*, *105*(3), 1318–1326. https://doi.org/10.1152/jn.00653.2010

Grabot, L., Kösem, A., Azizi, L., & van Wassenhove, V. (2017). Prestimulus Alpha Oscillations and the Temporal Sequencing of Audiovisual Events. *Journal of Cognitive Neuroscience*, *29*(9), 1566–1582. https://doi.org/10.1162/jocn_a_01145

Grandy, T. H., Werkle-Bergner, M., Chicherio, C., Schmiedek, F., Lövdén, M., & Lindenberger, U. (2013). Peak individual alpha frequency qualifies as a stable neurophysiological trait marker in healthy younger and older adults. *Psychophysiology*, *50*(6), 570–582. https://doi.org/10.1111/psyp.12043

Gray, M. J., & Emmanouil, T. A. (2020). Individual alpha frequency increases during a task but is unchanged by alpha-band flicker. *Psychophysiology*, *57*(2), e13480. https://doi.org/10.1111/psyp.13480

Grondin, S. (1993). Duration discrimination of empty and filled intervals marked by auditory and visual signals. *Perception & Psychophysics*, *54*(3), 383–394. https://doi.org/10.3758/BF03205274

Grondin, S. (2010). Timing and time perception: A review of recent behavioral and neuroscience findings and theoretical directions. *Attention, Perception, & Psychophysics*, *72*(3), 561–582. https://doi.org/10.3758/APP.72.3.561

Gruber, W. R., Klimesch, W., Sauseng, P., & Doppelmayr, M. (2005). Alpha Phase Synchronization Predicts P1 and N1 Latency and Amplitude Size. *Cerebral Cortex*, *15*(4), 371–377. https://doi.org/10.1093/cercor/bhh139

Gulbinaite, R., Viegen, T. van, Wieling, M., Cohen, M. X., & VanRullen, R. (2017). Individual Alpha Peak Frequency Predicts 10 Hz Flicker Effects on Selective Attention. *Journal of Neuroscience*, *37*(42), 10173–10184. https://doi.org/10.1523/JNEUROSCI.1163-17.2017

Haegens, S., Cousijn, H., Wallis, G., Harrison, P. J., & Nobre, A. C. (2014). Inter- and intra-individual variability in alpha peak frequency. *NeuroImage*, *92*, 46–55. https://doi.org/10.1016/j.neuroimage.2014.01.049

Haegens, S., Händel, B. F., & Jensen, O. (2011). Top-Down Controlled Alpha Band Activity in Somatosensory Areas Determines Behavioral Performance in a Discrimination Task. *Journal of Neuroscience*, *31*(14), 5197–5204.

https://doi.org/10.1523/JNEUROSCI.5199-10.2011

Haigh, A., Apthorp, D., & Bizo, L. A. (2021). The role of Weber's law in human time perception. *Attention, Perception, & Psychophysics*, *83*(1), 435–447. https://doi.org/10.3758/s13414-020-02128-6

Halgren, M., Ulbert, I., Bastuji, H., Fabó, D., Erőss, L., Rey, M., Devinsky, O., Doyle, W. K., Mak-McCully, R., Halgren, E., Wittner, L., Chauvel, P., Heit, G., Eskandar, E., Mandell, A., & Cash, S. S. (2019). The generation and propagation of the human alpha rhythm. *Proceedings of the National Academy of Sciences*, *116*(47), 23772–23782. https://doi.org/10.1073/pnas.1913092116

Händel, B. F., & Jensen, O. (2014). Spontaneous local alpha oscillations predict motion-induced blindness. *European Journal of Neuroscience*, *40*(9), 3371–3379. https://doi.org/10.1111/ejn.12701

Harris, A. M., Dux, P. E., & Mattingley, J. B. (2018). Detecting Unattended Stimuli Depends on the Phase of Prestimulus Neural Oscillations. *Journal of Neuroscience*, *38*(12), 3092–3101. https://doi.org/10.1523/JNEUROSCI.3006-17.2018

Harter, M. R. (1967). Excitability cycles and cortical scanning: A review of two hypotheses of central intermittency in perception. *Psychological Bulletin*, *68*(1), 47–58. https://doi.org/10.1037/h0024725

Hasuo, E., Nakajima, Y., Tomimatsu, E., Grondin, S., & Ueda, K. (2014). The occurrence of the filled duration illusion: A comparison of the method of

adjustment with the method of magnitude estimation. *Acta Psychologica*, *147*, 111–121. https://doi.org/10.1016/j.actpsy.2013.10.003

Herzog, M. H., Drissi-Daoudi, L., & Doerig, A. (2020). All in Good Time: Long-Lasting Postdictive Effects Reveal Discrete Perception. *Trends in Cognitive Sciences*, *24*(10), 826–837. https://doi.org/10.1016/j.tics.2020.07.001

Hindriks, R., & van Putten, M. J. A. M. (2013). Thalamo-cortical mechanisms underlying changes in amplitude and frequency of human alpha oscillations. *NeuroImage*, *70*, 150–163. https://doi.org/10.1016/j.neuroimage.2012.12.018

Hindriks, R., Van Putten, M. J. A. M., & Deco, G. (2014). Intra-cortical propagation of EEG alpha oscillations. *NeuroImage*, *103*, 444–453. https://doi.org/10.1016/j.neuroimage.2014.08.027

Hogendoorn, H. (2020). Motion Extrapolation in Visual Processing: Lessons from 25 Years of Flash-Lag Debate. *The Journal of Neuroscience*, *40*(30), 5698–5705. https://doi.org/10.1523/JNEUROSCI.0275-20.2020

Holcombe, A. O. (2009). Seeing slow and seeing fast: Two limits on perception. *Trends in Cognitive Sciences*, *13*(5), 216–221. https://doi.org/10.1016/j.tics.2009.02.005

Hughes, S., & Crunelli, V. (2005). Thalamic Mechanisms of EEG Alpha Rhythms and Their Pathological Implications. *The Neuroscientist*, *11*(4), 357–372. https://doi.org/10.1177/1073858405277450

Hughes, S., Lőrincz, M., Turmaine, M., & Crunelli, V. (2011). Thalamic Gap Junctions Control Local Neuronal Synchrony and Influence Macroscopic

Oscillation Amplitude during EEG Alpha Rhythms. *Frontiers in Psychology*, *2*. https://doi.org/10.3389/fpsyg.2011.00193

Iemi, L., Busch, N. A., Laudini, A., Haegens, S., Samaha, J., Villringer, A., & Nikulin, V. V. (2019). Multiple mechanisms link prestimulus neural oscillations to sensory responses. *eLife*, *8*, e43620. https://doi.org/10.7554/eLife.43620

Ivry, R. B., & Schlerf, J. E. (2008). Dedicated and intrinsic models of time perception. *Trends in Cognitive Sciences*, *12*(7), 273–280. https://doi.org/10.1016/j.tics.2008.04.002

Jackson, A. F., & Bolger, D. J. (2014). The neurophysiological bases of EEG and EEG measurement: A review for the rest of us. *Psychophysiology*, *51*(11), 1061–1071. https://doi.org/10.1111/psyp.12283

James, K. (1980). On Some Possible Characteristics of Information in J. J. Gibson's Ecological Approach to Visual Perception. *Leonardo*, *13*(2), 112–116. https://doi.org/10.2307/1577980

Jazayeri, M., & Shadlen, M. N. (2015). A Neural Mechanism for Sensing and Reproducing a Time Interval. *Current Biology*, *25*(20), 2599–2609. https://doi.org/10.1016/j.cub.2015.08.038

Jeffreys, D. A., & Axford, J. G. (1972). Source locations of pattern-specific components of human visual evoked potentials. I. Component of striate cortical origin. *Experimental Brain Research*, *16*(1), 1–21. https://doi.org/10.1007/BF00233371

Jensen, O., & Mazaheri, A. (2010). Shaping Functional Architecture by Oscillatory Alpha Activity: Gating by Inhibition. *Frontiers in Human Neuroscience*, *4*. https://doi.org/10.3389/fnhum.2010.00186

Karmarkar, U. R., & Buonomano, D. V. (2007). Timing in the Absence of Clocks: Encoding Time in Neural Network States. *Neuron*, *53*(3), 427–438. https://doi.org/10.1016/j.neuron.2007.01.006

Kasten, F. H., & Herrmann, C. S. (2022). The hidden brain-state dynamics of tACS aftereffects. *NeuroImage*, *264*, 119713. https://doi.org/10.1016/j.neuroimage.2022.119713

Keil, J., & Senkowski, D. (2017). Individual Alpha Frequency Relates to the Sound-Induced Flash Illusion. *Multisensory Research*, *30*(6), 565–578. https://doi.org/10.1163/22134808-00002572

Keil, J., & Senkowski, D. (2018). Neural Oscillations Orchestrate Multisensory Processing. *The Neuroscientist*, *24*(6), 609–626. https://doi.org/10.1177/1073858418755352

Keitel, C., Ruzzoli, M., Dugué, L., Busch, N. A., & Benwell, C. S. Y. (2022). Rhythms in cognition: The evidence revisited. *European Journal of Neuroscience*, *55*(11–12), 2991–3009. https://doi.org/10.1111/ejn.15740

Kelly, S. P., Gomez-Ramirez, M., & Foxe, J. J. (2008). Spatial Attention Modulates Initial Afferent Activity in Human Primary Visual Cortex. *Cerebral Cortex*, *18*(11), 2629–2636. https://doi.org/10.1093/cercor/bhn022

Kelly, S. P., Gomez-Ramirez, M., & Foxe, J. J. (2009). The strength of anticipatory

spatial biasing predicts target discrimination at attended locations: A high-density EEG study. *European Journal of Neuroscience*, *30*(11), 2224–2234. https://doi.org/10.1111/j.1460-9568.2009.06980.x

Kelly, S. P., & O'Connell, R. G. (2013). Internal and External Influences on the Rate of Sensory Evidence Accumulation in the Human Brain. *Journal of Neuroscience*, *33*(50), 19434–19441. https://doi.org/10.1523/JNEUROSCI.3355-13.2013

Kelly, S. P., Vanegas, M. I., Schroeder, C. E., & Lalor, E. C. (2013). The cruciform model of striate generation of the early VEP, re-illustrated, not revoked: A reply to Ales et al. (2013). *NeuroImage*, *82*, 154–159. https://doi.org/10.1016/j.neuroimage.2013.05.112

Kerzel, D. (2010). The Fröhlich effect: Past and present. In R. Nijhawan & B. Khurana (Eds.), *Space and Time in Perception and Action* (pp. 321–337). Cambridge University Press. https://doi.org/10.1017/CBO9780511750540.019

Kleiner, M. (2007). *What's new in Psychtoolbox-3?*

Klimesch, W. (1997). EEG-alpha rhythms and memory processes. *International Journal of Psychophysiology*, *26*(1), 319–340. https://doi.org/10.1016/S0167-8760(97)00773-3

Klimesch, W. (2011). Evoked alpha and early access to the knowledge system: The P1 inhibition timing hypothesis. *Brain Research*, *1408*, 52–71. https://doi.org/10.1016/j.brainres.2011.06.003

Klimesch, W., Sauseng, P., & Hanslmayr, S. (2007). EEG alpha oscillations: The inhibition–timing hypothesis. *Brain Research Reviews*, *53*(1), 63–88. https://doi.org/10.1016/j.brainresrev.2006.06.003

Knyazeva, M. G., Barzegaran, E., Vildavski, V. Y., & Demonet, J.-F. (2018). Aging of human alpha rhythm. *Neurobiology of Aging*, *69*, 261–273. https://doi.org/10.1016/j.neurobiolaging.2018.05.018

Kreegipuu, K., & Allik, J. (2003). Perceived onset time and position of a moving stimulus. *Vision Research*, *43*(15), 1625–1635. https://doi.org/10.1016/S0042-6989(03)00165-2

Krekelberg, B., & Lappe, M. (2001). Neuronal latencies and the position of moving objects. *Trends in Neurosciences*, *24*(6), 335–339. https://doi.org/10.1016/S0166-2236(00)01795-1

Kristofferson, A. B. (1967a). Attention and psychophysical time. *Acta Psychologica*, *27*, 93–100. https://doi.org/10.1016/0001-6918(67)90049-2

Kristofferson, A. B. (1967b). Successiveness Discrimination as a Two-State, Quantal Process. *Science*, *158*(3806), 1337–1339. https://doi.org/10.1126/science.158.3806.1337

Lange, J., Oostenveld, R., & Fries, P. (2013). Reduced Occipital Alpha Power Indexes Enhanced Excitability Rather than Improved Visual Perception. *Journal of Neuroscience*, *33*(7), 3212–3220. https://doi.org/10.1523/JNEUROSCI.3755-12.2013

Legg, C. F. (1968). Alpha rhythm and time judgments. *Journal of Experimental*

Psychology, *78*(1), 46–49. https://doi.org/10.1037/h0026149

Loewy, R. L., Bearden, C. E., Johnson, J. K., Raine, A., & Cannon, T. D. (2005). The prodromal questionnaire (PQ): Preliminary validation of a self-report screening measure for prodromal and psychotic syndromes. *Schizophrenia Research*, *79*(1), 117–125. https://doi.org/10.1016/j.schres.2005.03.007

Lopes da Silva, F. H., van Lierop, T. H. M. T., Schrijer, C. F., & Storm van Leeuwen, W. (1973). Organization of thalamic and cortical alpha rhythms: Spectra and coherences. *Electroencephalography and Clinical Neurophysiology*, *35*(6), 627–639. https://doi.org/10.1016/0013-4694(73)90216-2

Lörincz, M. L., Crunelli, V., & Hughes, S. W. (2008). Cellular Dynamics of Cholinergically Induced α (8–13 Hz) Rhythms in Sensory Thalamic Nuclei In Vitro. *Journal of Neuroscience*, *28*(3), 660–671. https://doi.org/10.1523/JNEUROSCI.4468-07.2008

Lőrincz, M. L., Kékesi, K. A., Juhász, G., Crunelli, V., & Hughes, S. W. (2009). Temporal Framing of Thalamic Relay-Mode Firing by Phasic Inhibition during the Alpha Rhythm. *Neuron*, *63*(5), 683–696. https://doi.org/10.1016/j.neuron.2009.08.012

Luck, S. (2005). *An Introduction to the Event-Related Potential Technique*. https://mitpress.mit.edu/9780262525855/an-introduction-to-the-event-related-potential-technique/

Luck, S. J., Heinze, H. J., Mangun, G. R., & Hillyard, S. A. (1990). Visual event-related potentials index focused attention within bilateral stimulus arrays. II.

Functional dissociation of P1 and N1 components. *Electroencephalography and Clinical Neurophysiology*, *75*(6), 528–542. https://doi.org/10.1016/0013-4694(90)90139-B

Mathewson, K. E., Gratton, G., Fabiani, M., Beck, D. M., & Ro, T. (2009). To See or Not to See: Prestimulus α Phase Predicts Visual Awareness. *Journal of Neuroscience*, *29*(9), 2725–2732. https://doi.org/10.1523/JNEUROSCI.3963-08.2009

Mathewson, K. E., Lleras, A., Beck, D. M., Fabiani, M., Ro, T., & Gratton, G. (2011). Pulsed Out of Awareness: EEG Alpha Oscillations Represent a Pulsed-Inhibition of Ongoing Cortical Processing. *Frontiers in Psychology*, *2*. https://doi.org/10.3389/fpsyg.2011.00099

May, E. S., Butz, M., Kahlbrock, N., Brenner, M., Hoogenboom, N., Kircheis, G., Häussinger, D., & Schnitzler, A. (2014). Hepatic encephalopathy is associated with slowed and delayed stimulus-associated somatosensory alpha activity. *Clinical Neurophysiology*, *125*(12), 2427–2435. https://doi.org/10.1016/j.clinph.2014.03.018

Melcón, M., Stern, E., Kessel, D., Arana, L., Poch, C., Campo, P., & Capilla, A. (2023). *Perception of near-threshold visual stimuli is influenced by pre-stimulus alpha-band amplitude but not by alpha phase* [Preprint]. Neuroscience. https://doi.org/10.1101/2023.03.14.532551

Menétrey, M. Q., Vogelsang, L., & Herzog, M. H. (2022). A guideline for linking brain wave findings to the various aspects of discrete perception. *European*

Journal of Neuroscience, *55*(11–12), 3528–3537. https://doi.org/10.1111/ejn.15349

Metzger, W. (1932). Versuch einer gemeinsamen Theorie der Phänomene Fröhlichs und Hazelhoffs und Kritik ihrer Verfahren zur Messung der Empfindungszeit. *Psychologische Forschung*, *16*(1), 176–200. https://doi.org/10.1007/BF00409732

Migliorati, D., Zappasodi, F., Perrucci, M. G., Donno, B., Northoff, G., Romei, V., & Costantini, M. (2020). Individual Alpha Frequency Predicts Perceived Visuotactile Simultaneity. *Journal of Cognitive Neuroscience*, *32*(1), 1–11. https://doi.org/10.1162/jocn_a_01464

Milton, A., & Pleydell-Pearce, C. (2017). Exploring the relationship of phase and peak-frequency EEG alpha-band and beta-band activity to temporal judgments of stimulus duration. *Cognitive Neuroscience*, *8*(4), 193–205. https://doi.org/10.1080/17588928.2017.1359524

Minami, S., & Amano, K. (2017). Illusory Jitter Perceived at the Frequency of Alpha Oscillations. *Current Biology*, *27*(15), 2344-2351.e4. https://doi.org/10.1016/j.cub.2017.06.033

Mioni, G., Shelp, A., Stanfield-Wiswell, C. T., Gladhill, K. A., Bader, F., & Wiener, M. (2020). Modulation of Individual Alpha Frequency with tACS shifts Time Perception. *Cerebral Cortex Communications*, *1*(1), tgaa064. https://doi.org/10.1093/texcom/tgaa064

Morrow, A., & Samaha, J. (2022). No evidence for a single oscillator underlying

discrete visual percepts. *European Journal of Neuroscience*, *55*(11–12), 3054–3066. https://doi.org/10.1111/ejn.15362

Murakami, I. (2001). A flash-lag effect in random motion. *Vision Research*, *41*(24), 3101–3119. https://doi.org/10.1016/S0042-6989(01)00193-6

Nakayama, R., Motoyoshi, I., & Sato, T. (2018). Discretized Theta-Rhythm Perception Revealed by Moving Stimuli. *Scientific Reports*, *8*(1), Article 1. https://doi.org/10.1038/s41598-018-24131-6

Navarra, J., Vatakis, A., Zampini, M., Soto-Faraco, S., Humphreys, W., & Spence, C. (2005). Exposure to asynchronous audiovisual speech extends the temporal window for audiovisual integration. *Cognitive Brain Research*, *25*(2), 499–507. https://doi.org/10.1016/j.cogbrainres.2005.07.009

Nijhawan, R. (1994). Motion extrapolation in catching. *Nature*, *370*(6487), 256–257. https://doi.org/10.1038/370256b0

Noguchi, Y. (2022). Individual differences in beta frequency correlate with the audio–visual fusion illusion. *Psychophysiology*, *59*(e14041). https://doi.org/10.1111/psyp.14041

Pelli, D. G. (1997). The VideoToolbox software for visual psychophysics: Transforming numbers into movies. *Spatial Vision*, *10*(4), 437–442. https://doi.org/10.1163/156856897x00366

Piéron, H. (1935). Le processus du métacontraste. [The process involved in "after-contrast."]. *Journal de Psychologie Normale et Pathologique*, *32*, 5–24.

Poole, D., Casassus, M., Gowen, E., Poliakoff, E., & Jones, L. A. (2022). Time

perception in autistic adults: Interval and event timing judgments do not differ from nonautistics. *Journal of Experimental Psychology: General*, *151*(11), 2666–2682. https://doi.org/10.1037/xge0001203

Powers, A. R., Hillock, A. R., & Wallace, M. T. (2009). Perceptual Training Narrows the Temporal Window of Multisensory Binding. *Journal of Neuroscience*, *29*(39), 12265–12274. https://doi.org/10.1523/JNEUROSCI.3501-09.2009

Prins, N. (2012). The psychometric function: The lapse rate revisited. *Journal of Vision*, *12*(6), 25–25. https://doi.org/10.1167/12.6.25

Prins, N., & Kingdom, F. A. A. (2018). Applying the Model-Comparison Approach to Test Specific Research Hypotheses in Psychophysical Research Using the Palamedes Toolbox. *Frontiers in Psychology*, *9*. https://doi.org/10.3389/fpsyg.2018.01250

Ramsay, I. S., Lynn, P. A., Schermitzler, B., & Sponheim, S. R. (2021). Individual alpha peak frequency is slower in schizophrenia and related to deficits in visual perception and cognition. *Scientific Reports*, *11*(1), Article 1. https://doi.org/10.1038/s41598-021-97303-6

Rassi, E., Wutz, A., Müller-Voggel, N., & Weisz, N. (2019). Prestimulus feedback connectivity biases the content of visual experiences. *Proceedings of the National Academy of Sciences*, *116*(32), 16056–16061. https://doi.org/10.1073/pnas.1817317116

Ro, T. (2019). Alpha Oscillations and Feedback Processing in Visual Cortex for Conscious Perception. *Journal of Cognitive Neuroscience*, *31*(7), 948–960.

https://doi.org/10.1162/jocn_a_01397

Ronconi, L., Oosterhof, N. N., Bonmassar, C., & Melcher, D. (2017). Multiple oscillatory rhythms determine the temporal organization of perception. *Proceedings of the National Academy of Sciences*, *114*(51), 13435–13440. https://doi.org/10.1073/pnas.1714522114

Ross, D. A. (1968). *Time Perception and Brain Rhythms* [Lehigh University]. https://www.proquest.com/openview/f269b4b9763197d92ff0ac4c72eb8b8a/1?pq-origsite=gscholar&cbl=18750&diss=y

Rouder, J. N., Morey, R. D., Verhagen, J., Province, J. M., & Wagenmakers, E.-J. (2016). Is There a Free Lunch in Inference? *Topics in Cognitive Science*, *8*(3), 520–547. https://doi.org/10.1111/tops.12214

Roy, M., Grondin, S., & Roy, M.-A. (2012). Time perception disorders are related to working memory impairment in schizophrenia. *Psychiatry Research*, *200*(2), 159–166. https://doi.org/10.1016/j.psychres.2012.06.008

Ruzzoli, M., Torralba, M., Morís Fernández, L., & Soto-Faraco, S. (2019). The relevance of alpha phase in human perception. *Cortex*, *120*, 249–268. https://doi.org/10.1016/j.cortex.2019.05.012

Salkind, N. J. (2006). *Encyclopedia of Measurement and Statistics*. SAGE Publications.

Salti, M., Bar-Haim, Y., & Lamy, D. (2012). The P3 component of the ERP reflects conscious perception, not confidence. *Consciousness and Cognition*, *21*(2), 961–968. https://doi.org/10.1016/j.concog.2012.01.012

Samaha, J., Bauer, P., Cimaroli, S., & Postle, B. R. (2015). Top-down control of the phase of alpha-band oscillations as a mechanism for temporal prediction. *Proceedings of the National Academy of Sciences*, *112*(27), 8439–8444. https://doi.org/10.1073/pnas.1503686112

Samaha, J., Boutonnet, B., Postle, B. R., & Lupyan, G. (2018). Effects of meaningfulness on perception: Alpha-band oscillations carry perceptual expectations and influence early visual responses. *Scientific Reports*, *8*(1), 6606. https://doi.org/10.1038/s41598-018-25093-5

Samaha, J., Gosseries, O., & Postle, B. R. (2017). Distinct Oscillatory Frequencies Underlie Excitability of Human Occipital and Parietal Cortex. *Journal of Neuroscience*, *37*(11), 2824–2833. https://doi.org/10.1523/JNEUROSCI.3413-16.2017

Samaha, J., Iemi, L., Haegens, S., & Busch, N. A. (2020). Spontaneous Brain Oscillations and Perceptual Decision-Making. *Trends in Cognitive Sciences*, *24*(8), 639–653. https://doi.org/10.1016/j.tics.2020.05.004

Samaha, J., & Postle, B. R. (2015). The Speed of Alpha-Band Oscillations Predicts the Temporal Resolution of Visual Perception. *Current Biology*, *25*(22), 2985–2990. https://doi.org/10.1016/j.cub.2015.10.007

Samaha, J., & Romei, V. (2024). Alpha-Band Frequency and Temporal Windows in Perception: A Review and Living Meta-analysis of 27 Experiments (and Counting). *Journal of Cognitive Neuroscience*, *36*(4), 640–654. https://doi.org/10.1162/jocn_a_02069

Sauseng, P., Klimesch, W., Stadler, W., Schabus, M., Doppelmayr, M., Hanslmayr, S., Gruber, W. R., & Birbaumer, N. (2005). A shift of visual spatial attention is selectively associated with human EEG alpha activity. *European Journal of Neuroscience*, *22*(11), 2917–2926. https://doi.org/10.1111/j.1460-9568.2005.04482.x

Schneider, K. A. (2018). The Flash-Lag, Fröhlich and Related Motion Illusions Are Natural Consequences of Discrete Sampling in the Visual System. *Frontiers in Psychology*, *9*. https://doi.org/10.3389/fpsyg.2018.01227

Shen, L., Han, B., Chen, L., & Chen, Q. (2019). Perceptual inference employs intrinsic alpha frequency to resolve perceptual ambiguity. *PLOS Biology*, *17*(3), e3000025. https://doi.org/10.1371/journal.pbio.3000025

Sherman, M. T., Kanai, R., Seth, A. K., & VanRullen, R. (2016). Rhythmic Influence of Top–Down Perceptual Priors in the Phase of Prestimulus Occipital Alpha Oscillations. *Journal of Cognitive Neuroscience*, *28*(9), 1318–1330. https://doi.org/10.1162/jocn_a_00973

Slagter, H. A., Prinssen, S., Reteig, L. C., & Mazaheri, A. (2016). Facilitation and inhibition in attention: Functional dissociation of pre-stimulus alpha activity, P1, and N1 components. *NeuroImage*, *125*, 25–35. https://doi.org/10.1016/j.neuroimage.2015.09.058

Sokoliuk, R., & VanRullen, R. (2019). Perceptual Illusions Caused by Discrete Sampling. In V. Arstila, A. Bardon, S. E. Power, & A. Vatakis (Eds.), *The Illusions of Time: Philosophical and Psychological Essays on Timing and*

Time Perception (pp. 315–338). Springer International Publishing. https://doi.org/10.1007/978-3-030-22048-8_17

Spaak, E., de Lange, F. P., & Jensen, O. (2014). Local Entrainment of Alpha Oscillations by Visual Stimuli Causes Cyclic Modulation of Perception. *Journal of Neuroscience*, *34*(10), 3536–3544. https://doi.org/10.1523/JNEUROSCI.4385-13.2014

Sponheim, S. R., Stim, J. J., Engel, S. A., & Pokorny, V. J. (2023). Slowed alpha oscillations and percept formation in psychotic psychopathology. *Frontiers in Psychology*, *14*. https://doi.org/10.3389/fpsyg.2023.1144107

Stevenson, R. A., Wilson, M. M., Powers, A. R., & Wallace, M. T. (2013). The effects of visual training on multisensory temporal processing. *Experimental Brain Research. Experimentelle Hirnforschung. Experimentation Cerebrale*, *225*(4), 479–489. https://doi.org/10.1007/s00221-012-3387-y

Stevenson, R. A., Zemtsov, R. K., & Wallace, M. T. (2012). Individual Differences in the Multisensory Temporal Binding Window Predict Susceptibility to Audiovisual Illusions. *Journal of Experimental Psychology. Human Perception and Performance*, *38*(6), 1517–1529. https://doi.org/10.1037/a0027339

Sur, S., & Sinha, V. K. (2009). Event-related potential: An overview. *Industrial Psychiatry Journal*, *18*(1), 70. https://doi.org/10.4103/0972-6748.57865

Surwillo, W. W. (1966). Time perception and the 'internal clock': Some observations on the role of the electroencephalogram. *Brain Research*, *2*(4), 390–392.

https://doi.org/10.1016/0006-8993(66)90008-4

Tarasi, L., & Romei, V. (2023). Individual Alpha Frequency Contributes to the Precision of Human Visual Processing. *Journal of Cognitive Neuroscience*, 1–11. https://doi.org/10.1162/jocn_a_02026

Tek, C., Gold, J., Blaxton, T., Wilk, C., McMahon, R. P., & Buchanan, R. W. (2002). Visual Perceptual and Working Memory Impairments in Schizophrenia. *Archives of General Psychiatry*, *59*(2), 146–153. https://doi.org/10.1001/archpsyc.59.2.146

Tenke, C. E., Schroeder, C. E., Arezzo, J. C., & Vaughan, H. G. (1993). Interpretation of high-resolution current source density profiles: A simulation of sublaminar contributions to the visual evoked potential. *Experimental Brain Research*, *94*(2), 183–192. https://doi.org/10.1007/BF00230286

Thoenes, S., & Oberfeld, D. (2017). Meta-analysis of time perception and temporal processing in schizophrenia: Differential effects on precision and accuracy. *Clinical Psychology Review*, *54*, 44–64. https://doi.org/10.1016/j.cpr.2017.03.007

Thut, G., Nietzel, A., Brandt, S. A., & Pascual-Leone, A. (2006). α-Band Electroencephalographic Activity over Occipital Cortex Indexes Visuospatial Attention Bias and Predicts Visual Target Detection. *Journal of Neuroscience*, *26*(37), 9494–9502. https://doi.org/10.1523/JNEUROSCI.0875-06.2006

Trajkovic, J., Di Gregorio, F., Ferri, F., Marzi, C., Diciotti, S., & Romei, V. (2021). Resting state alpha oscillatory activity is a valid and reliable marker of

schizotypy. *Scientific Reports*, *11*(1), Article 1. https://doi.org/10.1038/s41598-021-89690-7

Treisman, M. (1963). Temporal discrimination and the indifference interval: Implications for a model of the "internal clock." *Psychological Monographs: General and Applied*, *77*(13), 1–31. https://doi.org/10.1037/h0093864

Treisman, M., Faulkner, A., Naish, P. L. N., & Brogan, D. (1990). The Internal Clock: Evidence for a Temporal Oscillator Underlying Time Perception with Some Estimates of its Characteristic Frequency. *Perception*, *19*(6), 705–742. https://doi.org/10.1068/p190705

Valera, F. J., Toro, A., Roy John, E., & Schwartz, E. L. (1981). Perceptual framing and cortical alpha rhythm. *Neuropsychologia*, *19*(5), 675–686. https://doi.org/10.1016/0028-3932(81)90005-1

van Dijk, H., Schoffelen, J.-M., Oostenveld, R., & Jensen, O. (2008). Prestimulus Oscillatory Activity in the Alpha Band Predicts Visual Discrimination Ability. *Journal of Neuroscience*, *28*(8), 1816–1823. https://doi.org/10.1523/JNEUROSCI.1853-07.2008

van Kerkoerle, T., Self, M. W., Dagnino, B., Gariel-Mathis, M.-A., Poort, J., van der Togt, C., & Roelfsema, P. R. (2014). Alpha and gamma oscillations characterize feedback and feedforward processing in monkey visual cortex. *Proceedings of the National Academy of Sciences*, *111*(40), 14332–14341. https://doi.org/10.1073/pnas.1402773111

van Wassenhove, V., Herbst, S. K., & Kononowicz, T. W. (2019). Timing the Brain

to Time the Mind: Critical Contributions of Time-Resolved Neuroimaging for Temporal Cognition. In S. Supek & C. J. Aine (Eds.), *Magnetoencephalography* (pp. 855–905). Springer International Publishing. https://doi.org/10.1007/978-3-030-00087-5_67

Vanegas, M. I., Blangero, A., & Kelly, S. P. (2013). Exploiting individual primary visual cortex geometry to boost steady state visual evoked potentials. *Journal of Neural Engineering*, *10*(3), 036003. https://doi.org/10.1088/1741-2560/10/3/036003

VanRullen, R. (2016). Perceptual Cycles. *Trends in Cognitive Sciences*, *20*(10), 723–735. https://doi.org/10.1016/j.tics.2016.07.006

VanRullen, R., & Koch, C. (2003). Is perception discrete or continuous? *Trends in Cognitive Sciences*, *7*(5), 207–213. https://doi.org/10.1016/S1364-6613(03)00095-0

VanRullen, R., & Macdonald, J. S. P. (2012). Perceptual Echoes at 10 Hz in the Human Brain. *Current Biology*, *22*(11), 995–999. https://doi.org/10.1016/j.cub.2012.03.050

Venskus, A., Ferri, F., Migliorati, D., Spadone, S., Costantini, M., & Hughes, G. (2021). Temporal binding window and sense of agency are related processes modifiable via occipital tACS. *PLOS ONE*, *16*(9), e0256987. https://doi.org/10.1371/journal.pone.0256987

Venskus, A., & Hughes, G. (2021). Individual differences in alpha frequency are associated with the time window of multisensory integration, but not time

perception. *Neuropsychologia*, *159*, 107919. https://doi.org/10.1016/j.neuropsychologia.2021.107919

Wallace, G. L., & Happé, F. (2008). Time perception in autism spectrum disorders. *Research in Autism Spectrum Disorders*, *2*(3), 447–455. https://doi.org/10.1016/j.rasd.2007.09.005

Wearden, J. H., Norton, R., Martin, S., & Montford-Bebb, O. (2007). Internal clock processes and the filled-duration illusion. *Journal of Experimental Psychology: Human Perception and Performance*, *33*(3), 716–729. https://doi.org/10.1037/0096-1523.33.3.716

Wells, E. F., Bernstein, G. M., Scott, B. W., Bennett, P. J., & Mendelson, J. R. (2001). Critical flicker frequency responses in visual cortex. *Experimental Brain Research*, *139*(1), 106–110. https://doi.org/10.1007/s002210100721

White, C. T. (1963). Temporal numerosity and the psychological unit of duration. *Psychological Monographs: General and Applied*, *77*(12), 1–37. https://doi.org/10.1037/h0093860

White, P. A. (2018). Is conscious perception a series of discrete temporal frames? *Consciousness and Cognition*, *60*, 98–126. https://doi.org/10.1016/j.concog.2018.02.012

Whitney, D., & Cavanagh, P. (2000). Motion distorts visual space: Shifting the perceived position of remote stationary objects. *Nature Neuroscience*, *3*(9), Article 9. https://doi.org/10.1038/78878

Williams, E. A., Yüksel, E. M., Stewart, A. J., & Jones, L. A. (2019). Modality

differences in timing and the filled-duration illusion: Testing the pacemaker rate explanation. *Attention, Perception, & Psychophysics*, *81*(3), 823–845. https://doi.org/10.3758/s13414-018-1630-8

Woodman, G. F. (2010). A Brief Introduction to the Use of Event-Related Potentials (ERPs) in Studies of Perception and Attention. *Attention, Perception & Psychophysics*, *72*(8). https://doi.org/10.3758/APP.72.8.2031

Wutz, A., Melcher, D., & Samaha, J. (2018). Frequency modulation of neural oscillations according to visual task demands. *Proceedings of the National Academy of Sciences*, *115*(6), 1346–1351. https://doi.org/10.1073/pnas.1713318115

Wutz, A., Muschter, E., van Koningsbruggen, M. G., Weisz, N., & Melcher, D. (2016). Temporal Integration Windows in Neural Processing and Perception Aligned to Saccadic Eye Movements. *Current Biology*, *26*(13), 1659–1668. https://doi.org/10.1016/j.cub.2016.04.070

Zazio, A., Schreiber, M., Miniussi, C., & Bortoletto, M. (2020). Modelling the effects of ongoing alpha activity on visual perception: The oscillation-based probability of response. *Neuroscience & Biobehavioral Reviews*, *112*, 242–253. https://doi.org/10.1016/j.neubiorev.2020.01.037

Zhou, Y. J., Iemi, L., Schoffelen, J.-M., de Lange, F. P., & Haegens, S. (2021). Alpha oscillations shape sensory representation and perceptual sensitivity. *The Journal of Neuroscience*, JN-RM-1114-21. https://doi.org/10.1523/JNEUROSCI.1114-21.2021